BRNO UNIVERSITY OF TECHNOLOGY

Faculty of Electrical Engineering
and Communication

MASTER'S THESIS

Brno, 2024

Van Phi Nguyen

BRNO UNIVERSITY OF TECHNOLOGY

VYSOKÉ UČENÍ TECHNICKÉ V BRNĚ

FACULTY OF ELECTRICAL ENGINEERING AND COMMUNICATION

FAKULTA ELEKTROTECHNIKY
A KOMUNIKAČNÍCH TECHNOLOGIÍ

DEPARTMENT OF TELECOMMUNICATIONS

ÚSTAV TELEKOMUNIKACÍ

USE OF 5G FOR CONTROL OF UNMANNED AERIAL VEHICLES

VYUŽITÍ 5G PRO ŘÍZENÍ BEZPILOTNÍCH LÉTAJÍCÍCH PROSTŘEDKŮ

MASTER'S THESIS

DIPLOMOVÁ PRÁCE

AUTHOR Van Phi Nguyen

AUTOR PRÁCE

SUPERVISOR doc. Ing. Petr Číka, Ph.D.

VEDOUCÍ PRÁCE

BRNO 2024

BRNO UNIVERSITY OF TECHNOLOGY
FACULTY OF ELECTRICAL ENGINEERING AND COMMUNICATION

Master's Thesis

Master's study program **Information Security**

Department of Telecommunications

Student: Van Phi Nguyen ***ID:*** 246484

Year of study: 2 ***Academic year:*** 2023/24

TITLE OF THESIS:

Use of 5G for control of Unmanned Aerial Vehicles

INSTRUCTION:

The aim of the thesis is to verify the possibility of using 5G technology for drone control and to find out what parameters and limitations this method of control exhibits. The task will be to create a test setup involving a drone and a ground station, that will be interconnected via 5G, and perform testing on a suitable scenario. The drone will be equipped with a camera or other adequate sensors. The ground station will process data from the on-board camera/sensors. Based on the results of the data processing, the movement of the drone will be automatically controlled. The work will include an assessment of what applications, mission types or flight parameters this type of control is suitable for. The thesis will also include an analysis of the solution from the security point of view, i.e. an overview of possible ways of intentional interference with communication and the resulting impact.

RECOMMENDED LITERATURE:

[1] HU, Fei, Xin-Lin HUANG a DongXiu OU. UAV Swarm Networks: Models, Protocols, and Systems. CRC Press, 2021. ISBN 9780367457396.

[2] FALLGREN, Mikael, Markus DILLINGER, Toktam MAHMOODI a Tommy SVENSSON. Cellular V2X for Connected Automated Driving. Wiley, 2021. ISBN 978-1119692645.

[3] FAHLSTROM, Paul Gerin, Thomas James GLEASON a Mohammad H. SADRAEY. Introduction to UAV systems. Fifth edition. Wiley, 2022. Aerospace series. ISBN 978-111-9802-617.

Date of project specification: 5.2.2024 ***Deadline for submission:*** 21.5.2024

Supervisor: doc. Ing. Petr Číka, Ph.D.
Consultant: doc. Ing. Josef Bajer, Ph.D.

doc. Ing. Jan Hajný, Ph.D.
Chair of study program board

Abstract

This master's thesis explores the feasibility of utilizing 5G technologies within the private 5G network of the University of Defence (UNOB) in Brno, Czech Republic, for the control of unmanned aerial vehicles (UAVs). The research provides an in-depth analysis of aerial communications in UAVs, with a particular focus on the applications of 5G technologies. A central part of the study involves proposing a conceptual design for UAV test setups and providing a comprehensive outline of the execution of test scenarios. The assessment of each scenario is based on specific measured parameters and the methodologies used for these measurements. Furthermore, the thesis assesses the capabilities of remotely controlling 5G-connected UAVs from a Ground Control Station via the private 5G network, focusing on the processing of application data transmitted through this network. Finally, the study includes an evaluation of communication security concerns for UAVs and the potential security implications of the private 5G network.

Keywords

5G, aerial communications, cellular networks, MAVLink, NVIDIA Jetson AGX Orin Developer Kit, private 5G UNOB network, unmanned aerial vehicles (UAVs).

Abstrakt

Tato diplomová práce zkoumá možnost využití technologií 5G v rámci privátní 5G sítě Univerzity obrany (UNOB) v Brně, Česká republika, pro řízení bezpilotních létajících prostředků (UAVs). Výzkum poskytuje podrobnou analýzu leteckých komunikací u UAVs se zaměřením na aplikaci technologií 5G. Klíčovou součástí studie je návrh koncepčního designu pro testovací sestavy UAV a poskytnutí komplexního přehledu o provedení testovacích scénářů. Hodnocení každého scénáře je založeno na specifických měřených parametrech a metodologiích použitých pro tato měření. Dále práce hodnotí schopnosti dálkového ovládání UAV s podporou 5G z pozemní řídicí stanice prostřednictvím privátní 5G sítě, přičemž se zaměřuje na zpracování aplikačních dat přenášených touto sítí. Studie také zahrnuje hodnocení bezpečnostních rizik komunikace UAVs a potenciálních bezpečnostních důsledků privátní 5G sítě.

Klíčová slova

5G, letecká komunikace, mobilní sítě, MAVLink, NVIDIA Jetson AGX Orin Developer Kit, privátní 5G UNOB sítě, bezpilotní letadla (UAVs).

Rozšířený abstrakt

V posledních letech došlo k výraznému nárůstu využívání bezpilotních letadel (UAVs), a to nejen ve vojenských aplikacích, ale také v civilním a komerčním kontextu. Tento rostoucí zájem lze přičíst pokroku ve výrobní technologii bezpilotních letounů a snížení nákladů, díky čemuž jsou tato zařízení dostupnější široké veřejnosti. Současně vývoj komunikačních technologií, zejména rozvoj mobilních sítí 5G, sehrál zásadní roli při zvyšování schopností bezpilotních letounů, které jim umožňují operovat v dynamickém a složitém prostředí.

Cílem tohoto výzkumu je ve spolupráci s Katedrou letecké techniky Univerzity obrany (UNOB) v Brně ověřit možnosti využití technologií 5G pro řízení bezpilotních prostředků. Primárním cílem je identifikovat parametry a omezení spojená s tímto přístupem k řízení. Diplomová práce zahrnuje komplexní studium bezdrátové komunikace v bezpilotních letounech, se specifickým zaměřením na aplikaci mobilních sítí při provozu UAV. Kromě toho projekt poskytuje teoretické zázemí pro sítě 5G a zdůrazňuje nejnovější technologie a vynikající vlastnosti, které z nich činí vhodnou volbu pro komunikaci bezpilotních létajících prostředků.

Projekt především navrhuje koncepční návrh testovacího zařízení pro UAV a podrobně popisuje připravené scénáře pro provedení testů. V každém scénáři je hodnocení založeno na měřených parametrech a způsobu jejich měření.

Tyto výsledky dále hodnotí schopnost UAV pro automatické řízení prostřednictvím aplikace pro zpracování dat, která shromažďuje informace ze senzorů na UAV. Operace zpracování a řízení dat se provádějí na pozemní stanici a bezproblémově komunikují prostřednictvím vnitřní sítě 5G. Toto nastavení zajišťuje, že všechny řídicí příkazy a data senzorů jsou přenášeny efektivně, což umožňuje přesné řízení funkcí UAV na základě analýzy v reálném čase.

Nakonec tato práce zkoumá bezpečnostní aspekty v UAV komunikaci se zaměřením na základní bezpečnostní požadavky, riziky a možná řešení. Konkrétně zkoumá, jak privátní 5G sítě na UNOB řeší tyto bezpečnostní hrozby. Analýza zahrnuje podrobný přehled zranitelností spojených s UAV komunikací a strategií implementovaných v rámci privátní 5G, aby tato rizika zmírnila a zajistila robustní ochranu proti potenciálnímu narušení a neoprávněnému přístupu.

Bibliographic citation

NGUYEN, Van Phi. Využití 5G pro řízení bezpilotních létajících prostředků [online]. Brno, 2024 [cit. 2024-05-07]. Dostupné z: https://www.vut.cz/studenti/zav-prace/detail/159246. Diplomová práce. Vysoké učení technické v Brně, Fakulta elektrotechniky a komunikačních technologií, Ústav telekomunikací. Vedoucí práce Petr Číka.

Author’s Declaration

Author:	Bc. Van Phi Nguyen
Author’s ID:	246484
Paper type:	Master’s Thesis
Academic year:	2023/24
Topic:	Use of 5G for control of unmanned aerial vehicles

I declare that I have written this paper independently, under the guidance of the advisor and using exclusively the technical references and other sources of information cited in the project and listed in the comprehensive bibliography at the end of the project.

As the author, I furthermore declare that, with respect to the creation of this paper, I have not infringed any copyright or violated anyone’s personal and/or ownership rights. In this context, I am fully aware of the consequences of breaking Regulation S 11 of the Copyright Act No. 121/2000 Coll. of the Czech Republic, as amended, and of any breach of rights related to intellectual property or introduced within amendments to relevant Acts such as the Intellectual Property Act or the Criminal Code, Act No. 40/2009 Coll., Section 2, Head VI, Part 4.

Brno, May 07, 2024

----

author’s signature

Acknowledgement

I would like to express my deepest gratitude to my supervisor, doc. Ing. Petr Čika, Ph.D for his invaluable guidance and support throughout the entire research process.

I am deeply thankful to my consultant plk. gšt. doc. Ing. Josef Bajer, Ph.D, for his valuable contributions and constructive critique. His expertise, insightful feedback, and continuous encouragement played a pivotal role in shaping the direction of this master's thesis.

I would also like to acknowledge the Department of Aircraft Technology at University of Defence, Brno, Czech Republic for providing conductive environment for research and access to necessary resources.

I am grateful to Le Quy Don Technical Academy in Hanoi, Vietnam for providing financial support, which allowed me to conduct this research and helped me during my study in Brno, Czech Republic.

Finally, special thanks to my family and friends for their unwavering support and understanding throughout my master's study.

Brno, May 07, 2024 --

Author's signature

Contents

FIGURES

TABLES

INTRODUCTION

Unmanned aerial vehicles (UAVs), also commonly referred to as “drones”, are aircrafts without a human onboard. UAVs are piloted by remote control or embedded computer programs, that also can carry cameras, sensors, communication equipment, or other payloads. In the past, UAVs were primarily employed in military missions for remote surveillance and attack operations in dangerous areas, aimed at reducing the risks to human pilots. However, in recent years, people have witnessed an explosion of interest in using UAVs for civilian and commercial purposes, including aerial inspection, photography, precision agriculture, traffic management, search and rescue operations, package delivery, telecommunications, and many more.

Besides the development of UAVs, the evolution of communication technologies plays a pivotal role in enhancing their capabilities, enabling them to operate in dynamic and complex environments. In this context, the advent of the fifth generation of mobile networks, commonly referred to as 5G, presents a paradigm shift in wireless communication, offering unprecedented data speeds, low latency, and massive device connectivity.

The objective of this master’s thesis is to verify the possibility of employing 5G technologies, specifically within the private 5G network at the University of Defence (UNOB), Brno, Czech Republic, for the control of UAVs. The primary goal of this research is to explore the use of 5G technology for controlling UAVs and to identify the parameters and limitations of this control method. The project involves setting up a test environment with a UAV and a ground station connected via 5G. This UAV will have a camera or other sensors, and the ground station will process the data from these sensors. The UAV’s movements will be controlled automatically based on this processed data. The research will evaluate which applications, mission types, or flight parameters are suitable for this control method. Additionally, the study will analyze the security aspects, including potential methods of intentional interference with communication and their impacts.

The master’s thesis is structured into nine distinct sections. Chapter 1 focuses on the wireless communications of UAVs, analyzing the pros and cons of each communication technique. Chapter 2 provides an in-depth look at 5G networks, emphasizing their potential for enhancing aerial communications. Chapter 3 delves into how cellular networks have been applied to UAVs, reviewing the evolution of UAVs connectivity through different mobile network generations over the last twenty years.

In Chapter 4, the thesis introduces a proposed design for a testbed to evaluate a private 5G network at the University of Defence in Brno, Czech Republic, detailing the necessary hardware and software used in this research. Chapter 5 specifies the measurement parameters and the methods used to evaluate these tests.

Chapter 6 then describes the test scenarios and the results obtained. Following this, Chapter 7 examines the security aspects of UAV communications, specifically how the private 5G UNOB network addresses security threats. Chapter 8 evaluates the findings of this thesis and outlines the possible future work. The thesis concludes with a succinct summary of its findings.

1. UAVs WIRELESS COMMUNICATIONS

This chapter presents the study of UAVs wireless communications. This comprehensive study is conducted to clarify various types of wireless communications for UAVs, outlining both their advantages and disadvantages. This analysis is crucial for establishing a clear understanding of why cellular networks emerge as the suitable choice for UAVs.

1.1 Introduction to UAVs wireless communication

According to [1], the total number of UAVs will reach 86.5 million and cellular-connected UAVs will reach 6.5 million connections by 2025. The potential scale of the UAVs industry is staggering, with estimates suggesting it could reach around 80 billion US dollars in economic impact within the United States alone. This growth is anticipated to result in the creation of tens of thousands of new jobs in the coming decade [2]. Therefore, UAVs have been tagged as a promising technology to offer fertile business opportunities in the near future.

An essential enabling technology of unmanned aircraft systems (UASs) is wireless communication. The communication can be divided into payload and non-payload communication. The former one helps UAVs to transmit and/or to receive mission-related data (aerial images, high-speed video, UAVs operators, end users, and ground gateway). The latter is commonly known as control and non-payload communication (CNPC). CNPC exchanges safety-critical information with various parties such as remote pilots, nearby aerial vehicles, and air traffic controllers, to ensure safe, reliable, and efficient flight operation.

There are three CNPC types required for ensuring safe UAVs operations communication according to the International Telecommunication Union (ITU) [3]:

- Communication for UAVs command and control
- Communication for air traffic control (ATC) relay
- Communication supporting “sense and avoid”

UAV communication requirements were specified by the Third Generation Partnership Project – 3GPP (Table 1.1). Command and control data includes telemetry, waypoint updates for autonomous UAVs operations, real-time piloting, identity, flight authorization, navigation database updates, etc. On the other hand, application data consists of video (streaming), images, other sensor data, etc.

CNPC typically operates at a low data rate, e.g., 60 – 100 kbps, while demanding high reliability and minimal latency. The communication needs for UAVs command and control are similar across different UAV types, driven by shared safety considerations. However, the specific communication requirements can vary significantly, primarily influenced by their distinct applications.

Table 1.1 UAVs communication requirements specified by 3GPP [4]

	Data type	Data rate	Reliability	Latency
Downlink (ground station to UAV)	Command and control	60-100 kbps	10^{-3} packet error rate	50 ms
Uplink (UAV to ground station)	Command and control	60-100 kbps	10^{-3} packet error rate	N/A
	Application data	Up to 50 Mbps	N/A	Similar to ground user

1.2 Types of UAVs wireless communication

Wireless technology plays a crucial role in ensuring uninterrupted connectivity with exceptional reliability within three-dimensional space, accounting for both air-to-air and air-to-ground connections. The primary communication technologies encompass direct link, satellite, ad-hoc network, and cellular network (Fig. 1.1). These communication technologies find extensive application in military systems and various combat operations. Military applications include reconnaissance, armed engagements, and military training target tracking, among others.

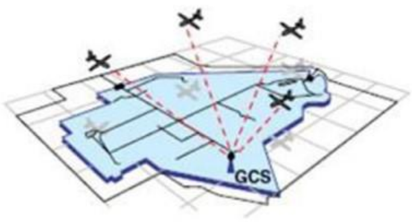

a) UAV direct communication

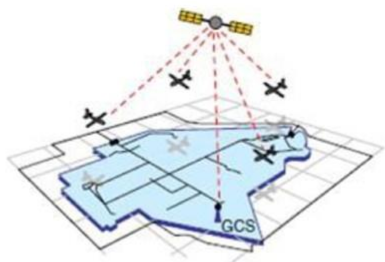

b) UAV communication via Satellite networks

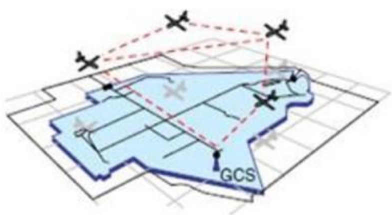

c) UAV communication via Ad -Hoc networks

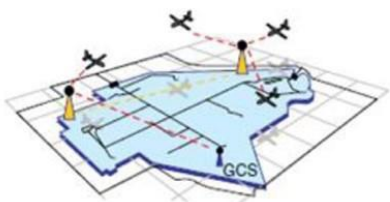

d) UAV communication via cellular networks

Fig.1.1 UAVs communication architecture [5]

- **Direct link** (Fig. 1.1a) is the direct point-to-point communication between UAVs and their associated ground node over the unlicensed band, e.g., the 2.4 GHz band. The ground node can be a remote controller or ground station. Although this communication is simple and low cost, it has big disadvantages of limited range, low data rate, being vulnerable to interface, and non-scalable. Due to the limited Line of

Sight (LoS) communication, the direct link can be easily blocked by obstacles, which results in poor reliability and low data rate.

- **Satellites** (Fig. 1.1b) play a vital role in facilitating data transmission between geographically distant UAVs and ground gateways. This connectivity is particularly valuable in remote regions where conventional terrestrial networks like Wi-Fi or cellular services are not available. Additionally, satellite signals support Global Navigation Satellite System (GNSS) modules in UAVs, enabling them to navigate and determine their precise location. However, there are several drawbacks to this communication. Firstly, the substantial distance between satellites and low-altitude UAVs or ground stations results in significant signal propagation loss and latency. Secondly, stringent limitations on size, weight, and power present challenges. Lastly, the elevated operational costs associated with satellite communication make it less feasible for widespread adoption.
- **An Ad-Hoc network** (Fig. 1.1c), also known as a Mobile Ad-Hoc Network (MANET), is a network that dynamically self-organizes without the need for infrastructure. It facilitates direct peer-to-peer communication among mobile devices such as laptops, cell phones, etc. These devices communicate using bandwidth-constrained wireless links, often utilizing standards like IEEE 802.11 a/b/g/n. Within a MANET, each device can change position over time, and their connectivity conditions with other devices can vary frequently. To enable communication between distant nodes, intermediate devices may assist in forwarding data through multi-hop relaying. However, this approach comes at the cost of increased energy consumption, reduced spectrum efficiency, and longer end-to-end delays. MANET finds application in scenarios like Flying Ad-Hoc Networks (FANET) and Vehicle Ad-Hoc Networks (VANET). In a smaller network, FANET proves to be a robust and flexible architecture for communication among UAVs. Nevertheless, in larger geographical areas, establishing a reliable routing protocol across the entire network becomes more complex due to the dynamic and intermittent link connections among flying UAVs.
- **Cellular networks** (Fig. 1.1d) offer a cost-effective solution for facilitating extensive UAV communication when compared to the aforementioned communication methods. This is thanks to taking advantage of both current and future cellular networks to establish communication links with UAVs. Cellular networks possess notable advantages, including extensive coverage, high-speed fiber optic data transmission, and advanced communication technologies. Consequently, employing such networks allows for the fulfillment of fundamental communication requirements for UAVs, spanning both CNPC and payload communication. This pivotal factor underscores why the project focuses on investigating the application of the cutting-edge 5G cellular network in UAV communication. However, it is worth acknowledging the limitations of cellular networks, which are unavailable in remote

areas such as seas, deserts, forests, etc. Nevertheless, a forward-looking approach entails integrating various communication types, including UAV-to-UAV, UAV-to-satellite, UAV-to-ground, and UAV-to-base-stations within cellular networks, to shape the blueprint for future developments in UAVs communication.

1.3 Use cases of cellular networks for UAVs communications

There are two paradigms in cellular UAVs communications, **cellular-connected UAVs** and **UAV-assisted wireless communications** [6], as illustrated in Fig. 1.2.

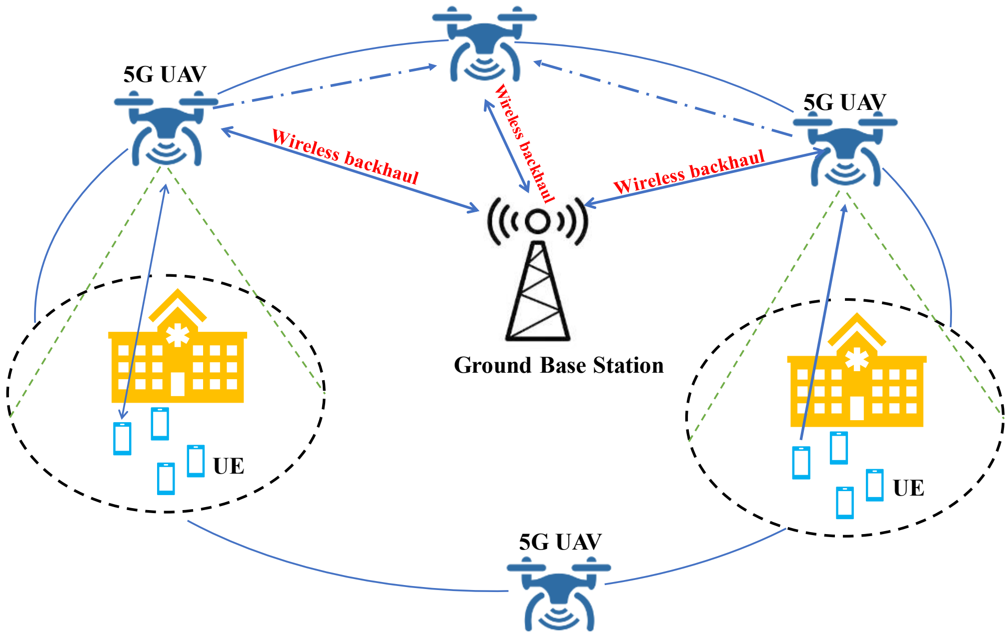

Fig.1.2 Application of UAV-assisted cellular communication in situations where users experience deep shadow fading or are situated at the cell's edge.

Within the first paradigm, several key advantages become apparent. Firstly, owing to the near-global coverage of cellular networks, a cellular-connected UAV allows ground-based pilots to command and control the UAV from a remote location, effectively extending its operational range without substantial limitations. Secondly, advanced cellular technologies and authentication mechanisms position cellular-connected UAVs to attain substantial performance enhancements compared to previously introduced technologies. This improvement is observed in terms of reliability, security, and data throughput. Additionally, a cellular-assisted localization service offers UAVs an alternative and supplementary method, in addition to the conventional satellite-based Global Positioning System (GPS), for enhancing UAVs navigation reliability. Lastly, the use of cellular-connected UAVs is a cost-effective solution, as it capitalizes on the existing worldwide network of cellular base stations, obviating the need for dedicated UASs infrastructure. As a result, cellular-connected UAVs are poised to benefit both the

UAVs and cellular industries, presenting promising business opportunities for exploration in the future.

On the other hand, the second paradigm, UAV-assisted wireless communications, is more possible and easier to install compact base stations or relays on UAVs, due to the ongoing reduction in manufacturing costs of UAVs and the shrinking size of communication equipment. This represents a significant improvement over traditional terrestrial communication systems, where stationary base stations or relays are typically fixed in place. UAV-supported communications offer several key advantages.

Firstly, UAV-mounted base stations and relays can be rapidly deployed as needed. This feature is particularly advantageous in scenarios such as temporary or unexpected events, emergency response, and search and rescue operations. Secondly, owing to their elevated position above the ground, UAV-based base stations and relays are more likely to establish LoS connections with ground users compared to their terrestrial counterparts. This results in more reliable communication links, as well as improved multiuser scheduling and resource allocation. Thirdly, thanks to the controllable high mobility of UAVs, UAV-based base stations and relays have an added degree of freedom in enhancing communication performance. They can dynamically adjust their positions in three-dimensional space to accommodate the communication needs of terrestrial networks.

From two paradigms, UAV applications that use mobile network connections have significant potential and they are poised for widespread development and utilization.

2. 5G OVERVIEW

This chapter introduces an overview of 5G technology, which contains its use cases, its development, and new technology suitable for cellular-connected UAVs.

2.1 Use cases of 5G

5G or fifth generation of wireless cellular technology, which is a significant advancement in telecommunications that offers a range of improvements over its predecessor, 4G LTE (long-term evolution). 5G builds on earlier generations (1G to 4G LTE), but it differs in several ways. It is designed for a wider range of applications than before: not only consumer applications such as voice, video and data but industrial applications such as machine-type communications [7]. As a result, a number of these applications require a peak data rate of several gigabits per second, others require latency as low as milliseconds, while others require a battery life of several years.

The 3GPP study [8] grouped use cases of 5G into five families that share common requirements and characteristics. The first three were also identified by the International Telecommunication Union (ITU) [9], which are:

- **Enhanced Mobile Broadband (eMBB)**, which calls for a higher data rate than LTE can provide. This service also provides a more uniform experience with low-latency communications over the extreme coverage area, and impressive performance as the number of users increases in terms of the peak data rate in ideal conditions, the expected data rate in more typical conditions, and the minimum in conditions of poor network coverage.
- **Massive machine-type communication (MTC)**, also known as the Internet of Things (IoT). These phrases both relate to wireless communications between autonomous machine-type devices that do not involve any direct human intervention.
- **Ultra-reliable Low-latency Communication (URLLC)**, also known as critical communication (CriC). This generic 5G service provides ultra-reliable low-latency communication links for network services with extreme requirements on availability, latency, and reliability, e.g., V2X communication and industrial manufacturing applications as shown below.

The last two have been separated out from those above by 3GPP:

- **Vehicle-to-everything Communication** refers to the exchange of information between a road vehicle and the mobile telecommunication network, and with other vehicles and pedestrians that are nearby. It is an aspect of URLLC. In recent years, LTE and LTE-Advanced Pro have offered more advantages for vehicle communications, such as a higher transmission and a lower level of interference, than using unlicensed spectrum, for example, some variants of Wi-Fi. However, these cellular communications were limited by LTE’s capabilities for data rate, latency, and reliability, which have been improved by 5G.

- **Network Operation (NEO)**, which requires optimizing and rerouting the traffic path in the case of low-latency applications, to interact with a client’s application servers and to re-configure a network to support new use cases as they arise.

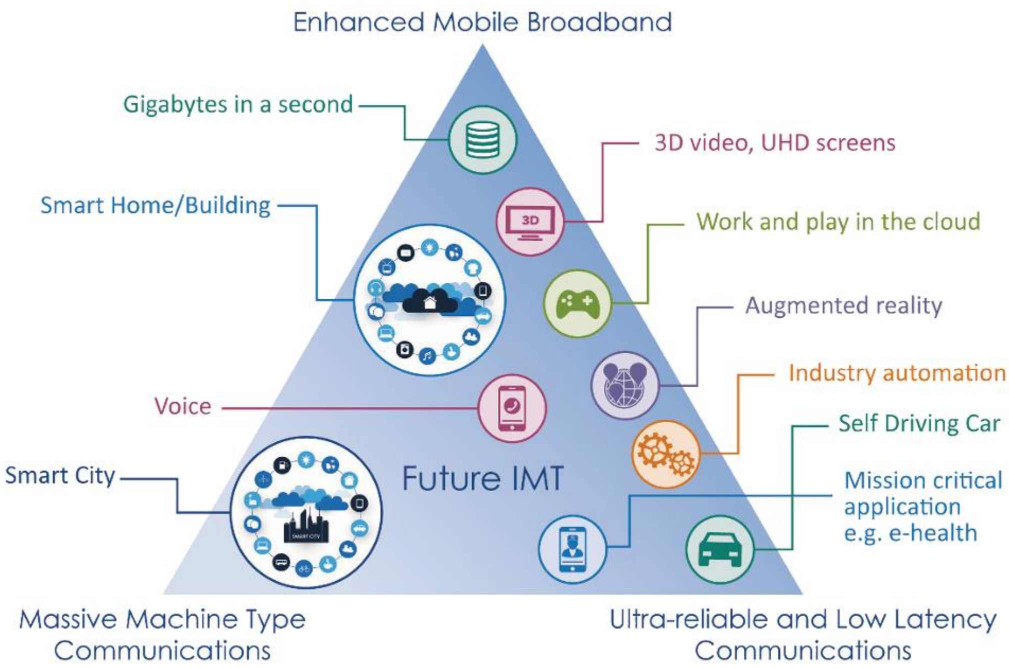

Fig.2.1 5G usage scenarios [10]

2.2 The development of 5G

The first three generations of mobile communication systems: the analog communication system 1G, Global System for Mobile Communications (GSM) 2G, and Universal Mobile Telecommunication System (UMTS) 3G have mostly concentrated on voice, instant messaging and the delivery of packet data in limited data rate by the means of the General Packet Radio Service (GPRS) and Enhanced Data Rates for GSM Evolution (EDGE) from 2G and from 3G with enhancement high-speed packet access (HSPA). Hence, voice calls were mostly handled by mobile telecommunication networks for a long time. The amount of mobile data grew slowly at first, but it overtook the amount of voice traffic in the 2010s [7] with the introduction of smartphones, notably the Apple iPhone in 2007, followed by devices based on Google’s Android operating system from 2008. With the expected increase in traffic, mobile networks will continue to be dominated by data, particularly video downloads.

To illustrate that issue, Fig. 2.2 shows the total traffic being handed in mobile telecommunication networks throughout the world, in units of exabytes ([EB] 10^{18} bytes, i.e., one billion gigabytes) per month. This figure shows that total global mobile data traffic – excluding traffic generated by Fixed Wireless Access (FWA) – reached 93 EB per month at the end of 2022 and is projected to grow by a factor of 3.5 to reach 329 EB per month in 2028. In 2027, all mobile data traffic growth will come from 5G, as 4G traffic declines. 5G's share of mobile data traffic was 15 percent at the end of 2022, an increase from 9% at the end of 2021. This share is forecast to grow to 66 percent in 2028.

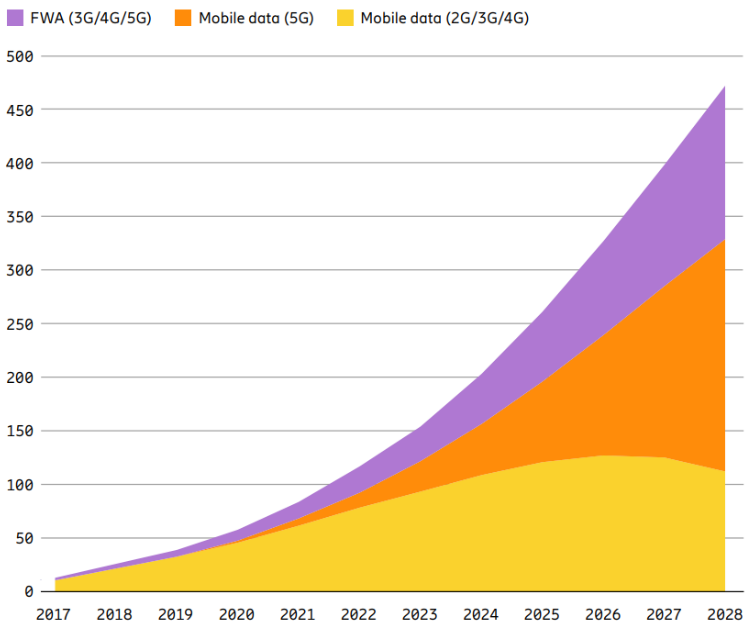

Fig.2.2 Global mobile network data traffic (EB per month) [11]

Around the world, about 240 service providers have now launched commercial 5G services, and around 35 have deployed or launched 5G standalone (SA) [12]. Owing to its substantial potential across a diverse array of applications, the emergence of 5G technology has garnered significant attention from industries and prompted serious investments in both developed and developing countries. Although traffic levels are continuing to grow, developed markets have become saturated with smartphones, and sales have begun to stall. To illustrate that, Fig. 2.3 shows Ericsson's measurements and forecasts of the number of mobile subscriptions worldwide. The most common 5G services launched by service providers for consumers are enhanced mobile broadband (eMBB), Fixed Wireless Access (FWA), gaming, and some AR/VR-based services. 5G subscriptions are forecast to reach 1.5 billion in 2023 and 9.1 billion in 2028.

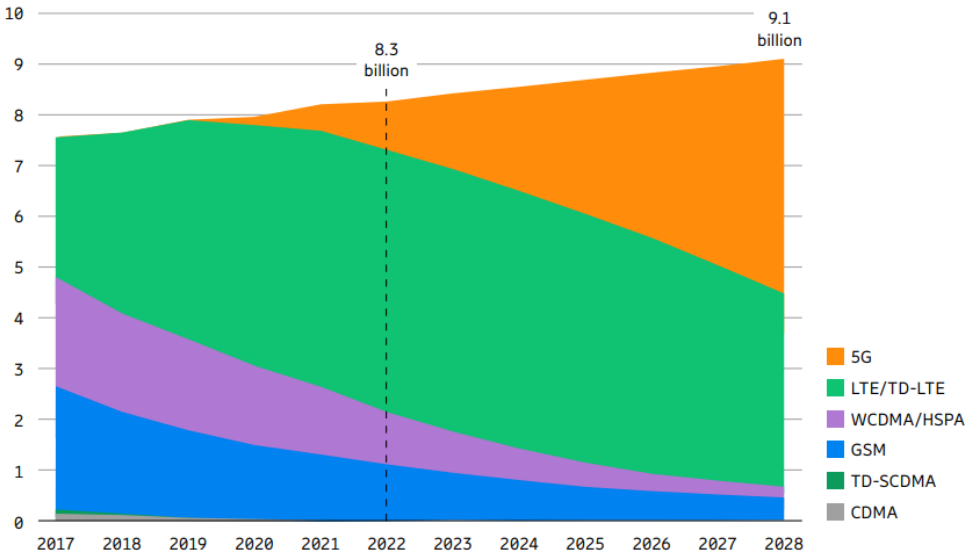

Fig.2.3 Mobile subscription by technology (billion) [11]

Although subscribers have also been making greater use of free Wi-Fi access and of third-party services for voice and messaging, which reduced network operators' revenue per bit, the 5G technology is still expected to have nearly exponential market growth in the next 8 years. In particular, the global 5G infrastructure market size was estimated at USD 5.82 billion in 2021 and is expected to hit around USD 98.57 billion by 2030 [13] , as shown in Fig. 2.4.

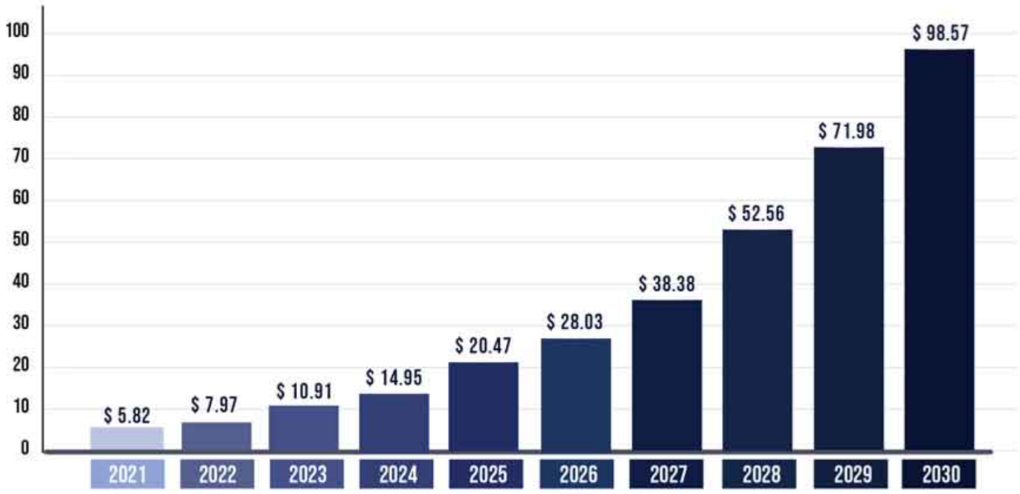

Fig.2.4 5G infrastructure market size, 2021 to 2030 [13]

2.3 New technologies in 5G

This section highlights the fundamental technologies within 5G networks. Moreover, the enhanced features of the 5G network's air interface make it well-suited for communication with UAVs.

2.3.1 Network Function Virtualization (NFV)

The core network of a mobile telecommunication system comprises a multitude of network elements, such as routers, signaling functions, and databases. Introducing new services frequently necessitates the incorporation of intricate, service-specific hardware, involving expensive design processes and entailing prolonged time-to-market. Furthermore, the ever-accelerating pace of technological and service innovations results in shorter hardware life cycles.

At the end of 2012, network operators started an initiative on Network Function Virtualization (NFV) [14]. In NFV, network elements are realized through software in the shape of virtualized network functions (VNFs). These VNFs may comprise one or more virtual machines, each running distinct software and processes, designed to replace custom hardware appliances, as presented in Fig. 2.5. Typically, a series of VNFs is employed sequentially to deliver valuable services to customers. NFV necessitates the presence of an orchestration framework that facilitates the proper instantiation, monitoring, and operation of both VNFs and Network Functions (NFs) like modulation, coding, multiple access, ciphering, and others.

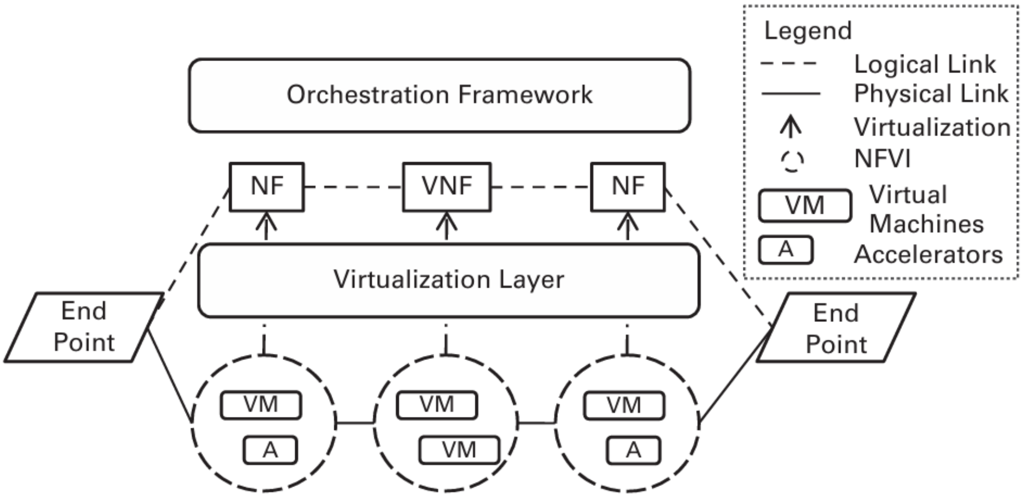

Fig.2.5 NFV framework [15]

NFV offers numerous advantages: the hardware is cost-effective and versatile; software development and upgrades are more straightforward, quicker, and cost-efficient; there is the potential to decouple software and hardware, allowing separate procurement from different vendors; and it becomes more accessible for new vendors to enter the market. Network operators in all the world were already adopting these techniques in their existing networks [16].

2.3.2 Software Defined Networking (SDN)

In addition to NFV, SDN is another important enabler for 5G future networks.

Software-defined networking (SDN) is an emerging paradigm, which breaks the vertical integration in traditional networks to provide the flexibility to program the network through (logical) centralized network control [16], as shown in Fig.2.6. SDN possesses the capacity to dynamically adjust its network parameters in response to its operating environment. The modular design of SDN presents an effective approach for enhancing network management by offering greater flexibility and simplicity. Within SDN, the centralized and cost-efficient architecture offers enhanced network visibility, enabling efficient resource utilization and superior performance. As smart programmable devices become more prevalent in the network landscape, SDN contributes to bolstering network security, improving energy efficiency, and enabling network virtualization, thereby enhancing overall network performance.

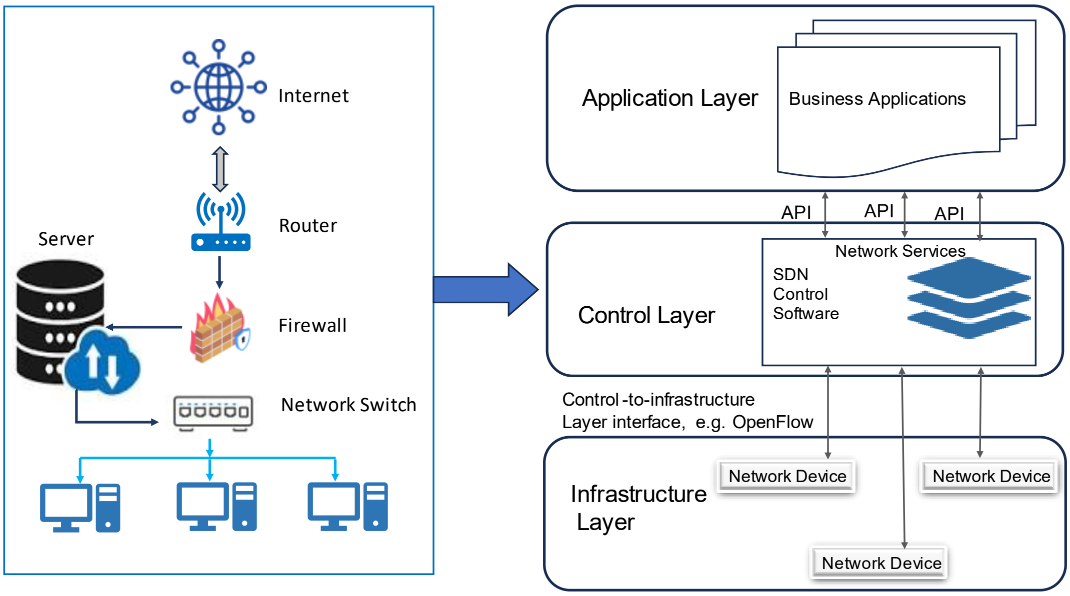

Fig.2.6 Comparison of the traditional network architecture and the simplified software-defined network (SDN) architecture, adapted from [15] and [17]

To summarize, NFV and SDN are complementary technologies: the first separates the hardware and software in a communication network, while the second separates its control and user planes.

2.3.3 Network Slicing

Network slicing is a key architectural feature in 5G that enables the creation of multiple virtual and independent networks on a shared physical infrastructure. They are virtual logical sub-networks which run on shared, underlying physical hardware, and which are realized by means of NFV and SDN [18], [19]. It allows network operators to divide their network resources into distinct, isolated, and customizable slices to better meet the diverse and specific requirements of different use cases, services, and applications. Each network slice is designed to cater to the unique needs of a particular set of users or applications. In other words, each network slice is optimized for the traffic that it carries, and isolated from each other due to data transport and security. In every main use case of 5G, with eMBB, MTC, and URLLC slices respectively optimized for a high data rate, a high connection density, low latency, and high reliability.

2.3.4 Technologies for the Air Interface

A primary demand in the realm of 5G is to facilitate a capacity expansion that is a thousandfold greater per unit area when contrasted with the prevailing LTE technology. This must be accomplished while maintaining a comparable cost structure and energy consumption per unit area as is observed in current cellular systems. Moreover, achieving this heightened capacity hinges on enhancing all three factors that collectively influence the system's capacity: More spectrum, a larger number of base stations per area, and an increased spectral efficiency per cell.

There are two important technologies: *millimeter waves* and *multiple antennas* [6], which are considered essential in contributing to the last stated factor. The former helps 5G be able to occupy a far wider bandwidth than it does at low radio frequencies, so its capacity can be far greater. It encompasses frequencies between approximately 30 GHz and 300 GHz, with bands typically falling within the range of 24 GHz to 100 GHz being the most relevant for 5G deployment.

The second one improves the coverage of the air interface at high radio frequencies through *beamforming* and improves its capacity at low radio frequencies through *massive multiple-input multiple-output* (massive MIMO) antennas.

2.4 Private 5G network at UNOB

The University of Defence, Brno, Czech Republic is launching a private standalone (SA) 5G network, supplied by the T-Mobile operator. The entire 5G SA technology is from Ericsson and runs on C-band frequencies. The installation covers both selected UNOB classrooms, and outdoor areas, which are planned by UNOB's decision. The main goal of this private network is to verify the contribution of 5G technology to applications of unmanned flying systems and unmanned ground systems, focusing on various areas such as control, data collection for decision-making, positioning, etc. The signal covers selected classrooms and specialized laboratories, areas between buildings to test outdoor UAV with a rare 64×64 antenna, and one of the facilities will house the 5G network core and antenna for network testing [20]. Fig.2.7 shows the private 5G SA network setup at UNOB. The blue lines indicate optical links. All information regarding the types of antennas and the positions of the 5G installations is presented in the figure below.

Fig.2.7 Private 5G SA network setup at UNOB, blue lines are illustrated for optical links, edited from mapy.cz

Interconnecting all eNodes is achieved through optical cables. Furthermore, the Ericsson Radio Dot Systems, designed to cater to a broader spectrum of indoor environments, establish connections to the Ericsson IRU 8846 communication board via CAT 6A Ethernet cables.

Fig.2.8 Ericsson AIR 6419 antenna.

For instance, the antenna used for the 5G NR node, Ericsson AIR 6419, is a lightweight Antenna Integrated Radio unit specifically designed for 5G mid-band TDD. Featuring 64 transmitters, 64 receivers, 192 antenna elements, a total carrier bandwidth of 200 MHz, and an impressive output power of up to 320 W, the AIR 6419 stands out as an Advanced Antenna System (AAS) for Massive MIMO. This powerful single antenna option empowers service providers to deliver a comprehensive 5G experience and enhanced capacity within a compact footprint. This antenna will play a vital role in all of this project's next tests.

3. RELATED WORKS

Recently, different studies for UAV communication using commercial 5G stand-alone (SA) and non-stand-alone (NSA) are mentioned. In support of this project's research goals, the thesis exclusively concentrates on initiatives associated with cellular network applications for UAVs (particularly in LTE-A and 5G), as well as security methodologies and remedies tailored to this type of connectivity. These studies can be categorized based on generations of cellular technologies.

3.1 Field experiments with 2G and 3G networks

The integration of mobile network connections in UAVs communication has evolved over the last two decades, involving the utilization of 2G and 3G networks.

Wzorek M et al. [21] developed a prototype network, which was created between two UAVs and a ground operator using GPRS technology. A graphical user interface (GUI) for a Sony Ericsson P900 mobile device provides the ground operator with a portable control interface for a UAV and its camera. Therefore, the GCS receives telemetry data (e.g. position, altitude, state, etc.) from the UAV in addition to an image stream from the camera. Based on the flight test, it was concluded that GSM network infrastructures can provide a useful means as a complementary communication channel for UAVs.

Daniel K. et al. [22] presented a coverage analysis for GSM networks for altitudes up to 500 m based on aerial Reference Signal Strength Indicator (RSSI) measurements. They gave evidence of available Radio frequency (RF) coverage in heights up to 500 m and the decent of the signal strengths with the altitude for urban and rural terrains.

In the work of F. Gonzalez et al. [23], these authors conducted the tests with an aircraft and connections with different cell towers in the UMTS network. Their aircraft is always in good condition of LoS to several transmission towers. Although there were not any optimized pointing angles for ground users from base station (BS) antenna orientations, the recorded results for the airborne environment were better than those recorded on the ground. Additionally, the measurement results showed good connections for the UAV altitude up to about 8500 ft (2590 m), beyond which the connection was lost. The maximum communication range was also observed to be 70 km from a single cell station. The average received power levels of the aerial users are 21% stronger than those on the ground, with latency in the order of 500 ms. Based on such results, the authors concluded that the 3G UMTS network could provide a possible solution for non-safety-critical communications for aerial users with moderate speed and altitude (below 4000 ft or 1220 m).

3.2 UAVs communications tests in 4G networks

Although there was limited research on UAVs supported by 2G/3G networks, the enthusiasm for utilizing 4G LTE and 5G networks to support UAVs has surged in recent years, both within academic circles and the industry field. In the below part of this section, this thesis aims to show the most relevant studies in 4G, LTE-A networks for UAVs communications.

In the master's thesis [24], Lassi Sundqvist explored the use of LTE for controlling multi-copter UAVs, focusing on field measurements. The study specifically measured the Reference Signal Received Power (RSRP) and Reference Signal Received Quality (RSRQ) for an LTE-connected UAV that ascended to a maximum altitude of 74 m, with a building positioned between the UAV's starting location and the BS. The findings indicated that RSRP initially rises and then falls with increasing altitude, peaking at around 34 m. Conversely, RSRQ showed a consistent decrease as altitude increased. This trend is attributed to the rise in interference, which becomes more significant than the improvement in RSRP at higher altitudes.

In [25], S.J. Maeng et al. analyzed the channel propagation of air-to-ground LTE links using an experimental dataset of raw LTE I/Q (in-phase/ quadrature-phase) samples at 3.51 GHz. To solve this issue, they introduced their own software AERID, which defined radio (SDR) base I/Q measurement and analysis framework for wireless signals, especially RSRP information for aerial experimentation. Additionally, the research reveals that an increase in 3D distances leads to a reduction in coherence bandwidth. This phenomenon is attributed to the heightened impact of ground reflection at greater distances.

Gharib et al. [26] performed an analysis in rural areas, examining the communication attributes between an aerial UAV and a commercial LTE network in Arizona, USA. Their findings indicated that rural areas exhibit better signal quality and reduced handover processes during low-elevation flights. Additionally, they observed a marginal decline in the performance of the 4G network with an increase in UAV velocity.

Afonso L. et al. [27] conducted flight tests with UAV altitudes varying from 10 m to 100 m to compare the latency performance of cellular-supported UAVs with three different technologies: EDGE, HSPA+, and 4G LTE. It was revealed that LTE achieved the best performance in terms of latency and jitter, with round-trip time (RTT) of 127 ms and a standard deviation of 48 ms for the worst-case scenario, and EDGE had the worst performance. Such results demonstrated the feasibility of (semi-)autonomous UAV operations over LTE network with low altitude (up to 100 m).

Amorim et al. [28] tried to find models for path loss exponents and shadowing for the radio channel between UAVs and 4G cellular networks (800 MHz frequency band). By employing a radio network LTE scanner mounted on UAV, these researchers captured RSRP and distance data at various points in 3D space, enabling the calculation of path loss samples at each location. Their results showed that path loss exponent decreases as the UAV moves up, approximating free space propagation for horizontal ranges up to tens of kilometers at UAV heights around 100 m.

In very similar topic [29], Amorim et al. analyze the end-to-end latency measured in a client-server application that emulates the traffic requirements for the UAV's and C2 link. The connectivity is provided by two real LTE-A networks to a client attached to a flying UAV. Measurements are performed at 4 different heights: ground level, 15 m, 40 m and100 m. In single operator scenarios, the reliability measured at the target latency, 50 ms, was between 99.6 % and 97.6 % in downlink, and 91.3% and 99.4% in uplink. These results are below the 99.9 % target reliability defined for UAVs and they show that several consecutive packets can be missed when the radio link connectivity degrades, leading to high (> 1 s) values for the 99.9% reliability of latency. Meanwhile, Xingqin Lin et al. in the study [30] presented field measurements conducted in a real commercial LTE network in Finland, demonstrating the suitability of terrestrial networks for connected UAVs at an altitude of 50 m and 150 m. Simulations were based on the latest 3GPP developments, including channel models, traffic models, antenna models, and network scenarios. The findings suggest that existing LTE networks designed for terrestrial use could support the initial deployment of low-altitude UAVs, although challenges related to interference and mobility may arise.

One of the biggest multinational semiconductor and telecommunications equipment company in the world – Qualcomm, in May 2017, published a report of their studies about "LTE unmanned systems" [31]. In this report, it was found that although the BS antennas are down tilted towards the ground, satisfactory signal coverage can still be achieved for altitude up to 400 ft (122 m) in the studied test. This result reinforced the study in [32] that, when the UAV moves higher, then number of detectable BSs increases too. However, in study [32] the SINR (Signal to Interference & Noise Ratio) of the best cell for the aerial user at the measured altitude of 150 m or 300 m is much lower than that of ground user.

3.3 State of the art in 5G networks

In recent years, numerous studies have emerged, focusing on the integration and implications of 5G UAVs connectivity. These studies play a crucial role in delving into the diverse ways in which 5G connections can enhance UAVs' capabilities. From optimizing real-time data transmission to refining control mechanisms, these investigations collectively illuminate the promising future that unfolds at the crossroads of 5G technology and UAVs innovation.

Bor-Yaliniz et al. [33] performed an analysis to determine if commercial 5G networks should be used to support UAVs. They found that there is no simple way to determine how best to utilize UAVs with 5G networks. However, by comparing a large number of 5G design options, like relaying and Cloud - Radio Access Network (C-RAN), they concluded that 5G slicing and modularity are network elements that provide flexibility to be utilized to support UAVs on the networks. They, however, performed no flight testing of 5G networks.

An early instance of 5G UAV flight testing is provided by Festaget et al. [34]. They performed long distance flight testing over a 7km course at a height of 100m, analyzing end-to-end latency. They concluded that cellular communication between UAVs and 5G base stations meets the demands for video streaming in principle, even when the network has not been optimized for aerial users. They also state that network slicing abilities in 5G networks have the potential to improve network performance further.

J. Sae et al. [35] considered an alternative to traditional drive testing, by conducting flight tests using an established, commercial grade 5G test network. They were able to calculate 4G and 5G radiation patterns within the 3D space. This led them to conclude that UAV flight testing with a smartphone as the measurement device is a reasonable alternative to drive testing for the purposes of evaluating the coverage capabilities of a given 5G network.

In the work conducted by Raheeb Muzaffar [36], practical experiments are developed using a commercial 5G base in Feichtendorf, Austria, where Magenta operates a 5G BSs, with a UAV performing flights at different heights using a mobile android tool for recording measurements. As general results, it is possible to observe that communication using 5G cannot be maintained during the entire flight time and oscillation for the 4G network [37] are frequent as there is an increase in altitude. This paper presented a study aimed at practical experiments involving 5G and UAVs, which generated very good results, and which should certainly be taken into account in any study aimed at both technologies.

Raouf et al. [38] performs network power measurements using UAV flight testing, allowing for comparison of aerial coverage between 4G LTE and commercial 5G low-mid band networks. Using the NSF AERPAW measurement platform in Raleigh NC, Raouf et al. performed flights at 140m and 180m for the urban and rural sites, respectively. They found that generally the measured signal power increases as UAV altitude increases, due to the better line-of-sight characteristics at high altitudes. They also found that the spectrum of down-link frequencies is significantly more crowded than the up-link spectrum in both environments.

To measure the coverage of 5G networks, Valentin P. et al. [39] employed Keysight's NEMO cell phones, which run Android application Nemo Handy to measure wireless diagnostics information of air interface and mobile application quality-of-service (QoS) and quality-of-experience (QoE). The measurement setup used a hexacopter, which mounts all the needed equipment.

In the latest work, Mohammed Grarib et al. [40] addresses the lack of performance evaluation studies for 5G-connected low-altitude UAV communication. Their paper comprehensively analyzes low-band and mid-band 5G network performance compared to LTE using real measurements from a commercial cellular network in a non-urban area. The study explores the impact of elevation and velocity on various key performance indicators (KPIs) such as RSRP, RSRQ, RSSNR, uplink throughput, and downlink throughput. Results show that increasing elevation generally degrades network performance, with mid-band 5G outperforming both low-band 5G and LTE in terms of throughput. The study concludes that mid-band 5G is a promising option for aerial communication.

Evaluating UAV communications in 2G and 3G networks appears relatively straightforward for assessing cellular network parameters and potential technological opportunities. For instance, in the study [21], the authors employed only the UDP protocol to measure latency, while in another study [20], a radiosonde connected to an embedded PC with ARM-7 CPU running on Linux OS, along with an altimeter for precise altitude measurement and GPS for geolocation, was used to measure only the RSSI parameter. However, with the advent of LTE-A and 5G, the utilization of mobile networks for UAV connections has expanded significantly, leading to a more comprehensive evaluation of network signal indicators.

Table 3.1 An overview of Related Works

Related Work	**LTE**	**5G**	**RSRP**	**SINR**	**RSRQ**	**Speed**	**Height.**	**Throughput**		**C/T[(a)]**	**Area[(b)]**	**Measurement Tools**
								UL	**DL**			
S. J. Maeng [25]	✓	×	✓	×	✓	✓	✓	×	×	T	R	KNO, QualiPoc, TEMS
Gharib et al. [26]	✓	×	✓	✓	✓	✓	✓	✓	✓	C	R	TEMS
Xingqin Lin et al. [30]	✓	×	✓	✓	×	✓	✓	✓	✓	C	S	TEMS
Sundqvist [24]	✓	×	✓	×	✓	×	✓	×	×	T	U	Nemo Handy (Keysight app)
J. Sae et al. [35]	✓	✓	✓	×	✓	✓	✓	✓	✓	T	S	MediaTek, QualiPoc
Festaget et al. [34]	✓	✓	✓	✓	×	✓	✓	✓	✓	T	S	ICMP echo, iPerf
Gharib M. et al. [40]	✓	✓	✓	✓	✓	✓	✓	✓	✓	C	S	RFInsights
Muzaff R. et al. [36]	✓	✓	✓	✓	×	×	✓	✓	✓	C	R	Wistron NeWeb NSA mobile test
Raouf A. F. et al. [38]	✓	✓	✓	×	×	×	✓	✓	✓	C	U, R	USRP & PyScript
Valentin P. et al. [39]	✓	✓	✓	×	×	✓	✓	×	×	C	R	Keysight's NEMO cell phones
This work	✓	✓	✓	✓	✓	✓	✓	✓	✓	T	U	ICMP echo, iPerf, PyScript

a) C/T: Commercial network versus testbed measurement
b) R: Rural, S: Suburban, U: Urban

Distinguishing itself from previous related works, this study focuses on the examination of a private 5G SA network provided by a commercial operator in the urban area. The forthcoming section details tests that evaluate specific and general mobile network parameters. The project leverages the capabilities of the hardware and software discussed in the subsequent section. Although the experiment's object is the private 5G SA network, the testbed setup employing the recommended hardware and software can be used for both test 4G LTE, 5G SA and 5G NSA.

4. CONCEPTUAL DESIGN OF THE TESTBED SETUP

One of the primary objectives of the master's thesis is to formulate a conceptual design for the test setup, encompassing coverage measurement and performance evaluation of the private 5G network at the University of Defence in Brno, Czech Republic. Given that the intended deployment of the setup is on a UAV, a key imperative for the implemented test is maximum portability and autonomy, facilitating continuous measurements while affixed to the UAV.

Fig. 4.1 illustrates the fundamental conceptual design of the testbed setup. The overarching framework of the testbed revolves around two available 5G modules – one installed on the UAV and another in the ground control station (GCS). Both modules function as cellular modem slave devices, designed to be orchestrated by a master processing unit. In this configuration, two NVIDIA Jetson AGX Orin Developer Kits serve as the master processing units, responsible for executing all data gathering and control functions within the testbed setup. When evaluating the coverage of the 5G base station in the next chapters, the GNSS module on the UAV transmits GPS data to the flight controller. Subsequently, this data is relayed to the single-board computer (SBC) for additional processing, specifically within the position tracking unit. Additionally, the 5G modules utilized in this study also independently support localization technology (as detailed in Section 4.1.3).

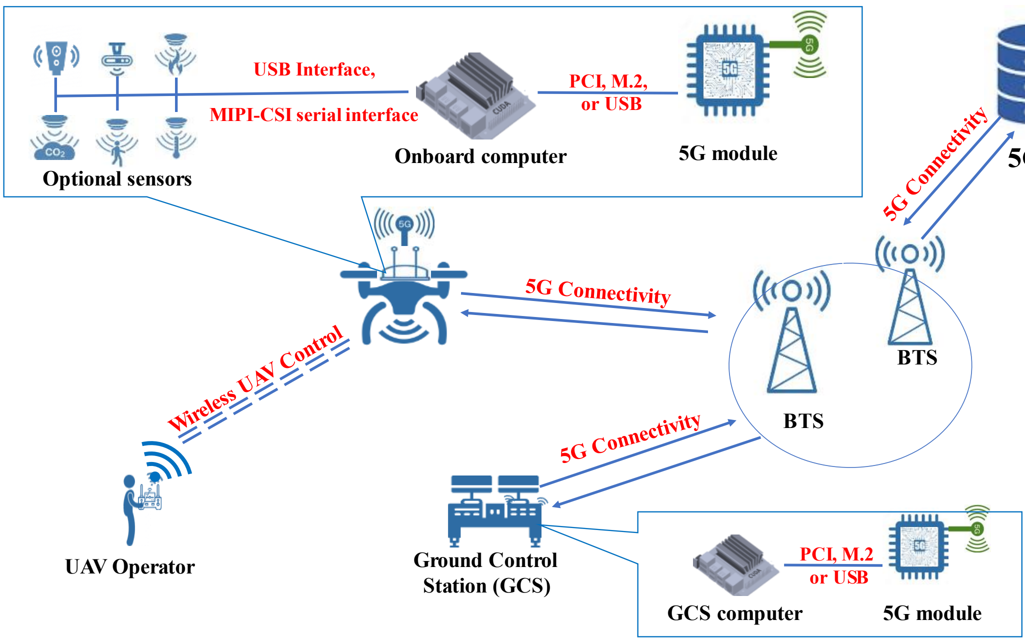

Fig.4.1 Basic conceptual design for the testbed setup

The entire experimental configuration on both the UAV and GCS necessitates a power supply primarily for the master processing unit. Utilizing the SBC provides the flexibility to connect a wide array of sensors, cameras, or other supplementary peripheral devices to enhance data collection and subsequent processing. This data can be uploaded to the server on the GCS or streamed live over the established 5G connection. The variety and quantity of additional devices only depend on the available physical connectors of the SBC. Mounted on the independently controlled UAV, the testbed demonstrates autonomous functionality, capable of conducting all essential measurements, cellular transmissions, and logging operations.

4.1 Hardware on the board

Considering the vast amount and diversity of available UAV models, it is worth mentioning the actual characteristics of the UAV used for this project. The selected UAV belongs to the Vertical Take-Off and Landing (VTOL) category, commonly recognized as a multirotor UAV. In the experiments described in this work, a quadcopter model is used (as shown in Fig. 4.2), equipped with a remote control operating in the 2.4 GHz band, a GPS receiver, a flight controller CubePilot Cube Orange and a SBC with external optional sensors. The SBC creates cellular communication in the private 5G SA network, which is used to communicate with a ground station or with other UAVs.

In addition to the primary components employed in this work for the 5G-connected UAV, consisting of a SBC – NVIDIA Jetson Orin AGX Developer Kit with a 5G module and a flight controller, there are essential components that are obligatory for every UAV, including:

- **Electronic Speed Controller (ESC)** supplies power to motors and individually regulates their speed through a Pulse Width Modulation (PWM) signal. The flight controller generates the required signal to modulate the motor speed.
- **Telemetry** and the **remote control** provide communication between the UAV and UAV operator on the ground.
- **Brushless DC motors** rotate the propellers and thus create thrust.
- **Li-Po battery** and **power module** deliver and transmit power to the flight controller, ESCs and all other electrical components.
- **A safety switch** that requires manual activation by the pilot to prevent any unintentional takeoff.
- An optional **buzzer** to provide feedback about the current state of the UAV.

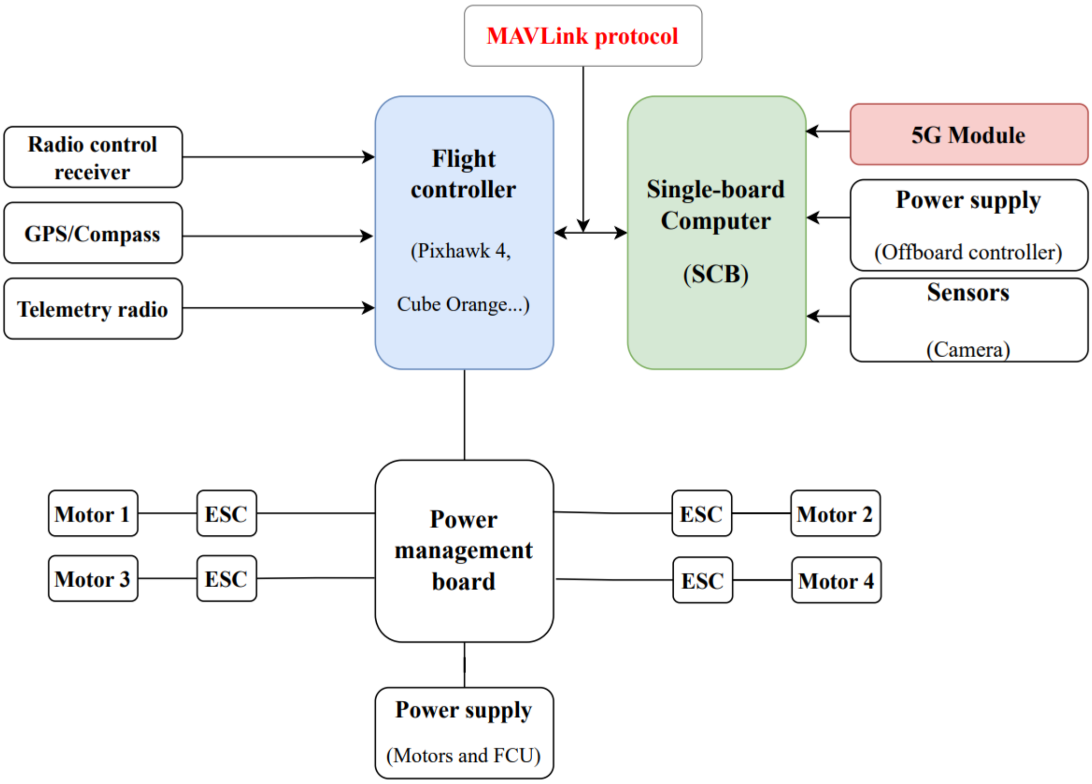

Fig.4.2 Basic hardware architecture of the 5G quadcopter UAV, adapted from [41]

The below sections emphasize and clarify the characteristics of primary hardware components.

4.1.1 Flight Controller: CubePilot Cube Orange

The CubePilot Cube Orange, as presented in Fig.4.3, stands out as the most advanced autopilot designed for open autonomous unmanned vehicles globally. Equipping with a high performance H7 processor, it incorporates a Cortex M7 with a double-precision (DP) FPU, 400 MHz c, a Cortex M4 running at 200 MHz, 2 MB of flash memory, and 1 MB of RAM. This dual core architecture provides high performance and stable solutions for flight. Additionally, ArduPilot firmware and PX4 fully support this flight controller.

Utilizing CubePilot Cube Orange offers several benefits. Firstly, the data from different sensors is gathered within the storage of flight controller for further process. In addition, MAVLink communication (as detailed in Section 4.2.2) allows connection between this flight controller and the master processing – SBC. In simpler terms, the SBC can engage in tasks such as reading and writing data, stabilization, and low-level control of the UAV through the flight controller.

Fig.4.3 Flight Controller: CubePilot Cube Orange

4.1.2 SBC: NVIDIA Jetson AGX Orin Developer Kit

The processing device is designed to execute the entire data collection process from diverse sources. Its functions encompass effectively utilizing the 5G module as a modem and ensuring sufficient memory space with a suitable read and write speed to accommodate the close to 1 Gbps data throughput offered by the 5G network at the University of Defence. The two NVIDIA Jetson AGX Orin Developer Kits on the UAV and GCS are installed with the Linux OS with supported NVIDIA manufacturer's Jetpack.

Fig.4.4 NVIDIA Jetson AGX Orin Developer Kit [42]

Powered either by a dedicated compact battery or drawing power from the shared current managed by the UAV's power management board, this developer kit serves as a potent and exceptionally portable processing master device. It provides extensive capabilities, offering scalable flash disk memory in the order of gigabytes for diverse data

Table 4.1 NVIDIA Jetson AGX Orin Developer Kit Technical Specifications [42]

JETSON AGX ORIN MODULE	
AI Performance	275 TOPs
GPU	NVIDIA Ampere architecture with 2048 NVIDIA® CUDA® cores and 64 tensor cores
CPU	12-core Arm Cortex-A78AE v8.2 64-bit CPU 3MB L2 + 6MB L3
DL Accelerator	2x NVDLA v2.0
Vision Accelerator	PVA v2.0
Memory	32GB/64GB 256-bit LPDDR5 204.8 GB/s
Storage	64GB eMMC 5.1
Video Encode	2x 4K60 | 4x 4K30 | 8x 1080p60 | 16x 1080p30 (H.265)
Video Decode	1x 8K30 | 3x 4K60 | 7x 4K30 | 11x 1080p60 | 22x 1080p30 (H.265)
REFERENCE CARRIER BOARD	
Camera	16 lane MIPI CSI-2 connector
PCIe	x16 PCIe slot supporting. x8 PCIe Gen4
M.2 Key	M x4 PCIe Gen
M.2 Key E	x1 PCIe Gen 4, USB 2.0, UART, I2S
USB	Type C: 2x USB 3.2 Gen2 with USB-PD support. Type A: 2x USB 3.2 Gen2, 2x USB 3.2 Gen1 Micro-B: USB 2.0
Networking	RJ45 (up to 10 GbE)
Display	DisplayPort 1.4a (+MST)
Others	40-pin header (I2C, GPIO, SPI, CAN, I2S, UART, DMIC) 12-pin automation header 10-pin audio panel header 10-pin JTAG header 4-pin fan header 2-pin RTC battery backup connector DC power jack Power, Force Recovery, and Reset buttons
Dimensions	110 mm x 110 mm x 71.65 mm (Height includes feet, carrier board, module, and thermal solution)

collection needs. The device supports various Ubuntu versions or Linux distributions based on Debian, delivering a range of services. Its versatility extends to accommodating different drivers, programs, applications, and scripts, making it a robust onboard and GCS computer capable of fulfilling all the primary functions of the testbed.

This computer platform is perfect for practical deep learning applications, transmission data in high rate and embedded systems. Additionally, it is the newest SBC developed by NVIDIA corporation, which provides eight times the performance of Jetson AGX Xavier with the same compact form factor and compatible pinouts, integrating NVIDIA Ampere architecture GPU, Arm Cortex-A78AE CPU, next-generation deep learning and vision accelerator, high-speed interface, faster memory bandwidth, and multi-mode sensor support, for supporting multiple concurrent AI application channels [42].

About the connection, the flight controller autopilot Pixhawk Cube Orange is interfaced with the NVIDIA Jetson AGX Orin Developer Kit through a UART connection, facilitating the transfer of MAVLink messages between the two devices. To ensure coherence among all data streams, the NVIDIA Jetson AGX Orin employs the Robot Operating System (ROS) for timestamp synchronization. Additionally, the MAVROS (MAVLink ROS) plugin can be utilized to convert MAVLink messages into ROS format, supporting diverse applications of the MAVLink protocol.

4.1.3 5G Modules

Since this project is focused on the implementation of the 5G testbed setup for a UAV, a vital requirement of key equipment is modern 5G supportive cellular modules. Over recent years, various companies have contributed to the development of a range of wireless modules and solutions for 5G cellular networks.

In this project, the author evaluates the functionality of two 5G modules that are utilized for measuring key 5G network parameters and other relevant applications. These modules are the SIM 8200EA-M2 manufactured by SIMCom and the 5G RM 502Q-EA by Quectel. Both modules are based on the same foundational technology, the Snapdragon X55 5G Modem-RF System by Qualcomm, and support 3GPP Release 15 for 5G technologies. This includes comprehensive support for the latest cellular technologies, spanning from standalone to non-standalone 5G NR. They also support 256QAM (Quadrature Amplitude Modulation) for both downlink and uplink, 4x4 MIMO layers for downlink, and 2x2 MIMO layers for uplink.

Additionally, the Quectel 5G module incorporates Qualcomm® IZat™ location technology Gen9C Lite in its GNSS receiver, enhancing its positioning capabilities to be quicker, more accurate, and more reliable. Conversely, the SIMCom module includes a port for a GNSS antenna that captures signals from multiple satellite systems including GPS, GLONASS, BeiDou, Galileo, and QZSS. The main characteristics of each module are detailed in Table 4.2 below.

Table 4.2 Key features of available modules

5G related parameters	SIM8200EA-M2	5G RM 502Q-EA
Form factor	M.2	M.2
Technology	5G NR SA/NSA 5G Sub-6GHz	5G NR SA/NSA 5G Sub-6GHz
Modulation	256QAM	256QAM
Spectrum	**Sub-6 GHz** DL 4X4 MIMO UL 2X2 MIMO	**Sub-6 GHz** DL 4X4 MIMO UL 2X2 MIMO
Transfer rate	**Sub-6G** DL: 4.0 Gbps UP: 500 Mbps	**SA Sub-6G** DL: 4.2Gbps UP: 450Mbps **NSA Sub-6G** DL: 5.0Gbps UP: 600/650Mbps
Supply voltage	3.135 – 4.4V. Typical 3.7V	3.135 – 4.4V. Typical 3.7V
Transmit power	23dBm	23 dBm ±2 dB
Idle mode	Available sleep mode (<5mA at supply voltage)	Available sleep mode 55 mA, USB 3.0 @Idle
Interfaces	SIM Card USB PCM I^2C Diversity Receiver	(U)SIM Card USB 2.0/3.0/3.1 PCIe Gen3
Other supported mode (DL/UL)	LTE (2 Gbps/200 Mbps) HSPA+ (42 Mbps/5.76 Mbps) GNSS	LTE (2 Gbps/200 Mbps) UMTS (42 Mbps/5.76 Mbps) GNSS
Operating temperature	Normal: -30°C to +70°C Extended: -40°C to +85°C	Normal: -30°C to +70°C Extended: -40°C to +85°C
Antennas	Cellular antenna x4 GNSS antenna x1	Cellular antenna x3 GNSS antenna x1
Driver support	Win7/Win8/Win10 Linux Android	Windows 7/8/8.1/10/11, Linux 2.6 - 6.3 Android 4.x - 13

A. Connection between the 5G modules and the NVIDIA SBC: M.2 or USB interface?

The 5G modules SIMCom SIM8200EA-M2 and Quectel RM502Q-EA, both 5G/LTE modems, utilize M.2 Type B connectors in the 2242 format. These modules, when used with a Hardware Attached on Top (HAT) or an expansion circuit board, require a nominal voltage of 3.7 V (ranging from a minimum of 3.125 V to a maximum of 4.4 V) and can draw currents up to 3 A for brief periods. The NVIDIA Jetson AGX Orin Developer Kit, however, lacks a compatible connector that meets these specifications. Additionally, the use of any 5G modems from manufacturers such as SIMCom, Quectel, or Telit involves not only power supply and network interfaces but also requires SIM card slots and antenna connectors. These features are not universally supported across all commercial developer kits, including those from Raspberry Pi, NVIDIA Kits, Intel NUC, etc.

The proposed solution, as illustrated in Fig.4.5, involves utilizing a carrier board equipped with an M.2 type B slot, a USIM or SIM card slot, its own power supply capable of delivering up to 3 A of current, antenna connectors, and a USB 3.0 connector to link the 5G modem board to a SBC. Additionally, this board will require thermal management solutions such as fans or heatsinks to dissipate heat effectively.

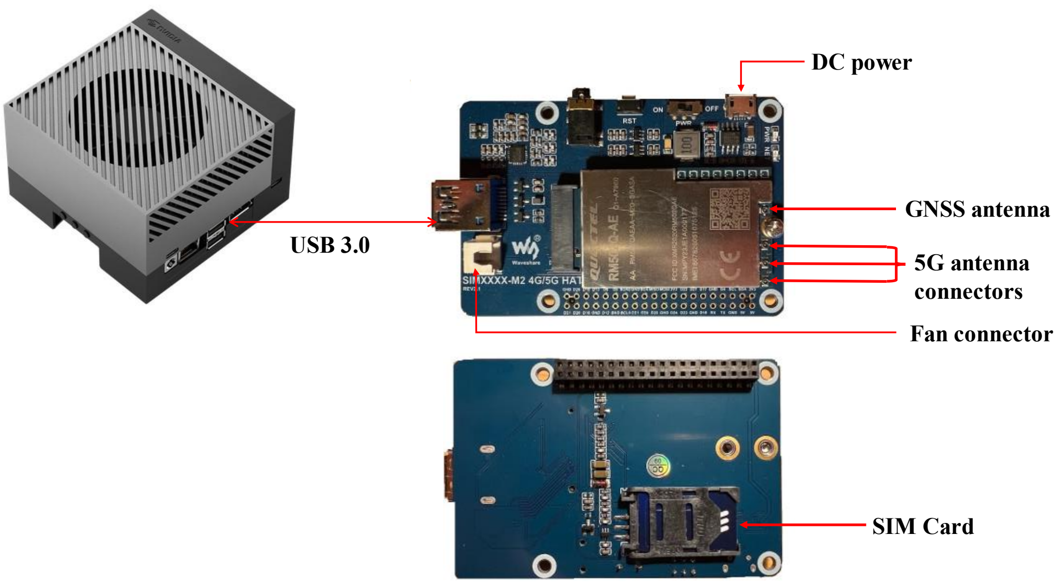

Fig.4.5 Proposal and confirmed connection between NVIDIA Jetson AGX Orin Developer Kit (left) and Quectel 5G RM502Q-EA module with its HAT (right).

The modules mentioned earlier, along with their corresponding development boards, function as fully subordinate cellular devices. They operate by responding to specific *AT - Commands* that are transmitted through the associated AT Serial port. Each 5G module is capable of supporting multiple virtual COM ports in Windows OS, or ttyUSB ports in Linux OS. These ports are all accessible via a single physical USB 3.0 connection.

B. Drivers 5G module for NVIDIA Jetson AGX Orin Developer Kit and other Kits

All NVIDIA Developer Kits operate on the NVIDIA JetPack SDK platform, which represents the most complete solution for developing AI applications. The JetPack SDK offers a comprehensive development environment tailored for AI development at the edge with hardware acceleration. It includes the Jetson Linux Driver Package, which encompasses a bootloader, Linux kernel, Ubuntu desktop environment, and a suite of libraries designed to enhance GPU computing, multimedia, graphics, and computer vision.

However, the JetPack SDK does not support drivers for all 5G modules. When unsupported, modifying the kernel source and compiling the necessary drivers become essential. In this study, the author primarily uses cellular modules equipped with Qualcomm chipsets that implement the Qualcomm MSM (QMI) interface. An open-source Linux in-kernel driver, known as *qmi_wwan*, supports this interface. This driver can be used in conjunction with ModemManager and NetworkManager to automate and manage connection establishment.

B.1. Driver for SIMCom SIM8200EA-M2

To assess the compatibility of the 5G connection, the author attempts to install drivers for this 5G module on both Windows 10 (PC) and Linux (Ubuntu 20.04 on NVIDIA Jetson AGX Orin Developer Kit). While the manufacturer provides a driver for Windows, there is no specific driver tailored for the Jetson AGX Orin, only a generic Linux driver. This is due to all versions of JetPack for Jetson AGX Orin not supporting this particular 5G SIMCom module – the support is limited to older versions of SIMCom modules.

To install and configure the driver on the Jetson AGX Orin and other NVIDIA Developer Kits, the following steps are taken:

- **Get the Kernel Source**: Download the kernel source from NVIDIA’s website, selecting the Jetson Linux version compatible with the NVIDIA product.
- **Modify and Install the Driver**: Install the Jetpack SDK driver package sources on a host PC running Linux and modify them to include the 5G module’s driver in the kernel.
- **Build the Kernel**: Compile the kernel on the host PC.
- **Update the Jetson Module**: Flash the newly built kernel from the host PC to the NVIDIA Jetson AGX Orin Developer Kit and run the newly compiled OS image on the NVIDIA Kit.

For Windows systems (up to Windows 10, with Windows 11 being less stable), the manufacturer provides a driver available on their official website. Once downloaded and executed, the auto-configuration generally completes successfully. However, despite these efforts, device managers or modem managers on both operating systems indicated that this module does not support 5G.

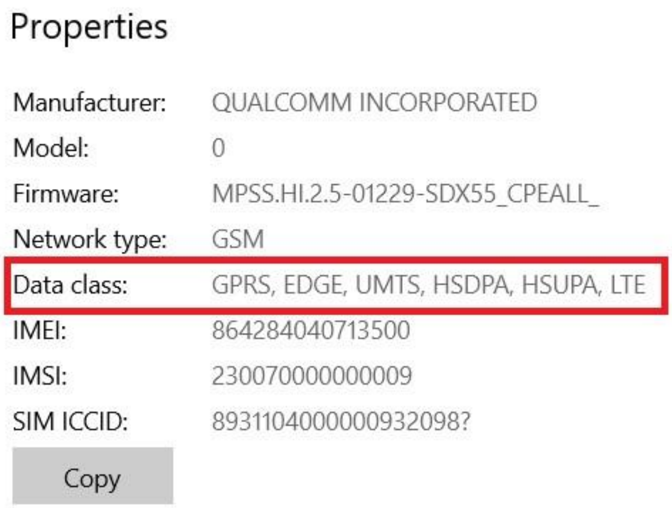

Fig.4.6 The data class of the SIM8200EA-M2 module shows that it does not support 5G

According to the specifications provided in the manual, the SIM8200-EA module is theoretically capable of supporting a range of Sub-6G SA mode frequencies, including n1, n2, n3, n5, n7, n8, n12, n20, n28, n38, n40, n41, n48, n66, n71, n77, and n78. This should enable it to operate on the private 5G UNOB network utilizing band n78. However, despite this theoretical compatibility, after installation of the necessary drivers, the SIM8200EA-M2 module's data class indicates that it supports only up to LTE, not 5G. Further testing on commercial 5G networks confirmed that this module does not function with 5G connectivity.

Subsequent chapters of this study will therefore focus solely on the capabilities of the Quectel RM502Q – EA modules, and all experiments will be conducted using these Quectel modules exclusively.

B.2. Driver for Quectel RM502Q-EA

During testing, the Quectel RM502Q-EA module demonstrated effective functionality with both commercial 5G networks and the UNOB private 5G network. Quectel provides a driver for Windows systems, supporting up to Windows 10, although it may operate on Windows 11 with less stability due to auto-configuration. For the NVIDIA Jetson AGX Orin Developer Kit, the driver comes pre-installed and does not require any modifications.

In Windows 10, after the initial installation of the USB driver needed to connect to the 5G module, it is essential to set up an additional driver, the USB MBIM driver. This driver is crucial for enabling the proper use of a USB 3.0 connection, which facilitates high-speed data traffic between the module and the PC. This setup is particularly important for 5G modems, as they are capable of higher data throughput. Typically, a USB connection to the modem defaults to being recognized as an Ethernet connection, operating at Ethernet speeds. Without the correct drivers, this default mode can act as a "bottleneck" in the data flow between the PC and the modem, thereby reducing the throughput achievable with 5G connectivity.

It is important to note that when switching between using Windows and Linux, the dial-up type of the Quectel RM500X needs to be configured using *AT commands*. This reconfiguration is necessary to ensure that the modem operates correctly across different operating systems and network setups.

```
AT+QCFG="usbnet",0 # driver type is NDIS(QMI); for Linux OS
AT+QCFG="usbnet",1 # driver type is ECM
AT+QCFG="usbnet",2 # driver type is MBIM; for Windows OS
AT+QCFG="usbnet",3 # driver type is RNDIS
AT+QCFG="usbnet",4 # driver type is NCM
```

After configuring all the necessary drivers and connecting the Quectel modem to the PC using a USB3.0 cable, the Device Manager in Windows should display all connected devices, including the Quectel modem and its associated port. This visibility in the Device Manager confirms that the modem is properly recognized and ready for use, ensuring it can operate at its full capacity for high-speed data transmission.

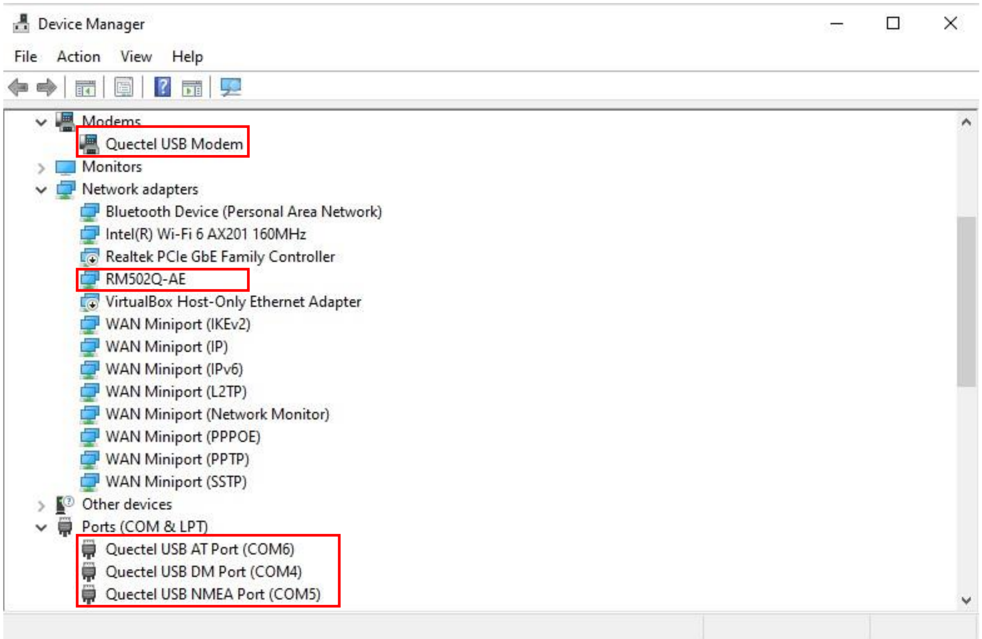

Fig.4.7 Windows Device Manager showing connected 5G module.

On the other hand, in Ubuntu 20.04 running NVIDIA Jetpack version 5.1.3, the NVIDIA Jetson AGX Orin Developer Kit fully supports the Quectel module. The *qmi_wwan* driver is already integrated into the kernel. When the modem is connected to the Jetson AGX Orin, after adjusting the dial-up type for the QMI driver, the configurations are automatically applied. To verify the success of the setup, you can use commands such as "*ifconfig*", "*usb-devices*", or inspect the output from the modem manager in the terminal of the Jetson AGX Orin. These tools provide detailed information about the connected devices and network interfaces, helping ensure that the modem is functioning correctly within the system.

```
/$ usb-devices

T:  Bus=02 Lev=02 Prnt=02 Port=00 Cnt=01 Dev#=  3 Spd=5000 MxCh= 0
D:  Ver= 3.20 Cls=00(>ifc ) Sub=00 Prot=00 MxPS= 9 #Cfgs=  1
P:  Vendor=2c7c ProdID=0800 Rev=04.14
S:  Manufacturer=Quectel
S:  Product=RM502Q-AE
S:  SerialNumber=63de9559
C:  #Ifs= 5 Cfg#= 1 Atr=a0 MxPwr=896mA
I:  If#= 0 Alt= 0 #EPs= 2 Cls=ff(vend.) Sub=ff Prot=30 Driver=option
I:  If#= 1 Alt= 0 #EPs= 3 Cls=ff(vend.) Sub=00 Prot=40 Driver=(none)
I:  If#= 2 Alt= 0 #EPs= 3 Cls=ff(vend.) Sub=00 Prot=00 Driver=option
I:  If#= 3 Alt= 0 #EPs= 3 Cls=ff(vend.) Sub=00 Prot=00 Driver=option
I:  If#= 4 Alt= 0 #EPs= 3 Cls=ff(vend.) Sub=ff Prot=ff Driver=qmi_wwan
/$ ifconfig
wwan0: flags=4305<UP,POINTOPOINT,RUNNING,NOARP,MULTICAST>  mtu 1500
        inet 172.16.0.7  netmask 255.255.255.240  destination 172.16.0.7
        unspec 00-00-00-00-00-00-00-00-00-00-00-00-00-00-00-00  txqueuelen 1000  (UNSPEC)
        RX packets 304749  bytes 12282038 (12.2 MB)
        RX errors 0  dropped 0  overruns 0  frame 0
        TX packets 2238948  bytes 3283548935 (3.2 GB)
        TX errors 7  dropped 0 overruns 0  carrier 0  collisions 0
```

Fig.4.8 Showing connection 5G module through USB 3.0 cable in the terminal of NVIDIA Jetson AGX Orin Developer Kit.

C. GNSS receiver in 5G module configuration

As noted earlier in this section, both Quectel and SIMCom 5G modules feature the Gen9C Lite technology for their GNSS receivers. The 5G M2 module requires a passive antenna to acquire positioning information. For the tasks of the 5G module's independent operations, configuring the GNSS receiver is crucial. Each of these modules includes a slot connector for attaching a GNSS antenna – designated as interface ANT4 in the SIMCom 8200EA-M2 and interface ANT3 in the Quectel RM502Q-EA.

It is important to ensure that the GNSS antenna is positioned facing the sky and located outdoors to optimize the reception of GNSS signals. To activate the GNSS receiver in the Quectel RM502Q-EA module, specific AT commands must be issued to enable the GPS functionality:

```
AT+QGPS = 1          #Turn on GPS positioning for Quectel module
AT+QGPSLOC = 1       #Get GPS positioning, modes can be 0, 1, 2
```

and in module SIMCom 8200EA-M2:

```
AT+CGPS = 1          #Turn on GPS positioning for SIMCom module
AT+CGPSINFO = 0      #Get GPS positioning
```

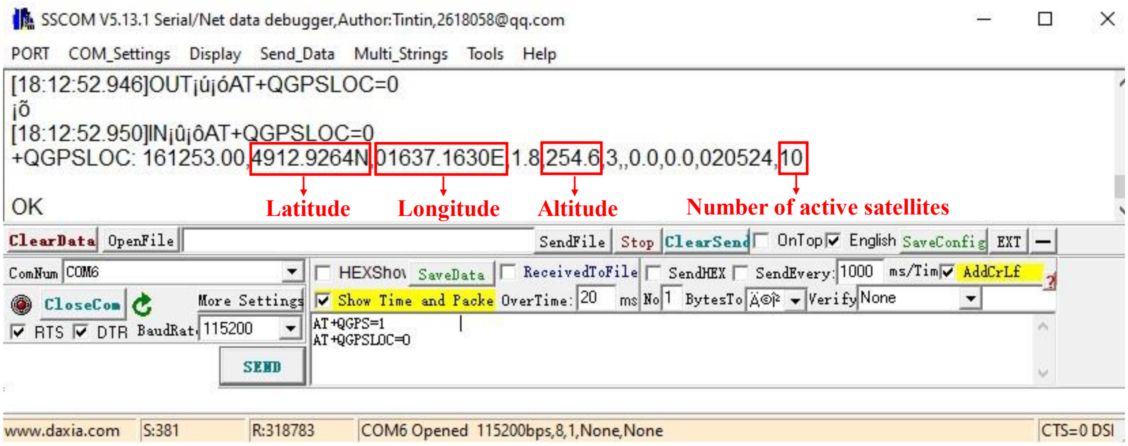

Fig.4.9 Getting GNSS information in the 5G Quectel RM502Q-EA module by AT commands in SSCOM software

For instance, in mode 1 of the Quectel 5G module for obtaining GPS positions, the command "AT+QGPSLOC=1" retrieves longitude and latitude in the formats ddmm.mmmmmm N/S and dddmm.mmmmmm E/W respectively. Additionally, altitude is reported as the absolute height of the 5G module above sea level, rounded to one decimal place in meters. These details are further illustrated in Fig. 4.9.

Where:

d	degree in the range 000 – 179
m	minute in the range 00.000000 – 59.999999
N/S	North latitude/South latitude
E/W	East longitude/West longitude

4.2 Software

For network performance measurement and analysis, this work employs standard open-source software tools, including *ICMP echo*, *iPerf*, *tcpdump*, and *Wireshark*. Link quality metrics or 5G signal quality are collected using the standard *AT command* set of the modem (detailed in Section 5.2). The transmitted data, based on IPv4, is sourced either from actual data collected by the camera and other sensors or emulated data generated by *iPerf*. Additionally, the emulated data represents a flexible approach to emulate realistic video and *Command and control (C&C or C2)* data patterns. Camera data streaming is implemented through H.264 or H.265 video encoding and MP4 containers, facilitated by the software tool *vlc*.

For C2 data transferring from the Jetson AGX Orin to the flight controller and between UAV-GCS, this study concentrates on using the MAVLink protocol.

4.2.1 iPerf

iPerf is a tool for active measurements of the maximum achievable bandwidth on IP networks [43]. It facilitates the adjustment of diverse parameters associated with timing, buffers, and protocols (TCP, UDP, SCTP with both IPv4 and IPv6). Following each test, it provides detailed reports on bandwidth, loss, and various other parameters.

The iPerf utility is equipped with a range of command-line parameters that enable the creation of highly customized network speed tests between hosts, end-user devices, or client-server setups. Moreover, iPerf is compatible with various operating systems, including Windows, Linux, macOS, and others, enhancing its versatility for network performance testing across diverse platforms. To facilitate the integration of iPerf with Python programs, this project employs the iPerf3 Python module. This module acts as a Python wrapper for the iPerf3 tool, allowing direct interaction with iPerf functionality from within a Python script. This integration provides a streamlined approach to conducting and automating network speed tests programmatically.

In terms of this study, the project aims to evaluate the KPIs between end-to-end devices (UAV-GCS connection) in the private 5G UNOB network by using open-source tools while considering the advantages and disadvantages of each tool. Table 4.3 below shows the use cases of each open-source tool that can be employed to measure 5G KPIs.

Besides open-source tools, it should be mentioned that there are also commercial tools such as Keysight tools (CyPerf, BreakingPoint Security, IxNetwork, IxLoad, LoadCore, Hawkeye, UsSim), VIAVI tools, Qmon, etc. These tools support a wide range of use cases from 5G drive and benchmark testing, 5G end-to-end QoS and QoE monitoring of network and services in live environments, continuous service, 5G coverage and performance assessment, etc.

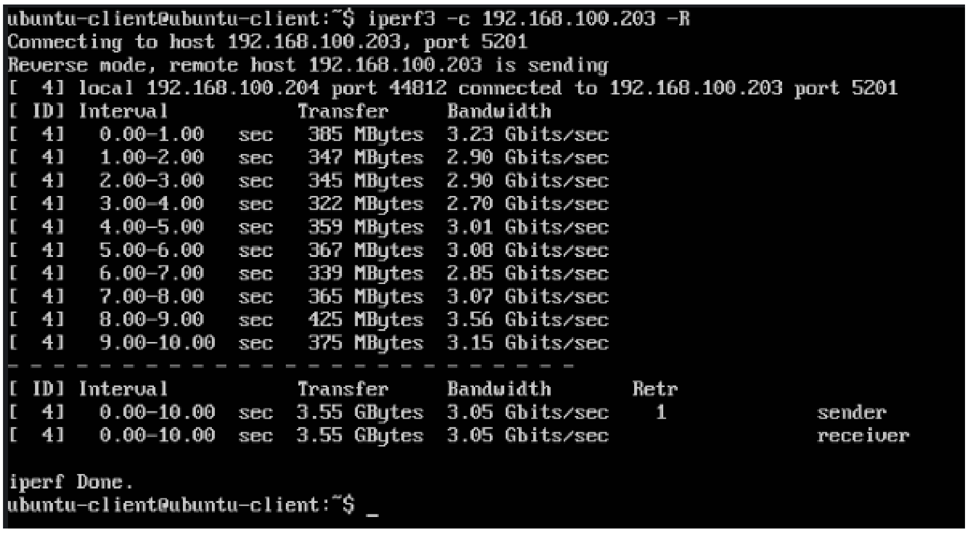

```
ubuntu-client@ubuntu-client:~$ iperf3 -c 192.168.100.203 -R
Connecting to host 192.168.100.203, port 5201
Reverse mode, remote host 192.168.100.203 is sending
[  4] local 192.168.100.204 port 44812 connected to 192.168.100.203 port 5201
[ ID] Interval           Transfer     Bandwidth
[  4]   0.00-1.00   sec   385 MBytes  3.23 Gbits/sec
[  4]   1.00-2.00   sec   347 MBytes  2.90 Gbits/sec
[  4]   2.00-3.00   sec   345 MBytes  2.90 Gbits/sec
[  4]   3.00-4.00   sec   322 MBytes  2.70 Gbits/sec
[  4]   4.00-5.00   sec   359 MBytes  3.01 Gbits/sec
[  4]   5.00-6.00   sec   367 MBytes  3.08 Gbits/sec
[  4]   6.00-7.00   sec   339 MBytes  2.85 Gbits/sec
[  4]   7.00-8.00   sec   365 MBytes  3.07 Gbits/sec
[  4]   8.00-9.00   sec   425 MBytes  3.56 Gbits/sec
[  4]   9.00-10.00  sec   375 MBytes  3.15 Gbits/sec
- - - - - - - - - - - - - - - - - - - - - - - - -
[ ID] Interval           Transfer     Bandwidth       Retr
[  4]   0.00-10.00  sec  3.55 GBytes  3.05 Gbits/sec    1             sender
[  4]   0.00-10.00  sec  3.55 GBytes  3.05 Gbits/sec                  receiver

iperf Done.
ubuntu-client@ubuntu-client:~$ _
```

Fig.4.10 Example of using iPerf to measure throughput between UE devices [44]

Table 4.3 Open-source tools and corresponding 5G KPIs, adapted from [45]

Tools	**5G KPIs**									
	One-way-latency	**Two-way-latency**	**Jitter**	**Availability**	**Reliability**	**Packet Loss**	**Area Traffic Capacity**	**Experienced Data rate**	**Guaranteed Data Rate**	**Data Volume**
	[ms]	**[ms]**	**[ms]**	**[%]**	**[%]**	**[%]**	**[bps/m²]**	**[Mbps]**	**[Mbits/s]**	**[Gbits]**
Ping		✓				✓				
iPerf			✓	✓		✓		✓	✓	✓
Bmon			✓							✓
NetEm	✓		✓	✓	✓	✓		✓	✓	✓
Ostinato	✓		✓	✓		✓		✓	✓	✓
TCPreplay								✓	✓	
Fping			✓			✓				
Moongen			✓	✓						
Curl							✓			
Ntopng			✓	✓		✓		✓	✓	
Cilium			✓	✓		✓		✓	✓	✓
TWAMP	✓	✓	✓			✓		✓	✓	

4.2.2 MAVLink protocol

The Micro Air Vehicle Link (MAVLink) protocol is used for communication with UAVs, and it offers numerous benefits. Notably, MAVLink is a lightweight serial protocol, enabling efficient data and command exchange between UAVs and GCS, between UAVs and SBC, utilized in real flight tests [46]. MAVLink protocol has two versions, version 1, and version 2. This study employs MAVLink version 2, which significantly surpasses its predecessor by featuring a 24-bit message ID that supports over 16 million unique message definitions, compared to the mere 256 messages permitted by the 8-bit message ID in version 1.

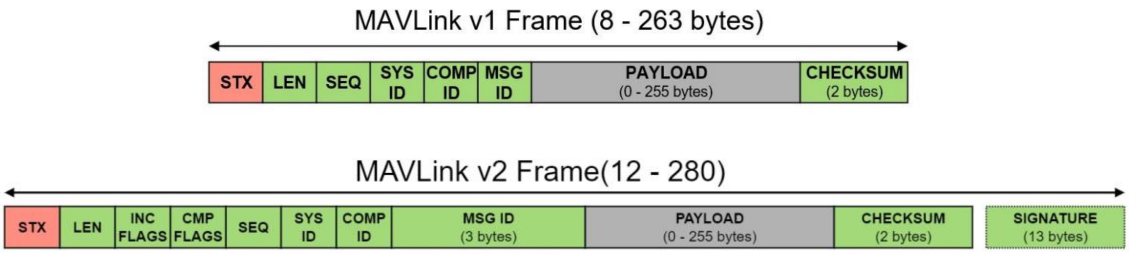

Fig.4.11 MAVLink 1.0 and MAVLink 2.0 Header [46]

Table 4.4 Explanation of MAVLink v2 frame [47]

Acronym	Content	Value	Explanation
STX	Packet start marker	0xFD	Indicates the start of the new packet.
LEN	Payload length	0 to 255	Indicates the length of the following payload section.
INC FLAGS	Incompati-bility Flags	–	Flags that must be understood for MAVLink compatibility (implementation discards packet if it does not understand flag).
CMP FLAGS	Compatibi-lity Flags	–	Flags that can be ignored if not understood (implementation can still handle packet even if it does not understand flag).
SEQ	Packet sequence number	0 to 255	Each component counts his send sequence. Allows to detect packet loss.
SYS	System ID (sender)	1 to 255	ID of the SENDING system. Allows to differentiate different MAVs on the same network.
COMP	Component ID (sender)	0 to 255	ID of the SENDING component. Allows to differentiate different components of the same system, e.g., the IMU and the autopilot
MSG ID	Message ID	3 B	ID of the message – the ID defines what the payloads "means" and how it should be correctly decoded.
Payload	Payload	0 to 255 B	Data of the message, which depends on the message type (i.e. Message ID) and contents.
Checksum	Checksum	2 B	CRC-16/MCRF4XX for message
Signature	Signature	13 B	Signature to ensure the link is tamper-proof.

The reliability of the MAVLink protocol is demonstrated through its capacity to support up to 255 concurrent systems on a single network, encompassing both offboard and onboard communications across various entities. Moreover, MAVLink is compatible with multiple programming languages including C, C++, JavaScript, and Python. In this study, the MAVLink protocol is implemented in Python and C++ program of SBC NVIDIA Jetson AGX Orin Developer Kit by using the *mavgen* library for both C++ and Python (Pymavlink).

MAVLink messages, integral to communication between unmanned systems and ground stations, are divided into two primary types [46]. State messages convey the system's current status from the unmanned vehicle to the ground station, detailing elements such as its identification, location, speed, and altitude. On the other hand, command messages originate from the ground station or an associated user program, directing the unmanned vehicle to perform specific tasks. These instructions might include commands for the UAV to take off, land, navigate to a designated waypoint, or carry out a complex mission involving multiple waypoints. Each type of message plays a crucial role in ensuring the effective operation and management of unmanned aerial systems.

In autonomous flights, the application data is transmitted to the GCS via a private 5G UNOB network. Upon receiving this data, the GCS server processes it and sends MAVLink commands back to the SBC on the UAV. These commands are then relayed to the flight controller, Cube Orange, which executes various movements and actions. The flow of data, from the UAV to the GCS and back to the UAV, is depicted in Fig.4.12. This illustration helps clarify the direction and sequence of data exchange essential for managing autonomous flight operations.

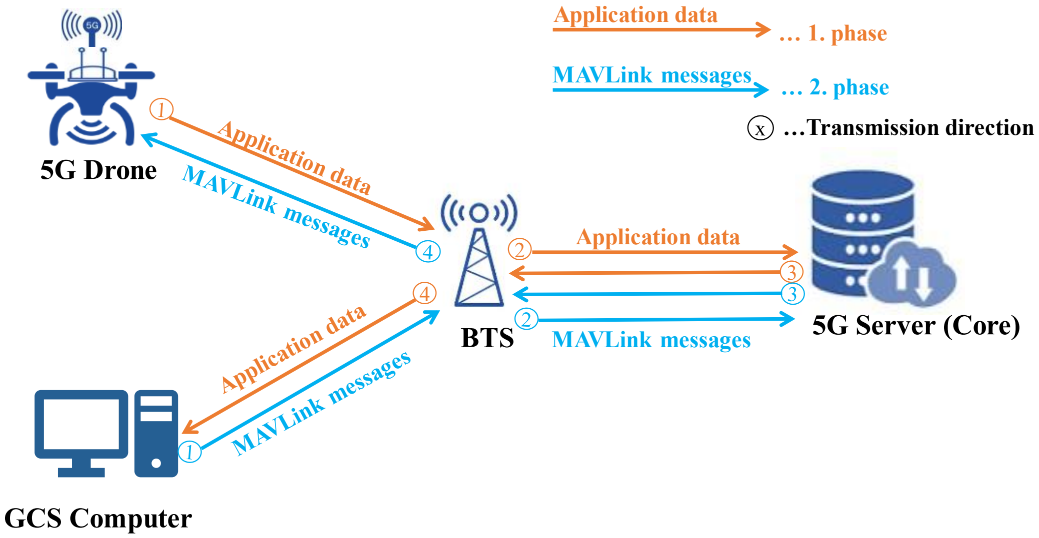

Fig.4.12 The directions of MAVLink data for controlling UAVs through private 5G UNOB network.

One of the key MAVLink state messages frequently utilized in subsequent chapters of this discussion is the GLOBAL_POSITION_INT message. This message is critical for retrieving location information from GPS sensors. As outlined in Table 4.5, GLOBAL_POSITION_INT provides a filtered global position, which integrates data from GPS sensors and accelerometers. The coordinates are presented in a GPS coordinate frame that uses a right-handed, Z-up system. The message is formatted as a scaled integer rather than a float, due to the higher precision required for accurate location data that scaled integers can provide over floats. This design ensures more reliable and precise positioning information, essential for navigational tasks.

Table 4.5 GLOBAL_POSITION_INT MAVLink message parameters [48]

Field Name	**Type**	**Units**	**Description**
time_boot_ms	uint32_t	ms	Timestamp (time since system boot).
lat	int32_t	degE7	Latitude, expressed
lon	int32_t	degE7	Longitude, expressed
alt	int32_t	mm	Altitude (MSL). Note that virtually all GPS modules provide both WGS84 and MSL.
relative_alt	int32_t	mm	Altitude above ground
vx	int16_t	cm/s	Ground X Speed (Latitude, positive north)
vy	int16_t	cm/s	Ground Y Speed (Longitude, positive east)
vz	int16_t	cm/s	Ground Z Speed (Altitude, positive down)
hdg	uint16_t	cdeg	Vehicle heading (yaw angle), 0.0...359.99 degrees. If unknown, set to: UINT16_MAX

4.2.3 GCS software

Mission Planner and QGroundControl, as shown in Fig.4.13, are comprehensive ground station applications designed for use with ArduPilot, an open-source autopilot system for various unmanned vehicles. These applications enable complete flight control and mission planning capabilities for any UAV that supports MAVLink communication. Pilots can utilize these tools to effortlessly plan flight missions, monitor the UAVs' location, track its flight path, and set waypoints using an interactive map. Additionally, these applications allow for the real-time inspection of the UAVs' status, displaying all relevant MAVLink parameters. Other features include viewing instrument data and streaming video directly from the UAVs, enhancing operational control and situational awareness.

Fig.4.13 MissionPlanner and QGroundControl interface

5. THE MEASURING PARAMETERS AND THE PROGRAM FOR MEASURING

This chapter defines the measuring parameters, which evaluate the quality of 5G signal and 5G end-to-end QoS. After that, the program for measuring is created to meet the above purposes.

5.1 Definition of the parameters

5.1.1 5G signal quality parameters

In order to evaluate the 5G network, including 5G signal coverage and 5G signal quality, this study focuses on measured Synchronization Signal – Reference Signal Received Power (SS-RSRP), as illustrated in Fig. 5.1, which has more informative results than other measured parameters like Synchronization Signal – Reference Signal Received Quality (SS-RSRQ) and Synchronization Signal – Signal to Interference plus Noise Ratio (SS-SINR).

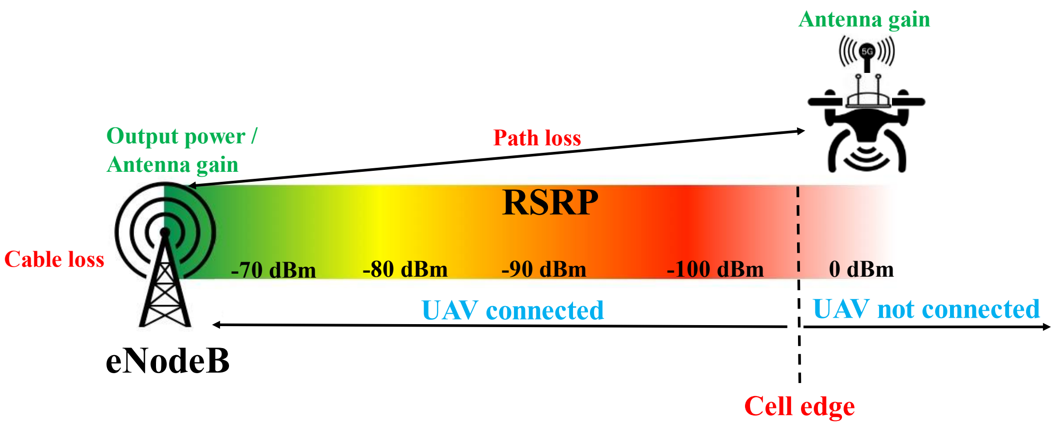

Fig.5.1 Illustration of RSRP measurement using a 5G-connected UAV

SS-RSRP is the linear average of the received secondary synchronization signal level. These signals, which are specific to each cell, are transmitted using the source elements (SE). RSRP enables the comparison of signal strengths from different cells within 5G networks, serving as a crucial parameter for processes like cell selection or handover. In essence, SS-RSRP in 5G is analogous to the RSRP parameter employed in LTE systems.

SS-RSRQ plays a crucial role in assessing the radio channel quality in the 5G NR networks. Differing from RSRP, which focuses solely on the desired signal strength, RSRQ incorporates interference levels by factoring in the Reference Signal Strength Indicator (RSSI) during its calculation. This parameter proves essential for tasks such as cell selection and handover, if the RSRP is not sufficient. This happens mainly in border parts of a cell. It is similar to the parameter RSRQ from LTE networks. However, the main difference is that 5G networks use Synchronization Signals (SS) and Channel State Information (CSI) instead of Reference Signals (RS).

SS-SINR is characterized as the linear average of the power contribution (measured in [W]) from the resource elements conveying secondary synchronization signals, divided by the linear average of the noise and interference power contribution (measured in [W]) across the resource elements carrying secondary synchronization signals within the identical frequency bandwidth. In 5G networks, SINR is communicated as a code through a measurement report to the eNodeB. This is the main difference between 3G and 4G.

The 5G modules used in this study do not provide RSSI measurements for the 5G frequency band, contrary to the initial plan for assessing signal coverage. RSSI reflects the average total received power, incorporating contributions from both the main and neighboring cells, along with noise and interference factors. Signal quality is monitored continuously up to more than 10 results every second, in parallel with tracking the precise location of the mobile measuring setup as it navigates around the Šumavská barrack, Černá Pole barrack and adjacent areas.

5.1.2 5G parameters in ITU standards

In theory, based on the earlier studies of 5G networks, the ITU prepared a set of parameters requirements for IMT-2020, which it published in November 2017. In this report, the ITU defines **peak data rate** is the maximum achievable data rate under ideal conditions (in bit/s), which is the received data bits assuming error-free conditions assigned to a single mobile station, when all assignable radio resources for the corresponding link direction are utilized (i.e. excluding radio resources that are used for physical layer synchronization, reference signals or pilots, guard bands and guard times) [49].

As per the ITU standards, **user plane latency** refers to the duration contributed by the radio network from the moment a packet is transmitted by the source to the moment it is received by the destination, measured in milliseconds [49]. It is defined as the **one-way** latency.

This study aims to measure the latency in the terms of **two-way-latency** or Round Time Trip (RTT). It means that latency is the time it takes for a device to send one small "echo – request" packet to the serving content server and the corresponding "echo – reply" packet back to the device. It is important to note that the data must first be routed through the Core 5G SA architecture before being sent to the terminal devices, as depicted in Fig.5.2. Consequently, the latency experienced between the 5G-connected UAV and the GCS server consistently exceeds that between the UAV and the Core 5G SA or between the GCS server and the Core 5G SA.

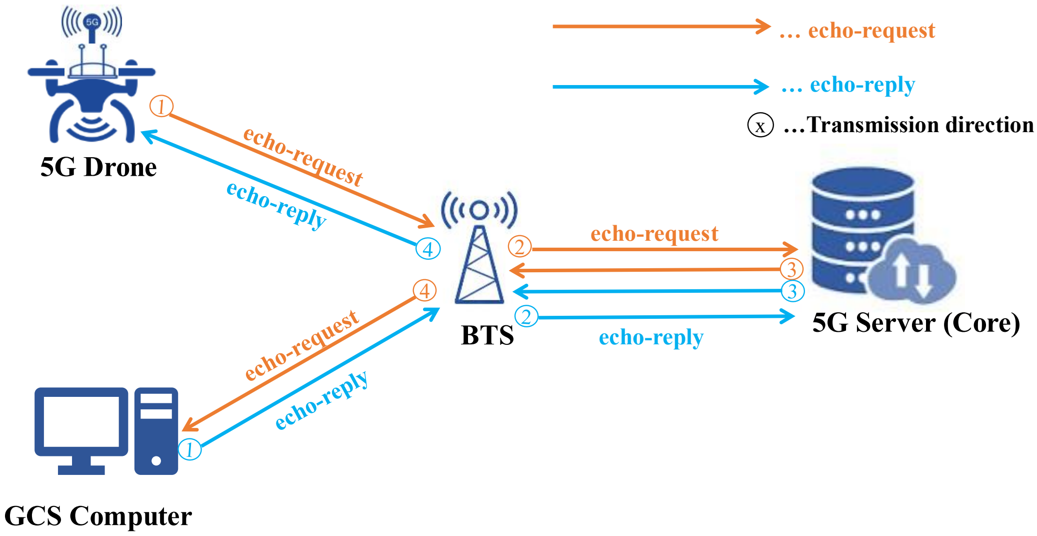

Fig.5.2 Illustration of RTT, two-way-latency UAV-GCS in ICMP protocol.

It is crucial to emphasize that the measured results will be assessed against the theoretical objectives set for the design of the 5G network. When comparing the requirements between LTE-Advanced and 5G networks, the design targets for 5G are far greater, as detailed in Table 5.1.

Table 5.1 Technical performance requirements for 5G [7]

Parameter	**LTE-Advanced**	**5G**	**Main 5G use case**
Peak data rate	500 Mbps (UL) 1000 Mbps (DL)	10 Gbps (UL) 20 Gbps (DL)	eMBB
Typical spectral efficiency a)	0.7 – 2.25 bits s^{-1} Hz^{-1} (UL) 1.1 – 3 bits s^{-1} Hz^{-1} (DL)	1.6 – 6.75 bits s^{-1} Hz^{-1} (UL) 3.3 – 9 bits s^{-1} Hz^{-1} (DL)	eMBB
Energy efficiency	n/a	Maximize	eMBB
Maximum UE speed	350 km h^{-1}	500 km h^{-1}	eMBB
User plane latency	5 ms	0.5 ms	URLLC
User plane reliability b)	n/a	99.999%	URLLC
Maximum coupling loss c)	n/a 164 dB	143 dB 164 dB	eMBB mMTC e)
Battery life d)	10 years	10–15 years	mMTC e)
Connection density	60 000 km^{-2}	1 000 000 km^{-2}	mMTC

a) Targets in various ITU performance environments.
b) Delivery of a 32-byte packet within 1 ms.
c) Data rate of 1 Mbps DL/30 kbps UL for eMBB, and 160 bps for mMTC.
d) Delivery of 200 uplink bytes per day, with a coupling loss of 164 dB, and a 5 Wh battery.
e) Addressed in Release 16 by integrating eMTC and NB-IoT into the 5G system.

5.2 Method of measuring the defined parameters

Link quality metrics are collected using the standard *AT command* set of the 5G modems.

AT commands are primarily used to configure a modem and establish its network connection. They can be used to interrogate the modem's Super SIM. They can also be used to get modem and connection status information, and this can be very helpful in debugging applications and in confirming that a modem is operating correctly: it has connected to the right network, is using the correct cellular technology, has roaming enabled, etc.

The AT commands are easily sent to the modem as plain text over a serial (UART) connection comprising two wires, one for receive (RX) and one for transmit (TX), or via USB. In the test, it's common to tap the modem's USB connection. This allows you to fire up a terminal and interact with the modem directly by issuing AT commands of your own.

The main commands for the signal quality requests of the current connectivity are "AT+QENG="servingcell"" [50] and "AT+CPSI?" [51] for Quectel and SIMCom modules respectively. The Quectel module responds with several lines – one for each connectivity band. In the 5G SA mode, the commands below in the bold positions highlight the 5G state, 5G mode, 5G band and other related information in the following order contain SS-RSRP, SS-RSRQ, SS-SINR. This line appears only if the NR5G band is detected [50].

```
AT+QENG="servingcell"

+QENG:"servingcell",<state>,"NR5G - SA",<duplex_mode>,<MCC>,<MNC>,
<cellID>,<PCID>,<TAC>,<ARFCN>,<band>,<NR_DL_bandwidth>,<RSRP>,<RSRQ>,
<SINR>,<scs>,<srxlev>                                 # In SA mode

+QENG:"servingcell",<state>,"LTE",<is_tdd>,<MCC>,<MNC>,<cellID>,<PCID>,
<earfcn>,<freq_band_ind>,<UL_bandwidth>,<DL_bandwidth>,<TAC>,<RSRP>,
<RSRQ>,<RSSI>,<SINR>,<CQI>,<tx_power>,<srxlev>  # In LTE mode
```

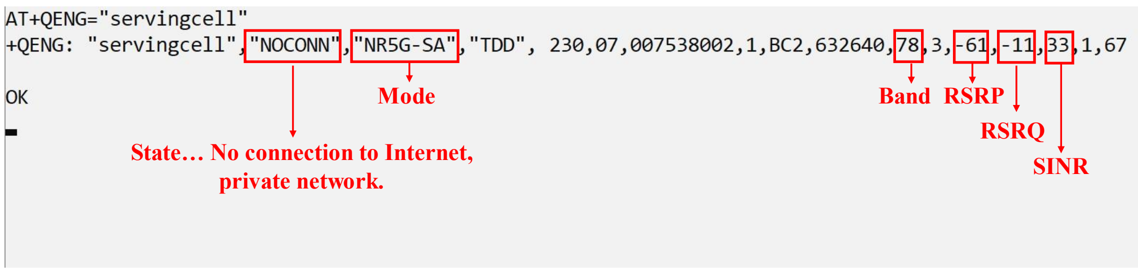

Fig.5.3 Example of getting 5G parameters in the private 5G UNOB network using Quectel 5G module

In the case of the SIMCom module, the same parameters are displayed when using AT commands "AT+CPSI?". In the NR5G mode, the commands below in the bold positions highlight the 5G state, 5G mode, 5G band and other related information in the following order contain SS-RSRP, SS-RSRQ, SS-SINR [51].

```
AT+CPSI=?

+CPSI:NR5G_SA,<OperationMode>[,<MCC>-<MNC>,<TAC>,<SCellID>,<PCellID>,
<FrequencyBand>,<earfcn><RSRP>,<RSRQ>,<SNR>]          # In NR5G mode

+CPSI:LTE,<OperationMode>[,<MCC>-<MNC>,<TAC>,<SCellID>,<PCellID>,
<FrequencyBand>,<earfcn>,<dlbw>,<ulbw>,<RSRQ>,<RSRP>,<RSSI>,<RSSNR>]
# In LTE mode
```

Once the list of AT-commands and responses is selected according to the used module, the future program should be performed a short "*ping"* session or "*iPerf"* session between the SBC on the UAV and the GCS computer to check the end-to-end connection presence. Further, these sessions will keep the 5G NR band in use and prevent the 5G modules from switching to idle mode.

Afterward, the future program in Section 5.3 will combine the functions of the GNSS module, 5G module with AT commands, and "*ping/iPerf"* session. This program will create log files with the defined pre-set columns, which will be used for all the measured data saving. These columns will be parameters: latitude, longitude, altitude (from GNSS module), 5G technology, 5G band, RSRP, RSRQ, SINR, data rate, latency, packet loss, and synchronization time.

5.3 Implemented software for the tested quality of 5G signal

The program described further represents a command-line interface software, created specifically for this work using Python. The program is written, compiled, and used on Linux OS of NVIDIA Jetson AGX Orin Developer Kit.

The figure below shows an activity diagram for the main function of the implemented tested quality of 5G signal program. The program starts with definition of all default parameters to be used further, which includes ttyUSB ports identification names of all used USB devices and sets of the AT commands and corresponding responses for both 5G modules (SIMCom and Quectel) and other different default parameters.

The first part of the program represents a preparation setup part in which all the necessary components are checked, peripheral devices are found, and serial communications are established and validated. The setup part starts with the "*USBfind*" function to access the list of serial connections of the current SBC and find the ports corresponding to the previous declaration. It is worth mentioning that used 5G modules have several virtual ttyUSB ports providing over a single USB connection, which specialized drivers to be recognized, as mentioned in Section 4.1.3. The establishing connection can be double-checked again as a network device in modem manager in Linux OS.

Find GPS signal: In case of successful finding, 5G module's port number is saved with detection flag change to the "*found*" state. The program continues to find GPS modules and get GPS signals. There are two ways to get GPS signals: by GPS antenna connected with 5G module, as mentioned in Section 4.1.3, or by own UAV's GPS antenna using MAVLink protocol, as mentioned in Section 4.2.2. In the first scenario, the AT commands get GPS signal from the passive GPS antenna connected to the 5G module. On the second scenario, SBC can get the GPS data through MAVLink protocol while SBC is connected to the flight controller.

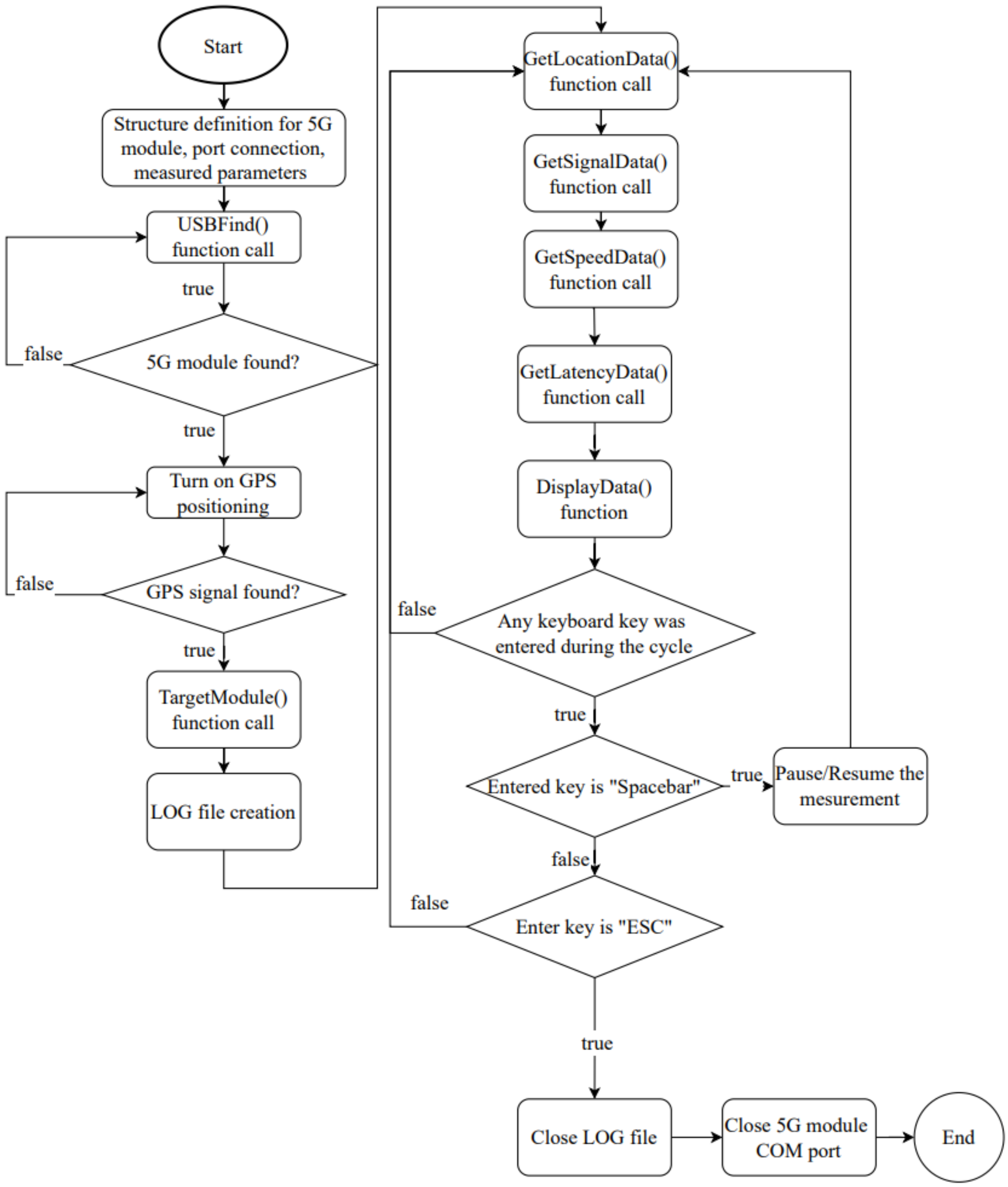

Fig.5.4 Basic activity for the main function of the implemented program.

Choosing target module: The testbed program proceeds with the *"TargetModule"* function, which is intended to define the actual list of AT-command and expected responses depending on the connected 5G module. Although the SIMCom SIM8200EA - M2 module does not support the UNOB private 5G network, in the near future, if users want to use other upgraded SIMCom, Quectel and Tellit 5G modules, using *“TargetModule”* function helps switch between the modules easily, as depicted in Fig.5.5. Section 5.2 presented the required AT-commands for each kind of 5G module to measure the signal quality.

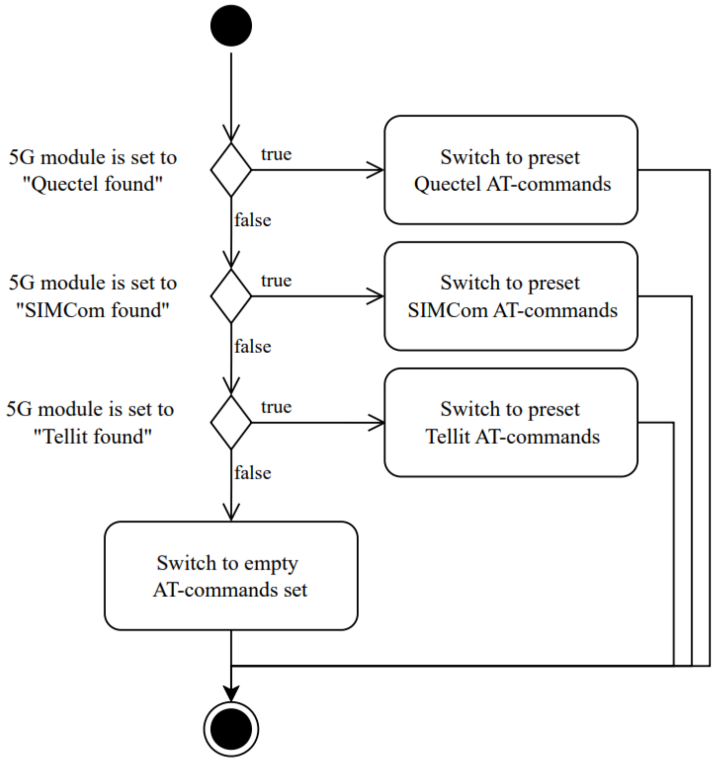

Fig.5.5 Diagram for choosing target module function

Log file creation: Once the list of AT-commands and responses are selected according to the used module, the program creates a log file with the defined columns pre-set, which will be used for all the measured data saving. When the log file is prepared, the preparation setup phase of the implemented program is finished, and the program moves to the second part represented with the main operational loop.

Operation loop: The operation loop contains five main parts “GetLocationData”, “GetSignalData”, “GetSpeedData”, “GetLatencyData” and “DisplayData”.

GetLocationData function consistently updates the UAV’s position by utilizing GPS signal. The positioning data is received continuously. As previously noted, through the MAVLink protocol, the SBC can readily access the GNSS signal from the flight controller equipped with a GPS sensor, which is an essential component for safe external flight. This GPS module transmits measured positioning information with only a few milliseconds of delay. In instances where the MAVLink signal is lost, the program can alternatively retrieve positioning data from the 5G module in use. However, the localization data from the UAV’s GPS sensor, accessed through the MAVLink protocol, is preferred. This is because it provides relative altitude data from the ground, a feature that the GPS antenna on the 5G module lacks.

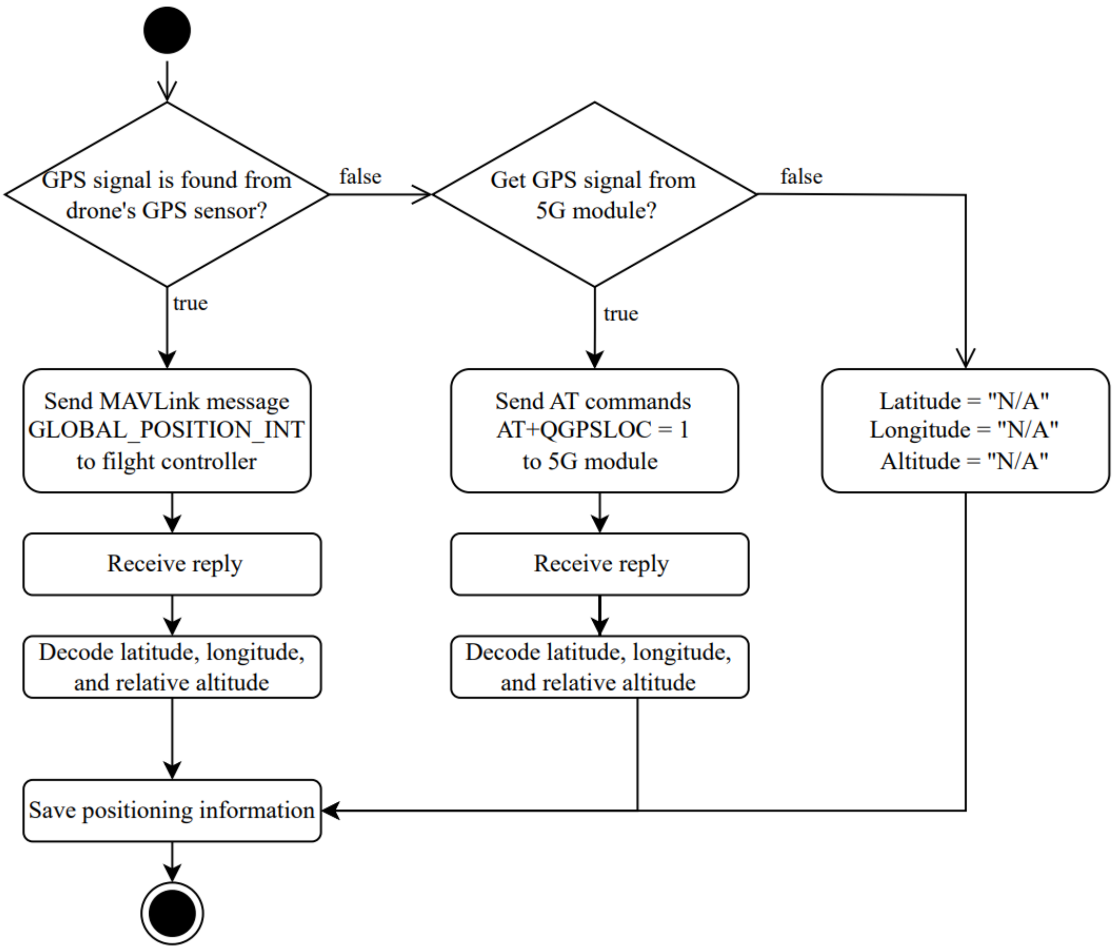

Fig.5.6 Diagram for getting GPS data function

GetSignalData function operates under the condition that a specific 5G module is defined and its ttyUSB ports have been successfully opened. In this scenario, the program sends a control AT-command to the 5G module to verify its operational status. This process is repeated until a correct response is received from the 5G module, ensuring its functionality. Once the program has verified the list of available serial devices, the "*TargetModule*" function is invoked. This function is responsible for redefining the AT - commands and the list of expected responses if the originally specified 5G module is replaced with a different one. This adjustment allows the system to maintain accurate communication protocols with the new module.

GetSpeedData function: This function is created to measure the throughput between the UAV and the GCS using *iPerf*. In this measurement, the GCS plays the role of server and the UAV as a client, as shown in Fig.5.7. The test employs both TCP and UDP traffic. By default, *iPerf3* sends TCP (UDP) traffic using a single flow, which could provide incorrect results when higher bandwidths than 1 Gbps are tested. In the test, to get more accurate results, the program uses a few parallel streams.

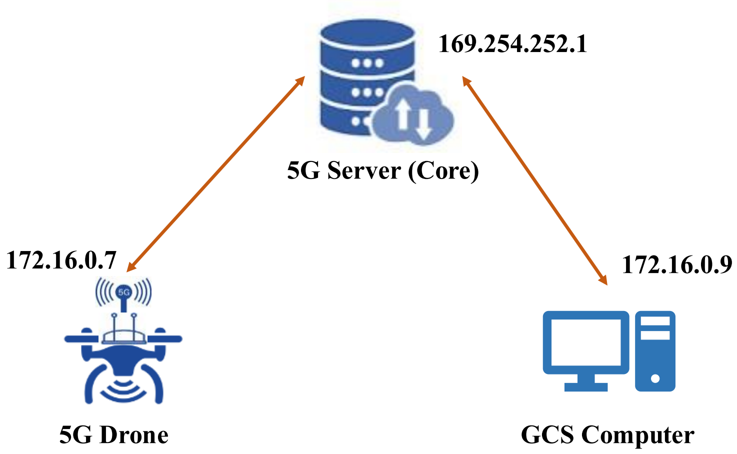

Fig.5.7 5G data flow of end-to-end connection in the private 5G UNOB network

The example commands below are employed for the separate iperf3 throughput test on the 5G-connected UAV.

Downlink:

- TCP: iperf3 -c 172.16.0.9 -t 20 -i 1 -P 20 -w 10M -R -p 15201
- UDP: iperf3 -c 172.16.0.9 -u -i 1 -t 20 -w 10M -b 1.1G -R -p 15201

Uplink:

- TCP: iperf3 -c 172.16.0.9 -t 20 -i 1 -P 20 -w 10M -p 15201
- UDP: iperf3 -c 172.16.0.9 -u -i 1 -t 20 -w 10M -b 1.1G -p 15201

In the GCS computer, for the server, the command iperf3 has to always be executed:

- iperf3 -s

GetLatencyData function: This function is initialized for measuring the RTT latency between the UAV and the GCS using ICMP protocol. As a result, we can get:

- Packet loss, which indicates the percentage of packets lost.
- RTT, which shows the time it takes for a packet to travel from the UAV's computer to the GCS computer and back. These values indicate the speed and stability of the 5G private network, including:
  - **Minimum**: The shortest time recorded.
  - **Average**: The average time over all ping requests.
  - **Maximum**: The longest time recorded.
  - **Mean Deviation**: The spread of RTT values

Another effect is the time duration of measuring by iPerf and ping, more measurements mean getting more accurate results. Therefore, the UAV will be held in every position in 10 – 15 s, which contains all the duration of iPerf and ping and other processes to perform one accurate and complete measurement. The UAV will be changed to a stable state as Stabilize or Loiter.

DisplayData function: The program proceeds to the stages of data visualization and logging after it has fully acquired positional data and signal quality measurements. This process is encapsulated within the "*DisplayData*" function. A tabular representation of the aggregated data is rendered in the console interface, as exemplified in the figure provided. This tabulation encompasses essential metadata such as the current timestamp and specifics pertaining to the operational status of the program, including ping server details, ping responses, and throughput metrics obtained via iPerf tests, to verify the reliability of the end-to-end connectivity. Additionally, the positioning data is also indicated in a separate row in the table, displaying indicators for the operational status of the GNSS antenna, whether integrated with the UAV or the 5G module, along with the geographical coordinates (latitude, longitude) and altitude measurements acquired.

```
|                 Module 5G          |Quectel_RM502Q-GL        |
|                 GNSS sensor        |PX4                      |
|--------------------------------------------------------------|

                          GPS data
|                 Type               |     Value      |  Unit  |
|------------------------------------|----------------|--------|
|Latitude                            |      35.5693156|degree  |
|Longitude                           |    -479.9438260|degree  |
|Altitude                            |    7196.5600000|meter   |

---------------------------------------------------------------|

                          5G KPI data
|                 Type               |     Value      |  Unit  |
|-----------------------------------------------------|--------|
|5G Band                             |n78             |-       |
|RSRP                                |-54             |dB      |
|RSRQ                                |-11             |dB      |
|RSSI                                |                |dB      |
|SNR                                 |33              |dB      |
|CSICQI                              |0               |dB      |
|End-to-end throughput               |           62.88|Mbps    |
|RTT min                             |          18.812|ms      |
|RTT max                             |          23.706|ms      |
|RTT average                         |          21.224|ms      |
|PING_stddev                         |               0|-       |
```

Fig.5.8 Example of displaying all the collected information

The subsequent figure presents an illustrative example of a log file format. The recorded outcomes are methodically archived in a predetermined sequence, delineated by semicolons (";"), facilitating subsequent data manipulation. This structured format enables efficient data importation into software environments such as Microsoft Excel, where the log file can be seamlessly converted into tabular formats for user-friendly interaction, or into Python for the generation of heatmaps depicting the coverage of private 5G networks. Following the comprehensive logging of the acquired data, it is systematically purged from the program’s internal process memory to maintain optimal performance and data integrity.

6. TEST SCENARIOS AND RESULTS

This chapter presents prepared scenarios for test execution and their results in the private 5G SA network at UNOB.

6.1 Scenario A: Maximum UAV-to-GSC throughput

In this scenario, the UAV flies at a short distance around the Černá Pole barrack of University of Defence, Brno, Czech Republic, within a flight height under 30 m to measure the maximum data throughput. Fig.6.1 shows the experimental protocol, which includes two distinct flights: vertical flights 50 m away from the BS (point A, liftoff from the ground to a height of 30 m), and horizontal flights from point B to point C with different heights under 30 m. The UAV starts at point B (200 m from BS), flies 150 m far away from the BS to point C with a speed of 3 m/s and returns to point B. These horizontal flights are repeated at different altitudes to gather comprehensive data. The GCS remains fixed at point A throughout these tests.

Fig.6.1 The pre-set trajectory for scenario A

Table 6.1 presents the complete dataset from the measurements conducted during both vertical and horizontal flight tests. In these experiments, the UAV functions as the client, while the GCS serves as the server. The downlink (DL) refers to the data transmission pathway from the GCS to the UAV, whereas the uplink (UL) denotes the reverse data transmission from the UAV to the GCS.

This assessment encompasses the evaluation of both DL and UL speeds in both TCP and UDP, along with the measurement of latency between the SBC on the UAV and the GCS computer. The same methodology is applied to throughput measurements at different altitudes under 30 m. The integrated testbed, affixed to the UAV platform, executed a maximum number of consecutive measurements under 10 m, 20 m, and 30 m above ground level from a potentially static position. The parameters indicated 5G signal's quality are measured more than 10 times per second. The end-to-end throughput of UAV – GCS connection is mostly dependent on the time of iPerf measurements. To mitigate potential UAV-related effects on the measured signal, the UAV equipped with 5G modules consistently oriented itself towards the base station antenna at each measurement position.

Table 6.1 End-to-end UAV-GCS measurement results

Experiment			**Throughput [Mbps]**		**Latency RTT [ms]**	
Type	**Range**	**Link**	**Max**	**Mean ± stddev**	**Min**	**Mean ± stddev**
Vertical flight	**Takeoff – 10 m**	**DL TCP**	69.4	63.8 ± 1.5	15.7	24.1± 4.6
		DL UDP	68.9	67.6 ± 6.0		
		UL TCP	39.5	31.1 ± 4.6		
		UL UDP	46.1	37.9 ± 5.1		
	10 m – 20 m	**DL TCP**	64.7	63.6 ± 0.6	16.9	25.9 ± 4.4
		DL UDP	68.6	67.7 ± 0.7		
		UL TCP	34.7	31.2 ± 3.3		
		UL UDP	49.6	37.1 ± 8.9		
	20 m – 30 m	**DL TCP**	63.9	63.5 ± 0.2	18.0	25.8 ± 4.9
		DL UDP	68.5	68.1 ± 0.4		
		UL TCP	35.7	28.2 ± 5.5		
		UL UDP	43.3	36.2 ± 4.6		
Horizontal flight	**Under – 10m**	**DL TCP**	75.5	60.3 ± 7.6	17.6	32.1 ± 20.6
		DL UDP	68.8	67.6 ± 0.5		
		UL TCP	4.7	1.7 ± 1.5		
		UL UDP	35.7	22.9 ± 3.9		
	Altitude 15m	**DL TCP**	64.7	62.7 ± 1.7	17.7	29.6 ± 18.8
		DL UDP	68.9	67.7 ± 0.8		
		UL TCP	6.9	2.7 ± 2.1		
		UL UDP	22.2	22.0 ± 0.2		
	Altitude 30m	**DL TCP**	65.5	62.6 ± 2.1	20.2	26.9 ± 4.6
		DL UDP	68.4	67.6 ± 0.7		
		UL TCP	4.1	3.1 ± 0.7		
		UL UDP	21.9	21.8 ± 0.1		

During vertical flight tests at point A, the DL and UL throughput, including both TCP and UDP protocols, present minimum fluctuation with changes in the UAV's altitude. The DL throughput between UAV – GCS with peaks above 69 Mbps (for TCP) and 68 Mbps (for UDP). The average throughput DL is always more than 63 Mbps (with both TCP and UDP). Besides, the UL with UDP is slightly better than UL with TCP. The maximum UL UDP is 49.6 Mbps and average UL UDP through all flights is more than 36 Mbps. On the other hand, the maximum UL TCP is 39.5 Mbps and averages around 28 – 31 Mbps.

In the vertical test conducted at point A, the proximity of the test site to the 5G antenna (within 50 m) ensures that the SINR parameter remained stable despite increases in altitude, peaking at 39 dBm with an average of 36.19 ± 1.50 dBm. However, a notable decrease in the RSRP parameter was observed as the altitude increased. The data represented in Fig.6.2 indicates that the current setup is less effective for UAVs operating at higher altitudes. The RSRP parameter peaks at -51 dBm and has an average value of -63.84 ± 5.78 dBm.

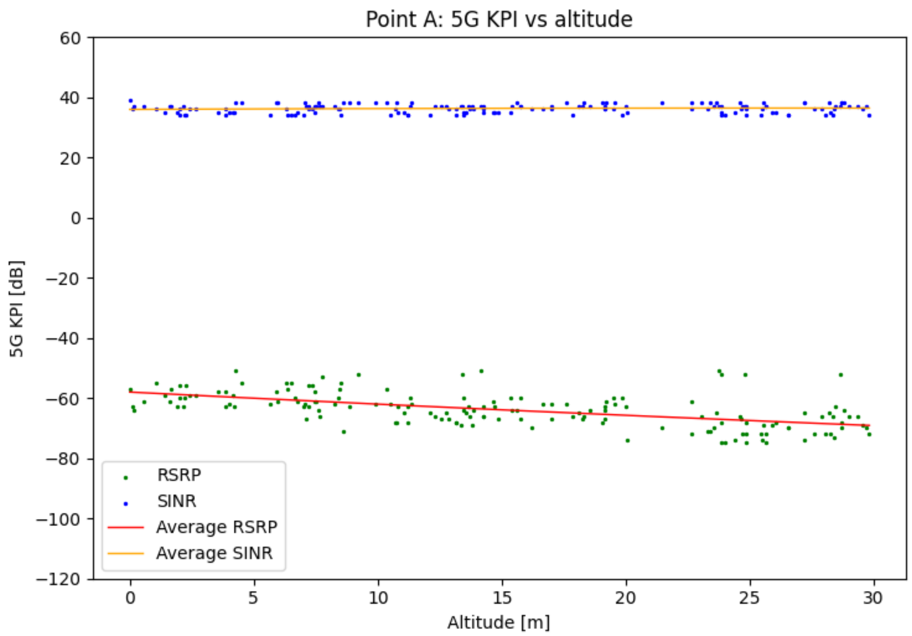

Fig.6.2 Measurement results in the vertical flights at point A: 5G KPI vs altitude

In the horizontal flight B-to-C far away from the BS, the DL remained unaffected by the distance, terrain, or potential obstacles. However, a significant disparity is observed between the UL performances of TCP and UDP protocols. The UL UDP throughput averages 22 Mbps, reaching a peak of 35.7 Mbps. Conversely, the UL TCP throughput is markedly lower, averaging only 2 Mbps and peaking at nearly 7 Mbps. The results indicate that distance exerts a minor negative impact on DL performance, but the effect on uplink UL throughput is more pronounced, exhibiting a decline correlated with reductions in both SS-RSRP and SS-SINR.

The reduction in RSRP and SINR in the horizontal flights is directly linked to increasing distance from the 5G antenna. The RSRP values are confined to a range of -100 dBm to -80 dBm, peaking at -83 dBm with an average of -92.61 ± 4.34 dBm. Similarly, SINR values span from 10 to 30 dB, with a maximum of 33 dBm and an average of 21.57 ± 6.22 dBm. This decline in signal quality with distance is further confirmed in additional tests, particularly in scenario B. There is also a clear correlation between critical 5G signal quality indicators and the performance of both upload and download data transmission links. These findings are further illustrated by comparing RSRP and SINR parameters across vertical and horizontal flights, as shown in Fig.6.3.

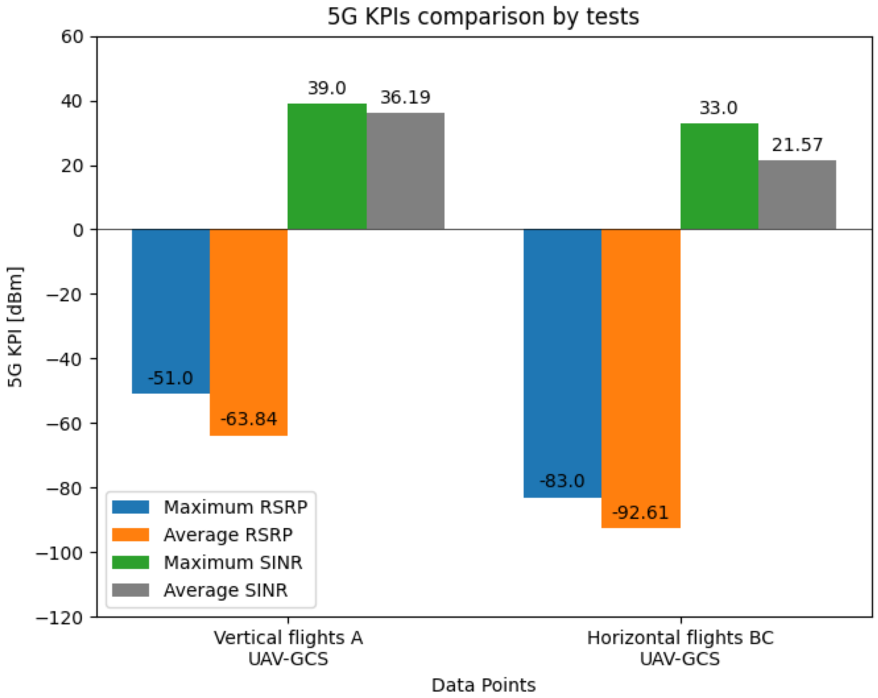

Fig.6.3 5G KPIs comparison by tests.

The results indicate that distance exerts a minor negative impact on DL performance, but the effect on uplink UL throughput is more pronounced, especially in TCP protocol, exhibiting a decline correlated with reductions in both RSRP and SINR.

These findings in both vertical and horizontal flights align closely with those reported by Festag et al. [34], measuring end-to-end throughput across the T-Mobile commercial mobile network in Germany, involving 6 BSs. The difference in this study is that, the signal quality maintained by each antenna, along with their specific distances, ensured that the results are not influenced by any handover effects.

The latency observed in both vertical and horizontal flight configurations exceed 15 ms, typically ranging between 20 ms to 30 ms. This latency can primarily be attributed to the necessity of data transfer through the Core 5G SA architecture before transmission to the terminal devices, as illustrated in Fig.6.1. Even when the GCS and the UAV are in the same test place, the data is not transmitted directly, always has to be transferred through 5G CORE and back the nearest 5G base station. The Fig.4.12, Fig.5.2, Fig.5.7, Fig.6.1 illustrated this data direction. Furthermore, the connection of two Ericsson 5G antennas to the 5G Core SA via dual single-mode fiber optic cables contributes to the aggregated latency, predominantly due to transfer delays.

This study also examines the transmission quality of this UAV connected solely to a 5G CORE network. The results from UDP link measurements indicate that during vertical flights at location A, the DL speed, from the 5G CORE to the UAV, reaches a maximum of 217.5 Mbps, with an average of 183.6 ± 15.5 Mbps, and the upload UL speed peaked at 46.4 Mbps, averaging 38.0 ± 3.9 Mbps. In horizontal flights between points B and C, the maximum DL speed was 177.5 Mbps, with an average of 94.4 ± 20.9 Mbps, while the maximum UL speed was consistent at 38.9 Mbps, averaging 34.3 ± 2.8 Mbps. The accompanying chart details these findings, presenting specific results for both vertical and horizontal flight paths in relation to the throughput between the UAV and the 5G CORE network.

The comparison presented in Fig.6.5 indicates that the latency associated with UAV - CORE is significantly reduced, approximately half that of UAV-GCS. This reduction can be attributed to a halving of the transmission distance, as elucidated in Fig.6.4. Furthermore, data throughput for UAV-CORE surpasses that of UAV-GCS. Nevertheless, integrating the GCS within the 5G CORE infrastructure does not fulfill the operational requirements for GCS mobility and falls outside the scope of this investigation.

Finally, for detailed information on each test, additional graphs are presented in Appendix A - of this thesis.

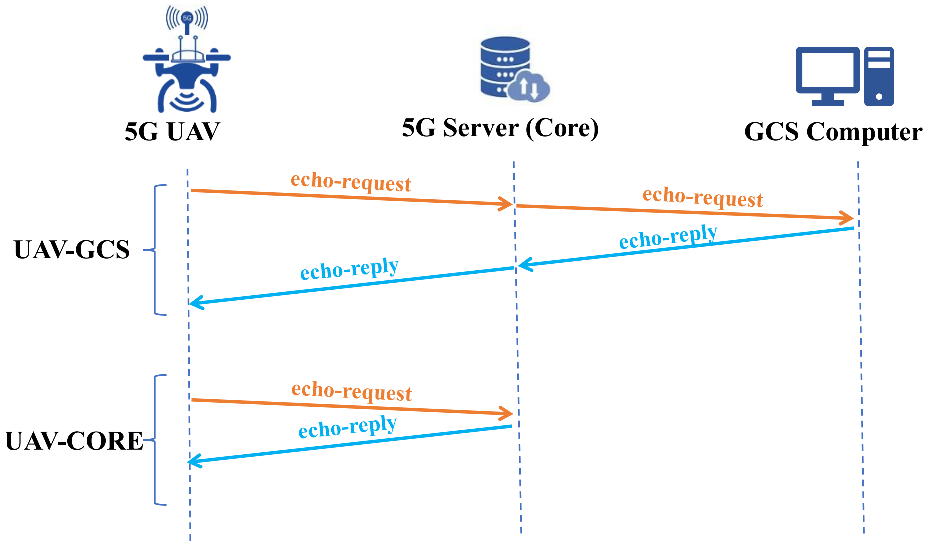

Fig.6.4 Latency through ICMP packets explanation UAV-GCS, UAV-CORE

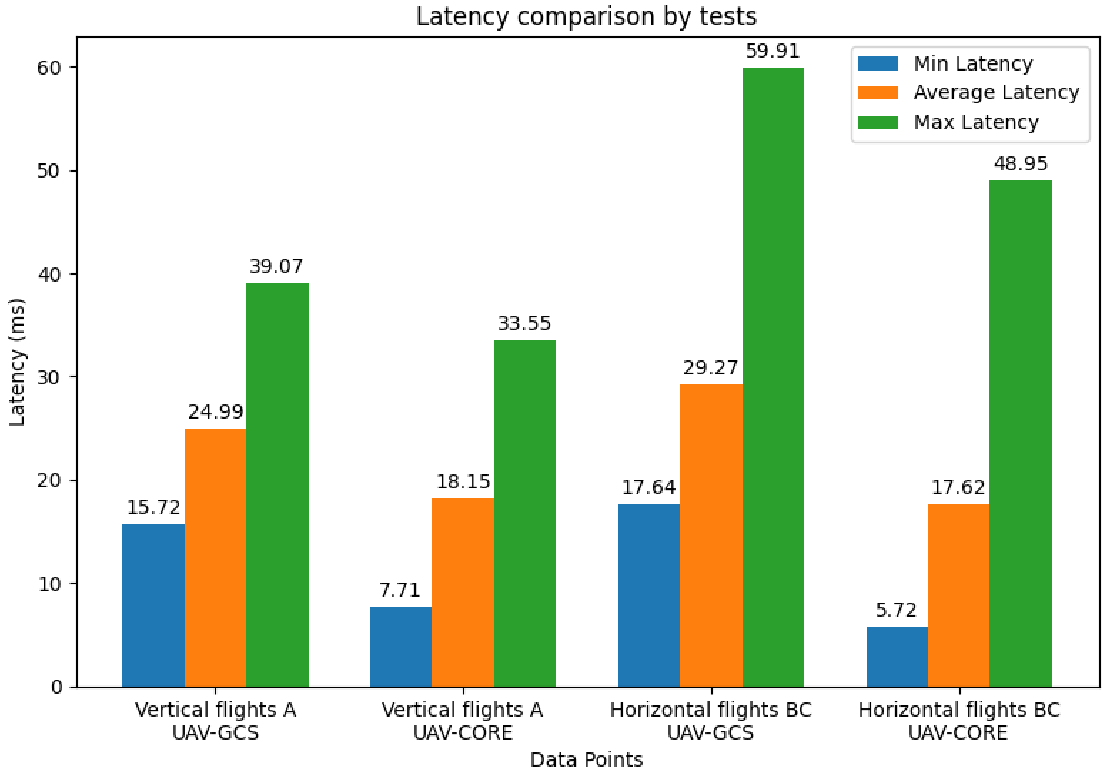

Fig.6.5 Latency comparison by tests.

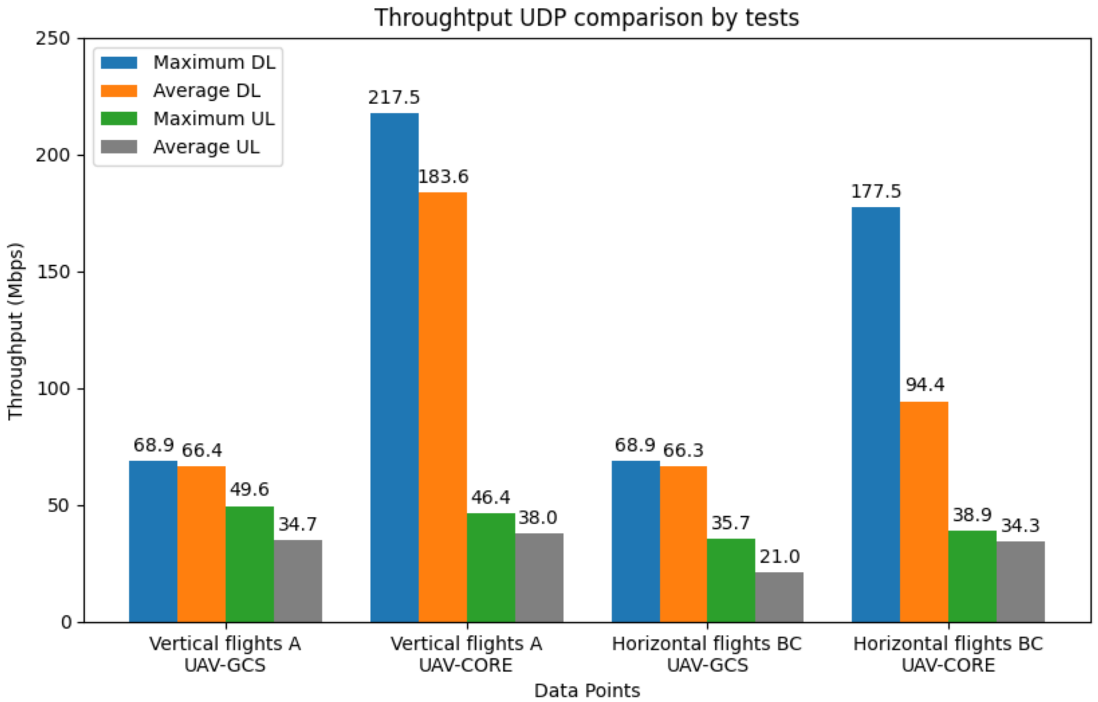

Fig.6.6 Throughput UDP comparison by tests

6.2 Scenario B: Long-range flights and the coverage of the base stations

Contemporary mobile networks are predominantly engineered for terrestrial communications, which can lead to challenges in aerial applications such as UAVs communications. The wireless connection between UAVs and the GCS often exhibits compromised signal quality, evidenced by low received signal strength and a correspondingly diminished SINR. This issue is primarily due to the orientation of base station antennas, which are down tilted to optimize coverage for ground-level devices. Furthermore, UAVs operating at high altitudes are likely to encounter signals from multiple base stations simultaneously. This increases the complexity of managing connections, resulting in more frequent handover procedures for UAVs than for terrestrial users, who typically receive signals from a smaller number of base stations.

The T-Mobile operator, which provides the 5G network for the UNOB, offers software that simulates BS coverage at both Šumavská and Černá Pole barracks. This tool performs an orientation simulation for outdoor coverage, assuming conditions without any negative impacts from attenuation, essentially depicting an ideal environment, as depicted in Fig.6.7, Fig.6.9.

In this scenario, the UAV navigates within the designated spaces authorized by the Czech Civil Aviation Authority (CAA) and in accordance with European Union Regulation 2019/947 set forth by the European Union Aviation Safety Agency (EASA).

The UAV navigates around the antenna area at Černá Pole barrack and Šumavská barrack, Brno, Czech Republic to assess signal quality in these regions. The flight positions will vary from proximity to gradually extending to more distant locations. In case a connection is sustained, the study seeks to determine the signal quality and key parameters of the private 5G network by AT commands in the 5G Quectel module.

The flight results showed consistent results from T-Mobile's simulations. The test gets more than 10 results of AT commands per second. Signal quality indicators for 5G (RSRP and SINR) deteriorate as the UAV increases its distance from the antenna. This degradation can be attributed to energy attenuation over distance, further affected by urban structural elements such as signal obstructions and physical obstacles. Optimal signal quality through the tests is generally observed within a distance of 150 m from the antenna, where RSRP exceeds - 80 dBm and SINR surpasses 25 dBm. These levels are sufficient to meet the communication requirements of UAVs.

The analysis of 5G quality metrics in relation to the distance from the antenna is depicted in the subsequent charts for two military areas, Černá Pole and Šumavská. The absence of a handover phenomenon leads to a degradation of the 5G signal quality as the distance from the antenna increases. Factors typical of urban environments, such as building density, physical obstructions, and electromagnetic interference from vehicular traffic and other radio sources, further influence the signal quality.

Table 6.2 below displays the color range used to draw the coverage map for both antennas at Šumavská barrack and Černá Pole barrack.

Table 6.2 RSRP color ranges

	Color	Min RSRP [dBm]	Max RSRP [dBm]
1		-70	–
2		-75	-71
3		-80	-76
4		-85	-81
5		-90	-86
6		-95	-91
7		-100	-96
8		-105	-101
9		-110	-106
10		-115	-145

In Černá Pole, specifically between positions 1 and 2 in Fig.6.8, the RSRP index shows a notable decline across the two buildings, despite the flight path extending above the buildings' height. In contrast, the Šumavská military zone, depicted in Fig.6.10 at points 1 and 2, experiences signal interference from the surrounding trees.

Nonetheless, the signal integrity at Šumavská barrack, where the UAV testing area is comparatively smaller and devoid of nearby obstacles, ensures that the UAV maintains a line of sight with the antenna, resulting in excellent signal quality. The SINR and RSRP parameters consistently remain at optimal levels, reflecting superior signal quality. A similar scenario is observed in the Černá Pole military zone, where the building housing the 5G antenna aids in maintaining high-quality signal reception.

Furthermore, this study provides two additional graphs illustrating the relationship between the 5G KPIs and distance from the antenna at both Černá Pole and Šumavská barracks, shown in Fig.6.11 and Fig.6.12. These graphs support the previous comments and evaluations.

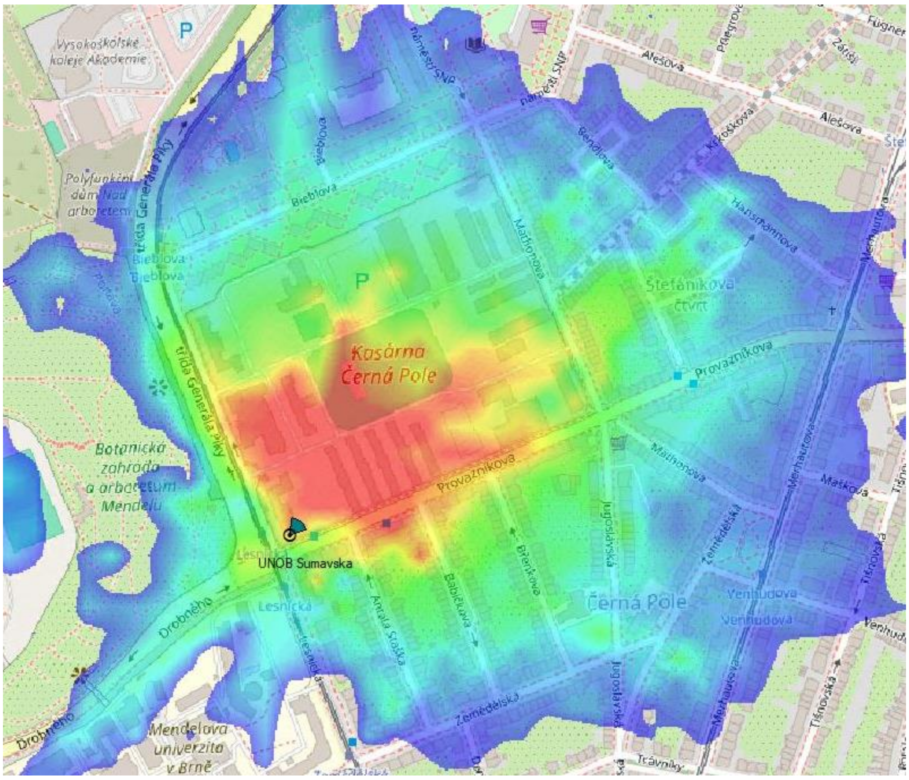

Fig.6.7 The coverage of the BS at Černá Pole barrack from T-Mobile simulation software

Fig.6.8 The coverage of the BS at Černá Pole barrack in the real flight test, altitude 15 m, the figure at the top-right is the preset waypoints in QGroundControl

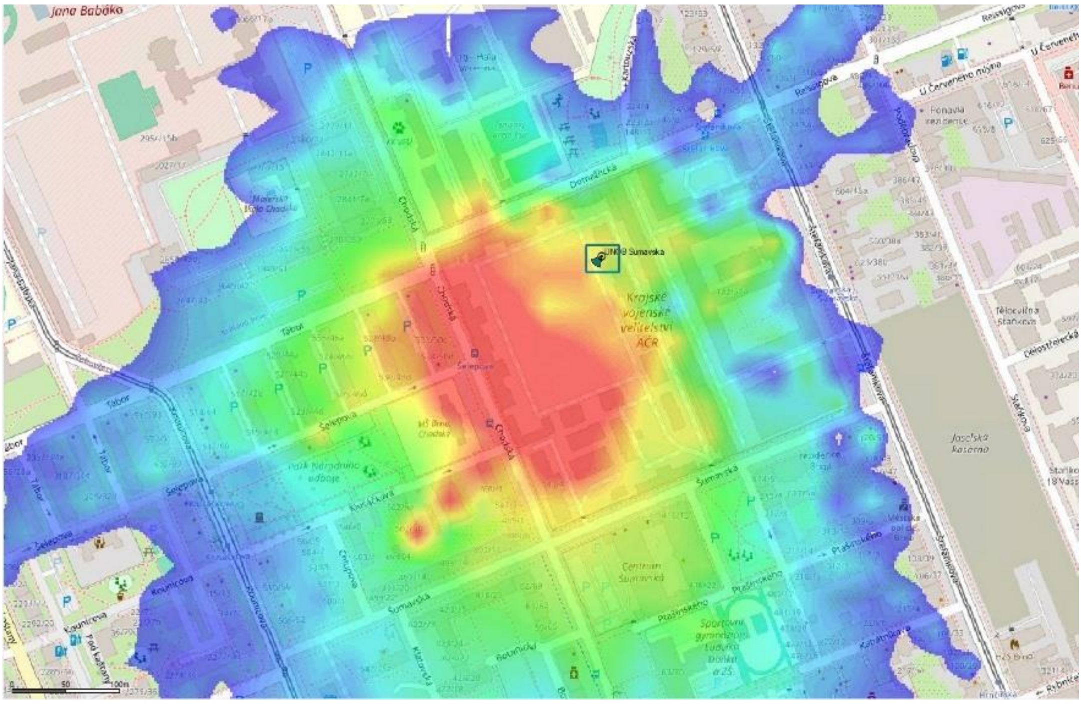

Fig.6.9 The coverage of the BS at Šumavská barrak from T-Mobile simulation software

Fig.6.10 The coverage of the BS at Šumavská barrack in the real flight test, altitude 15 m, the figure at the top-right is the preset waypoints in QGroundControl.

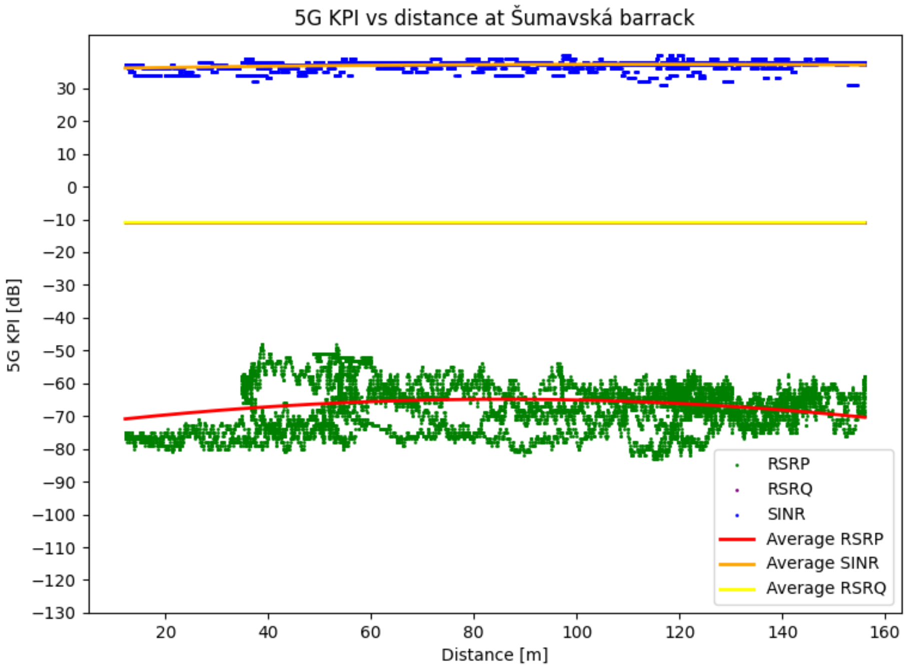

Fig.6.11 5G signal quality at altitude of 15 m vs distance from the 5G antenna at Šumavská barrack.

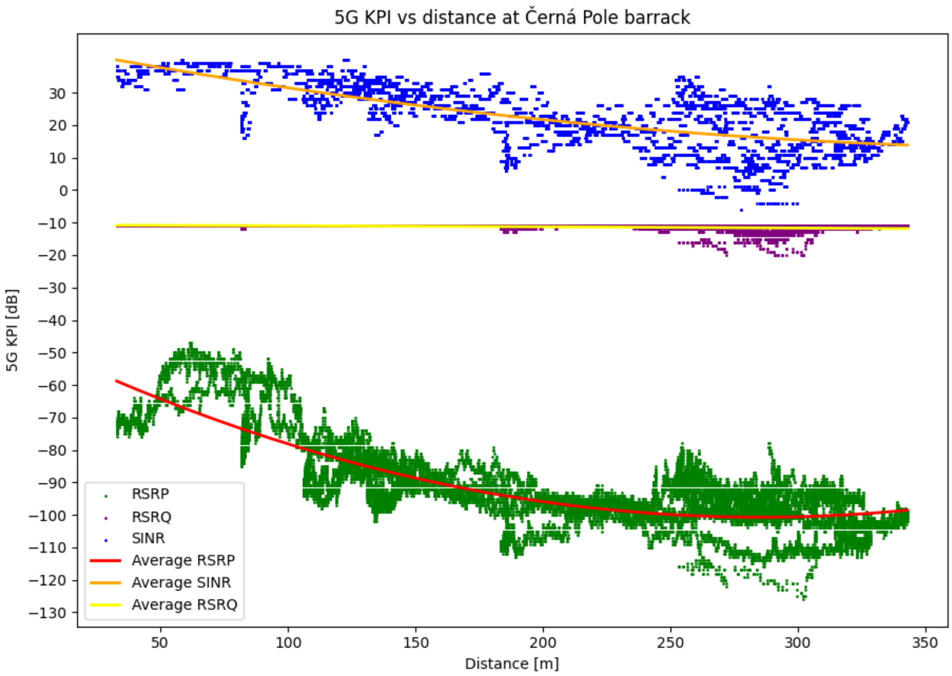

Fig.6.12 5G signal quality performance at altitude 15 m height vs distance from the 5G antenna at Šumavská barrack.

6.3 Scenario C: Remote control

Due to the favorable measurements of 5G signal quality parameters at the Šumavská barracks, the research has progressed to conducting experiments in UAV remote control utilizing a private 5G UNOB network. In this scenario, the GCS is positioned at the Černá Pole barracks, while the 5G-connected UAV operates within Šumavská barrack as shown in Fig.6.13. Communication between the GCS and the UAV is facilitated solely through 5G network links. At the GCS, operators are responsible for the supervision of control tasks, management of C&C data exchanges, which include telemetry and waypoints essential for the UAV's autonomous navigation by utilizing the GCS software QGroundControl. They also oversee real-time piloting, perform identity verification, authorize flights, and update navigation databases, among other duties. Moreover, the GCS receives application data, which encompasses video streams, images, and additional data from various sensors.

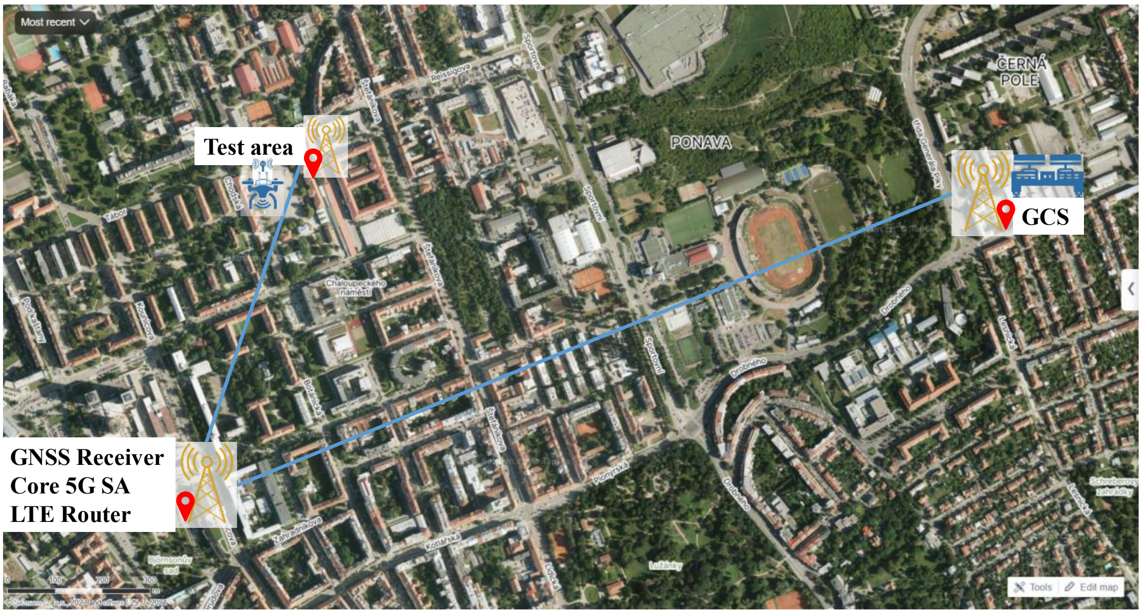

Fig.6.13 Scenario C: Remote control, edited from mapy.cz

The UDP protocol is used instead of TCP in QGroundControl station, because of its utility in supporting real-time and efficient UAV operations. Due to its connectionless nature, UDP minimizes communication delays and overhead, making it particularly suitable for this scenario where timely and continuous data transmission is critical, such as in UAV navigation and monitoring. UDP's simplicity allows for rapid data handling and the protocol's ability to multicast enhances its applicability in situations involving multiple receiving stations. By enabling data to be sent simultaneously to multiple locations, UDP ensures that all relevant parties receive crucial flight data concurrently, which is essential for synchronized operations and safety. Thus, despite lacking mechanisms for ensuring data reliability, UDP's speed and multi-receiver capabilities affirm its value in UAV control systems where performance and immediate data dissemination are crucial.

Fig.6.14 shows the setup connection to the 5G-connected UAV at Šumavská barrack from the GCS at Černá Pole barrack using QGroundControl software, users navigate to the Application Settings > Comm Links menu, add the UAV's SBC IP private 5G address as a UDP connection, and then use the "add server" button to complete the setup. Similarly, in Mission Planner, users select UDP as the connection type in the startup window and set a baud rate, typically 115200. Upon clicking the "connect" button, the connection is established.

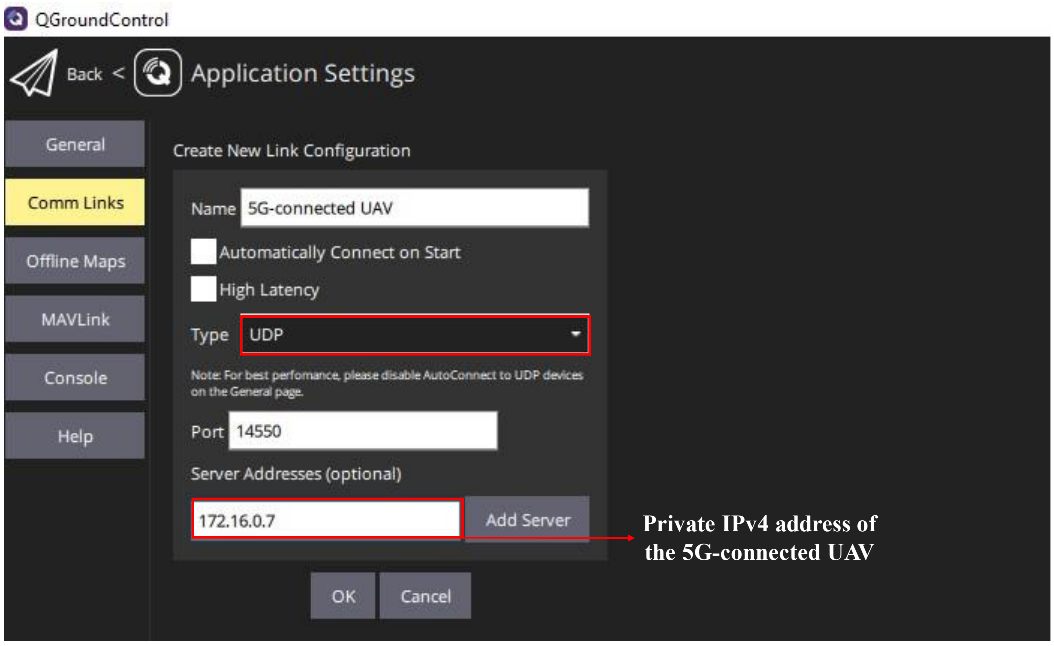

Fig.6.14 Example of the connection to the 5G-connected UAV from GCS by QGroundControl

With a basic flight setup as illustrated in Fig.6.15, the GCS uploads the mission plan to the UAV via the private 5G UNOB network. Throughout the flight, the UAV sends MAVLink state messages back to the GCS, maintaining a stable uplink throughput of 3 to 4 kBps during the tests, as depicted in Fig.6.16. The peak data rate observed was 3.568 kBps, with an average rate of 3.312 ± 0.095 kBps.

Fig.6.15 Preset flight waypoints at Šumavská barrack in QGroundControl from the GCS at Černá Pole barrack

Moreover, the UAV incorporates the NVIDIA Jetson AGX Orin Developer Kit to operate a camera server, which is pivotal for regular monitoring and surveillance tasks. Data throughput for this application, depicted with the blue line in Fig.6.16, is facilitated by video capture using a Sony IMX214 sensor, achieving a resolution of 1024 × 768, and pre-encoded with the H265 MPA codec. The maximum video data rate recorded is 5.457 Mbps, with an average rate of 5.196 ± 0.078 Mbps.

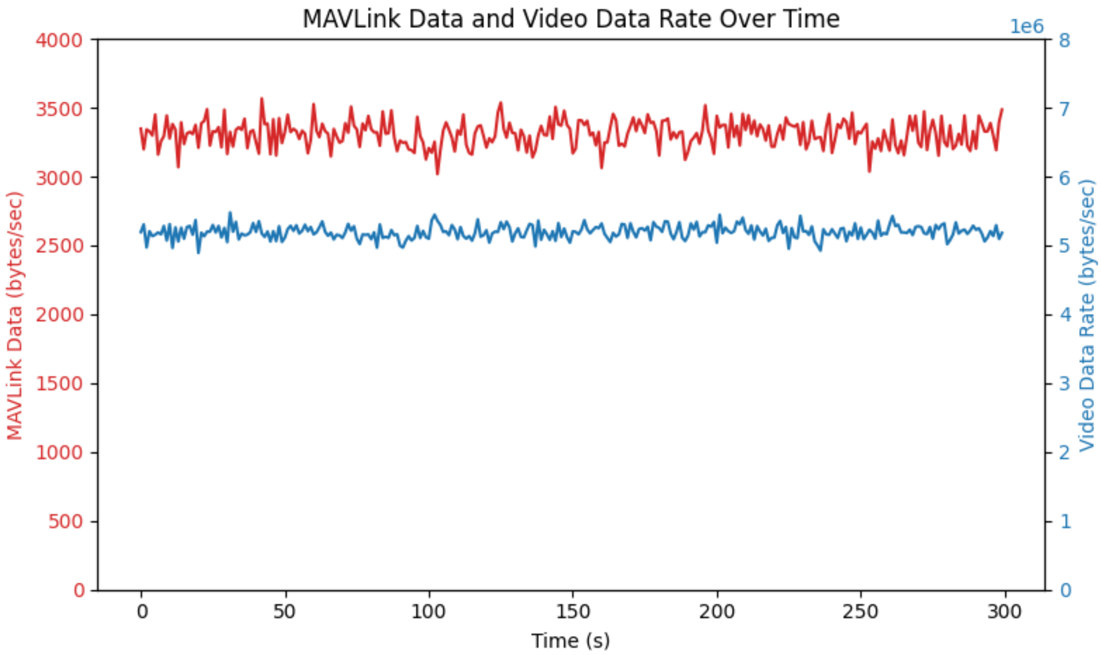

Fig.6.16 MAVLink state messages and video data rate between 5G UAV-GCS captured by Wireshark

Additionally, this study demonstrates the feasibility of deploying remote UAV control tasks within commercial mobile networks, utilizing a Virtual Private Network (VPN) to address connectivity challenges.

In commercial cellular networks, even when the GCS and the SBC on the UAV utilize different network operators, they can simply connect to the internet. However, each is typically assigned a private IP address by their respective carrier, which restricts direct connectivity due to the non-public nature of these addresses. This is a common issue when the GCS and UAV are on different networks and are unable to directly communicate over the internet due to private IP addressing [52]. To overcome this limitation, the use of a VPN is proposed as an effective solution. The diagram in Fig.6.17 explains the operation of this VPN setup. A server is set up with a static IP address, for instance, 35.236.55.229, which can be hosted on cloud platforms like Google Cloud Platform, Amazon Web Services, or Microsoft Azure, etc.

In the specified setup, once the UAV connects to the Vodafone network, for example, it is assigned a public IP address of 46.135.27.50, and similarly, the GCS obtains the IP address 46.135.20.10 upon connection. Both the UAV and the GCS run VPN client software that connects to the VPN server operating on the cloud server. This configuration allows both devices to receive VPN IP addresses: the UAV receives 10.6.0.6, and the GCS receives 10.6.0.8. With these VPN-assigned IP addresses, the UAV can directly communicate with the GCS using the IP address 10.6.0.8.

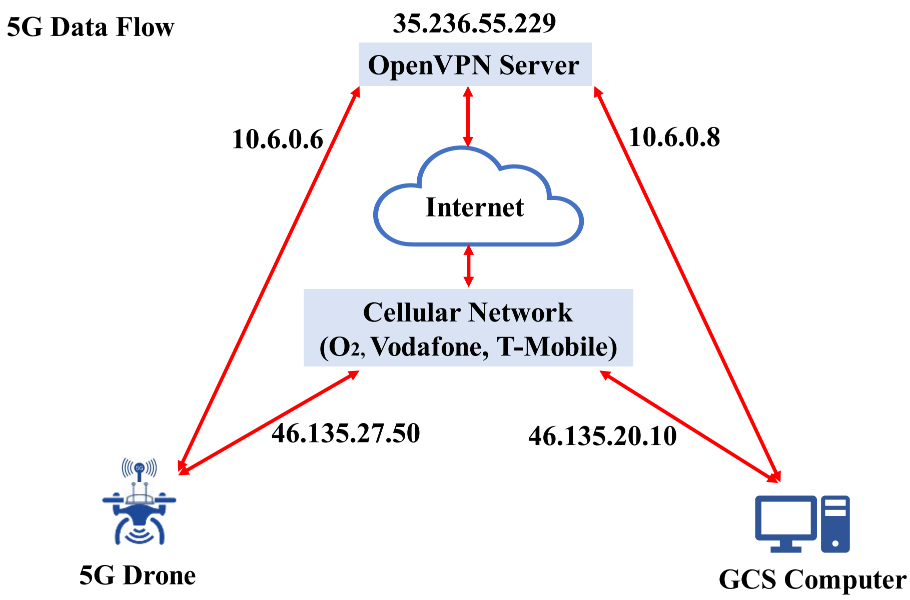

Fig.6.17 OpenVPN for remote control in commercial cellular networks, adapted from [52]

To ensure consistent IP addressing, which is crucial for reliable communication, each network endpoint (the UAV and the GCS) is assigned a unique security certificate. This certificate ensures that each time they connect to the VPN, they receive the same IP address, enhancing the stability and reliability of the remote-control connection. This method ensures seamless and secure communication between the UAV and GCS, crucial for effective remote operations in diverse network environments.

6.4 Scenario D: Autonomous flight using 5G

The findings from scenario B, showing the extent of antenna coverage, coupled with the consistent transmission of MAVLink messages in experiment C, indicate that autonomous flight methods through private 5G UNOB network can be implemented using the MAVLink protocol. This approach enables two types of automatic control: stationary and non-stationary.

The first method involves using fixed flight plans provided by GCS software like MissionPlanner and QGroundControl. In this method, UAVs execute predefined tasks without the ability to adapt to changes in their environment, such as avoiding obstacles or tracking objects, etc. Results from part C confirm that the private 5G UNOB network can effectively control UAVs in this manner.

The second method integrates flight planning either through the GCS or directly on the SBC installed on the UAVs. This setup allows UAVs to execute flight programs and receive control signals from the GCS, which processes data from cameras, LiDAR or other sensors attached to the UAV. These flight programs offer comprehensive control features and enable UAVs to transmit application data back to the GCS. The GCS then processes this data to send responsive control signals to the UAV.

During the tests in this scenario, an autonomous landing procedure is executed using two NVIDIA Jetson AGX Orin Developer Kits, one on the UAV and another at the ground station, employing control MAVLink statements from the Pymavlink library (Python library for MAVLink messages). The UAV navigated to a designated landing area and descended onto a target marked on the ground, as depicted in Fig.6.18. This scenario evaluates the ability to control 5G-connected UAV from GCS by processing application data transferred through private 5G UNOB network.

The landing target uses ArUco markers, as shown in Fig.6.19, which are binary square fiducial markers utilized for estimating camera pose. They hold significant potential for identification and three-dimensional localization [53], similar to QR codes but containing only identifiers. ArUco markers come in various configurations ($N \times N$, where N can be 4, 5, 6, or 7) but all feature a distinctive black border that aids in rapid detection and identification in images.

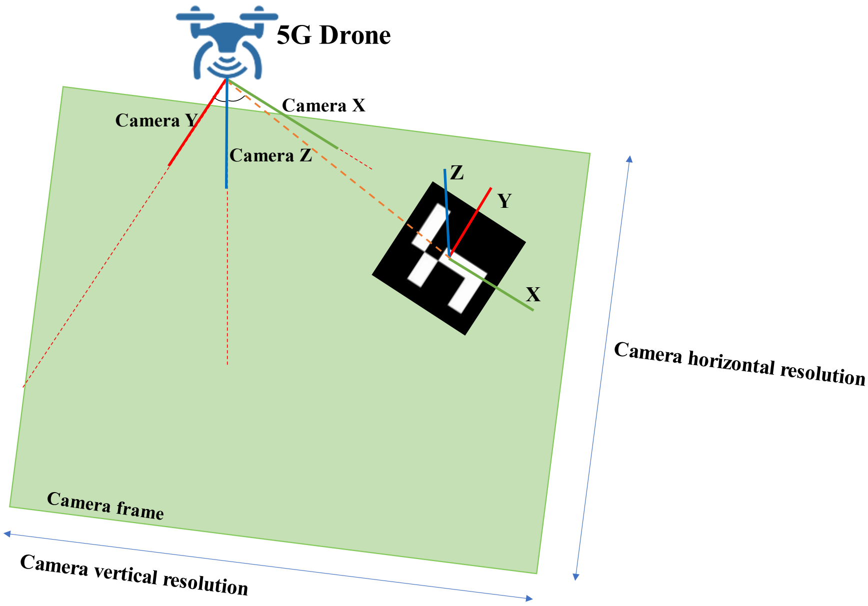

Fig.6.18 Visual representation of the landing target, adapted from [54].

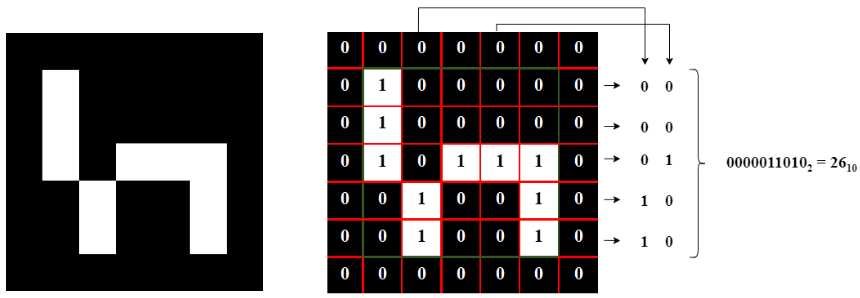

Fig.6.19 Example of an ArUco marker, ORIGINAL configuration library, and decoding [55]

The 5G-connected UAV's primary function is to capture images and transmit them to the GCS. Here, the GCS processes these images to detect landing targets using the OpenCV library and then communicates with the UAV by sending MAVLink messages to guide it back to the designated landing area. The transmission and reception of data, including images and MAVLink messages, are facilitated through the socket API for TCP. This protocol is chosen to ensure optimal data integrity and quality necessary for accurate image processing. The workflow of transmitting application data and MAVLink messages is illustrated in Fig.6.21 below.

OpenCV, or the Open Computer Vision Library, manages the image processing tasks. It calculates the poses and orientations of the markers relative to the camera's frame of reference. After processing the images, OpenCV outputs either the position of the ArUco marker within the image frame, specified as coordinates (x_{pixel}, y_{pixel}) in pixels, or the marker's relative position, denoted as P(x, y, z), with respect to the camera in meters. The used cameras need to be calibrated before the image processing. All the processes related to image processing, marker identification, detection and localization is executed in the SBC NVIDIA Jetson Orin on the GCS, as detailed in Fig.6.20.

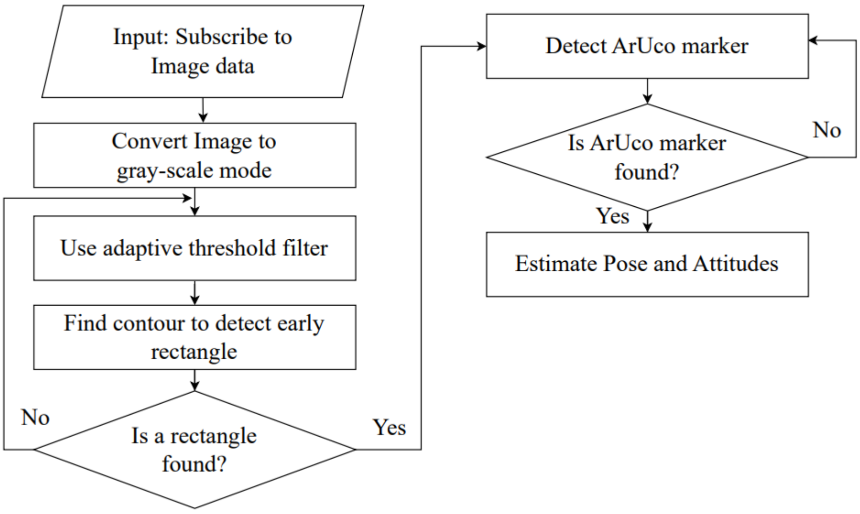

Fig.6.20 Image processing in GCS [55].

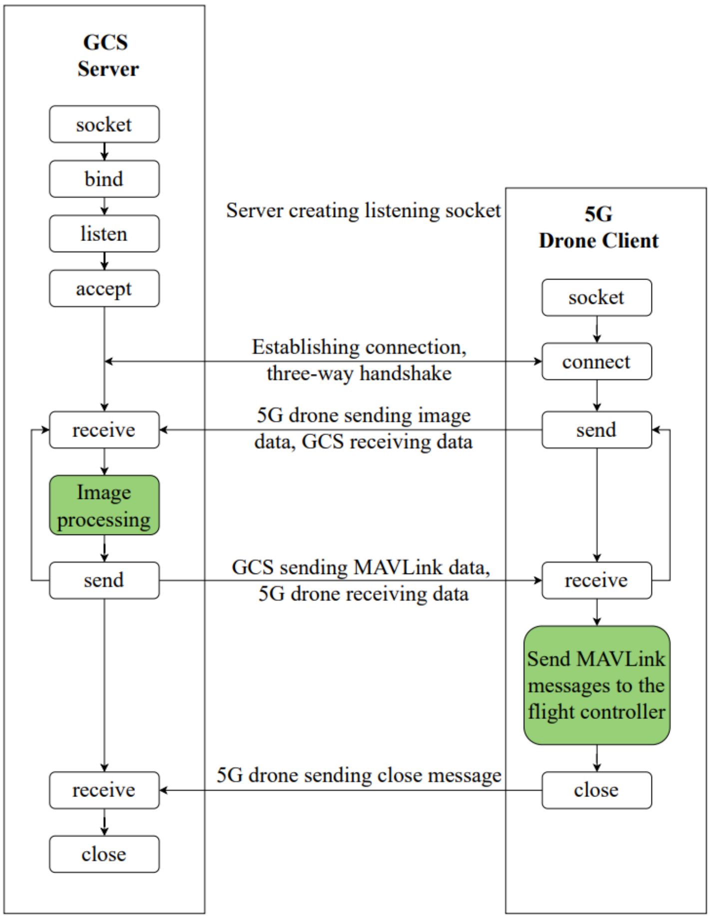

Fig.6.21 TCP flow socket between the GCS and the 5G-connected UAV, adapted from [56].

In this study, the most critical MAVLink control message utilized is the "*Landing_Target*". MAVLink version 2 allows this message to carry two types of parameters to guide the UAV towards the landing platform. The first parameter is the relative position, P(x, y, z), of the marker with respect to the camera, derived from the image processing output. The second parameter includes two angular offsets, *angle_x* and *angle_y*, which represent the x and y-axis angular deviations from the center of the image to the target, and a distance parameter, z, indicating the distance from the UAV to the marker.

To enable Precision Landing mode, a rangefinder must be active. This can be achieved through two methods: employing a physical rangefinder or configuring a virtual "MAVLink rangefinder". This project utilizes the latter, leveraging the depth parameter obtained from the ArUco marker. The algorithm employs a virtual distance sensor based on the *Distance_Sensor* message form within the MAVLink protocol. The configuration of this virtual rangefinder includes setting its minimum and maximum range distances. The altitude, represented by parameter z in $P(x, y, z)$, is estimated through the pose and attitudes of the ArUco markers and is transmitted via the MAVLink message during precision landing.

The frequency at which these MAVLink messages are broadcast is crucial for achieving the desired landing precision and speed. According to MAVLink documentation, the "*Landing_Target*" and "*Distance_Sensor*" messages should be broadcast at rates of 10-50 Hz and 5-20 Hz [57], respectively, to maintain effective control and accuracy during the landing process. To ensure this MAVLink messages rate, the camera sensor Sony IMX214 is set to capture video with resolution 640 × 480 and 30 FPS.

This study tested an autonomous mission based on the author's prior success in [41], [55] with an automatic landing mission using the MAVLink protocol. In the previous successful task, the video data (from the same Sony IMX214 sensor with this study) was processed directly on the NVIDIA Jetson Nano SBC (the basic version of the NVIDIA Kit line) mounted on the UAV, instead of being transmitted to the GCS via this 5G private 5G network. This study aims to investigate whether the private 5G UNOB network could support this type of mission, which requires MAVLink messages frequency at high speed and low latency.

However, the results showed significant delays when transmitting images from the UAV to the GCS and reconstructing them on the GCS server. Fig.6.22 indicates that most of the delay is due to video transmission and reconstruction at the GCS, with a minimum delay of 172.1 ms and an average delay of 357.99 ± 219.93 ms. In contrast, the image processing speed at the GCS ranged from a minimum of 1.68 ms to an average of 5.051 ± 1.08 ms. The latency for sending MAVLink messages from the GCS back to the UAV had a minimum of 8.40 ms and an average latency of 10.11 ± 3.33 ms.

These delays prevented achieving the required MAVLink message frequency for the autonomous precision landing task.

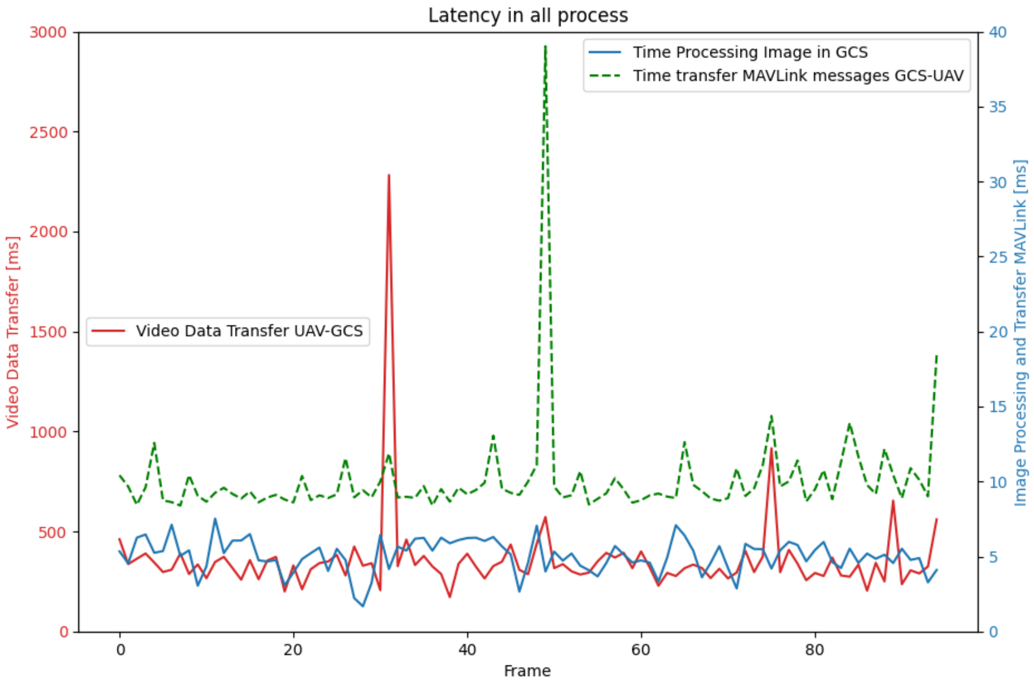

Fig.6.22 Latency in all process, contains the sending video data UAV-GCS, image processing in the GCS and sending MAVLink messages GCS-UAV.

To compare with the process when the video data is processed entirely on the SBC on the 5G-connected UAV, without involving the GCS, the SBC transmitted MAVLink messages (*Landing_Target* and *Sensor_Distance*) at a stable rate of 19 to 25 Hz (messages/s). Fig.6.23 compares the MAVLink messages rate (both two messages) between processing video data directly on the onboard SBC and processing it on the GCS.

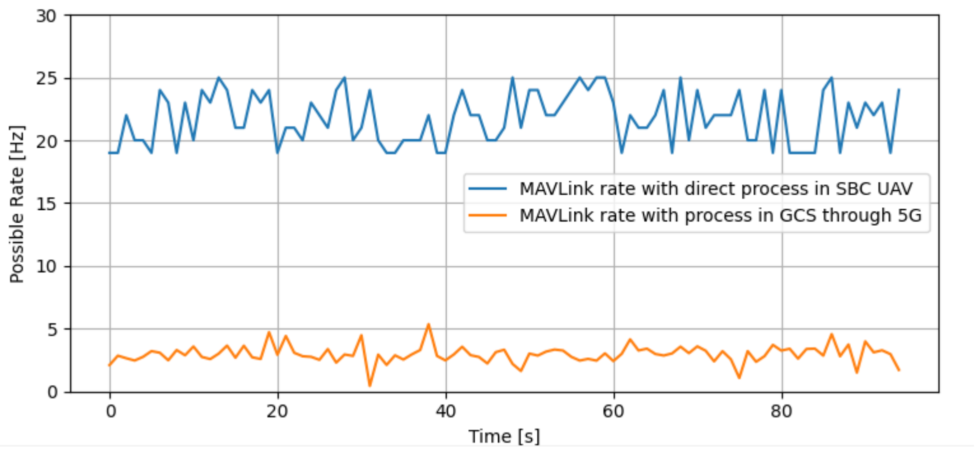

Fig.6.23 Comparison of the MAVLink messages rate

To clarify the influence of the delay on the accurate landing process using the MAVLink protocol, the experiment utilized a setup in Gazebo/ROS simulation. The significant delay prevents the UAV from promptly updating its relative position to the ArUco marker in the horizontal plane (Ox, Oy), causing it to repeatedly overshoot the landing target, as shown in Fig.6.24. This results in the UAV flying back and forth over the target, leading to instability and compromising flight safety. Fig.6.24 represents the UAV's relative position to the ArUco marker in the Ox and Oy directions (the red and blue lines) respectively.

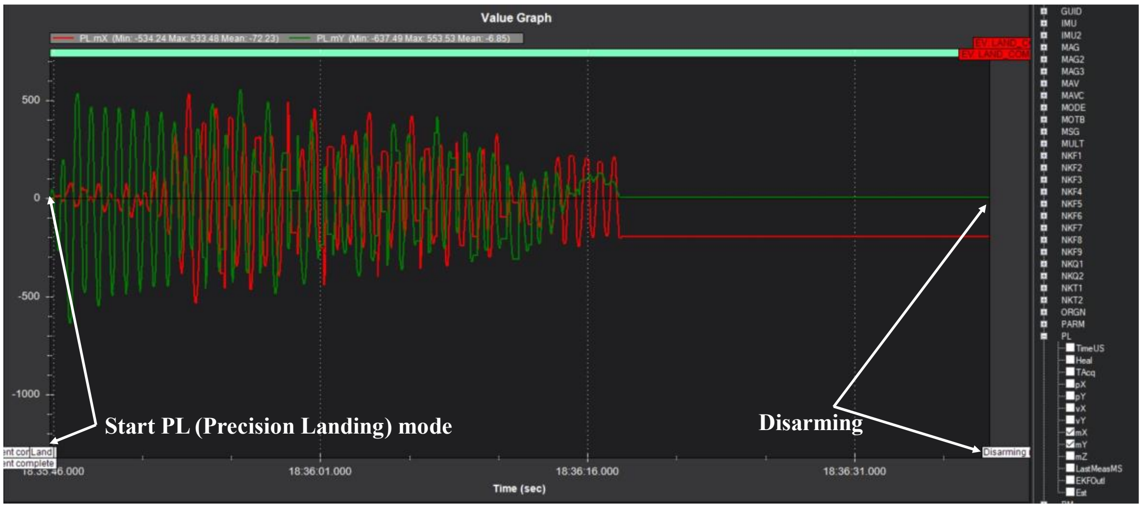

Fig.6.24 Relative position between the UAV and the landing target in MAVLink Precision Landing mode, video data transferring to GCS, results presented in Mission Planner.

With image processing done directly on the onboard SBC, without transferring to the GCS, the precision landing mode using the MAVLink protocol is achieved with minimal oscillation as presented in Fig.6.25.

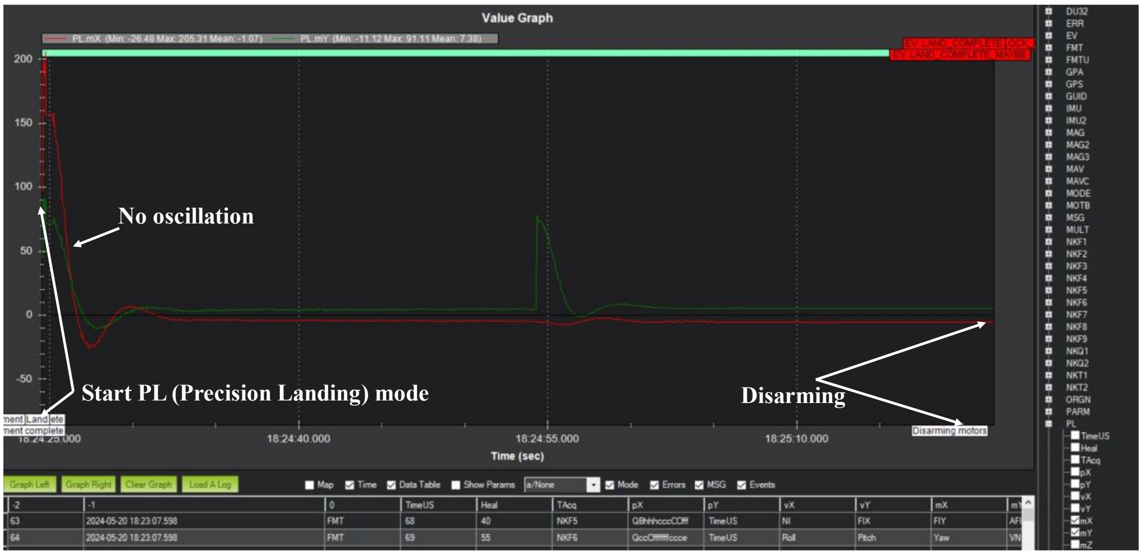

Fig.6.25 Relative position between UAV and the landing target in MAVLink Precision Landing mode, video data processing on the UAV, results presented in Mission Planner.

Thus, it can be concluded that for tasks requiring the UAV to interact directly with the environment and respond quickly, such as detecting landing destinations, the experiments in this thesis have demonstrated that the latency is too high. This makes it impossible to perform these tasks with the author's current setups, programs, and the current state of the private 5G UNOB network.

For tasks that do not require real-time interaction with the environment, the private 5G UNOB network can effectively transmit flight missions from the GCS to the UAV, as shown in Scenario C, or send application data one-way from the UAV to the GCS. For flight missions that require high interaction with the environment, the application data from different sensors onboard should be processed directly on the UAV's SBC.

7. UAV COMMUNICATION SECURITY

This chapter offers an overview of security in UAV communications, focusing both on general practices and specifically on those employed in 5G-connected UAVs. Additionally, it introduces security measures specific to the private 5G UNOB network. The discussion underscores the importance of 5G communication as a foundational element in ensuring that connections between UAVs and GCS maintain the highest level of security.

7.1 Security in UAVs communication

The main communication links of the UAV communication system are between the GCS and the flight controller (GCS – UAV) and between the flight controllers (UAV – UAV). Information flow in the UAV system is presented in Fig.7.1. As mentioned in Chapter 1, since all the communication channels are wireless, it suffers from security weakness.

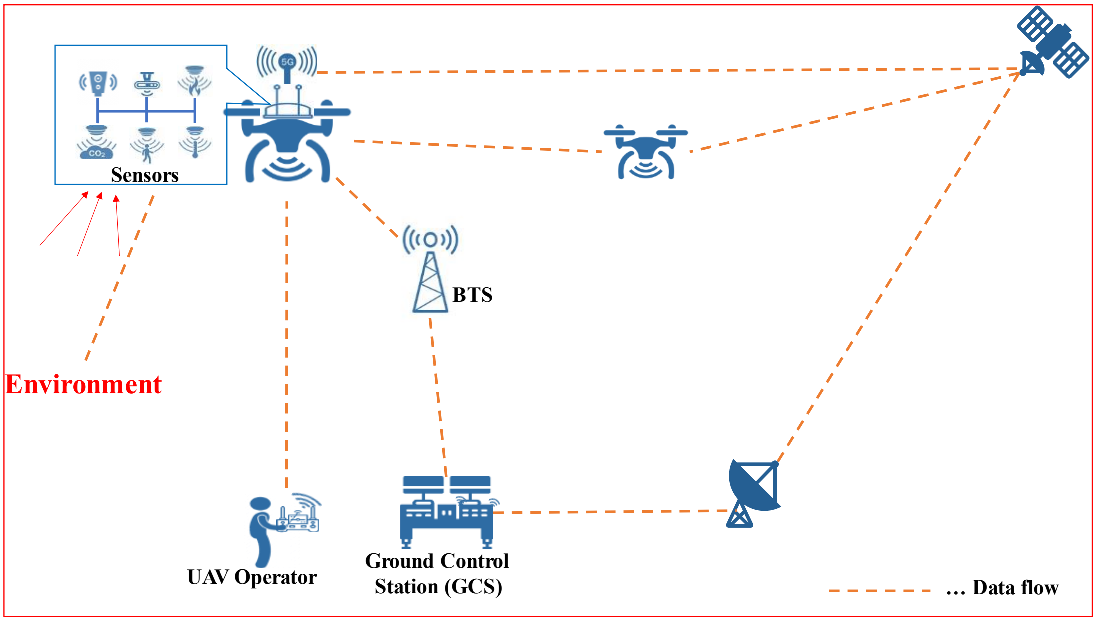

Fig.7.1 Information flow in UAVs-GCS system

In this study, UAV communication based on MAVLink protocol is set up on a private 5G network. Therefore, aspects of MAVLink protocol security and security on the private 5G UNOB network are considered.

7.1.1 Security requirements

According to [46], [58], this study summarizes the most critical requirements for securing MAVLink protocol and 5G communications, which include confidentiality, integrity, availability, authentication, non-repudiation, authorization, and privacy. These elements are essential to ensuring the robustness and trustworthiness of communication systems.

Information confidentiality ensures that private data is exchanged securely between parties. It safeguards against unauthorized leaks of sensitive information within the network between a 5G-connected UAV and a GCS. This protection is crucial as it prevents potential adversaries from intercepting commands sent from the GCS to the UAV, and vice versa.

Information integrity ensures the C&C data, as well as application data exchanged between GCS and the UAV, remains unchanged and uncorrupted, whether accidentally or deliberately. This protection is crucial to guard against unauthorized modification of information.

Availability is the ability in which the communication between the UAV and GCS remains constant and accessible, even during system failures or attempts by attackers to disrupt the communication channel. Continuous operation and maintenance are essential to keep the system running reliably without interruptions. The service must also be consistently available to meet the demands of users or operators at the GCS.

Authorized access means that only specifically allowed UAVs and GCS, in this case, which are connected to the private 5G UNOB network with designated SIM cards and assigned IP addresses, have permission to access and exchange C&C and application data.

Authentication within the private 5G UNOB network is crucial as it involves multiple entities interacting and sharing information. It is necessary to confirm the identities of these entities and the origin of the information, ensuring that all communications are legitimate. This process helps the 5G Server (CORE) verify that data received is indeed from a credible source. The details of this authentication process will be elaborated in the following sections, particularly regarding wireless communication security.

Non-repudiation ensures that key parties, such as the GCS and UAV, cannot deny their participation in sending or receiving data.

Privacy protects sensitive communication details and conceals the identities of the UAV and GCS from potential eavesdroppers. The data exchanged, including sensitive MAVLink parameters and private 5G signals, must be kept confidential, especially in sensitive environments like military operations to prevent unauthorized access.

7.1.2 Possible security threats

In the absence of an encrypted channel, when MAVLink interfaces with other communication forms such as radio links, satellite links, or ad-hoc networks, it lacks inherent security procedures. Specifically, MAVLink does not natively offer the CIA (Confidentiality, Integrity, and Availability) security services. Consequently, the GCS communicates with UAVs over an unauthenticated and unencrypted channel. This openness renders MAVLink susceptible to various malicious attacks. These attacks can be categorized as Interception (Attacks against the systems confidentiality), Modification

(Attacks against the system integrity), Interruption (Attacks against the systems availability) and Fabrication (Attacks on authenticity) [46], as illustrated in Fig. 7.2. Additionally, 5G communication also faces one more kind of threat from insider attack vectors, as indicated in Fig. 7.2.

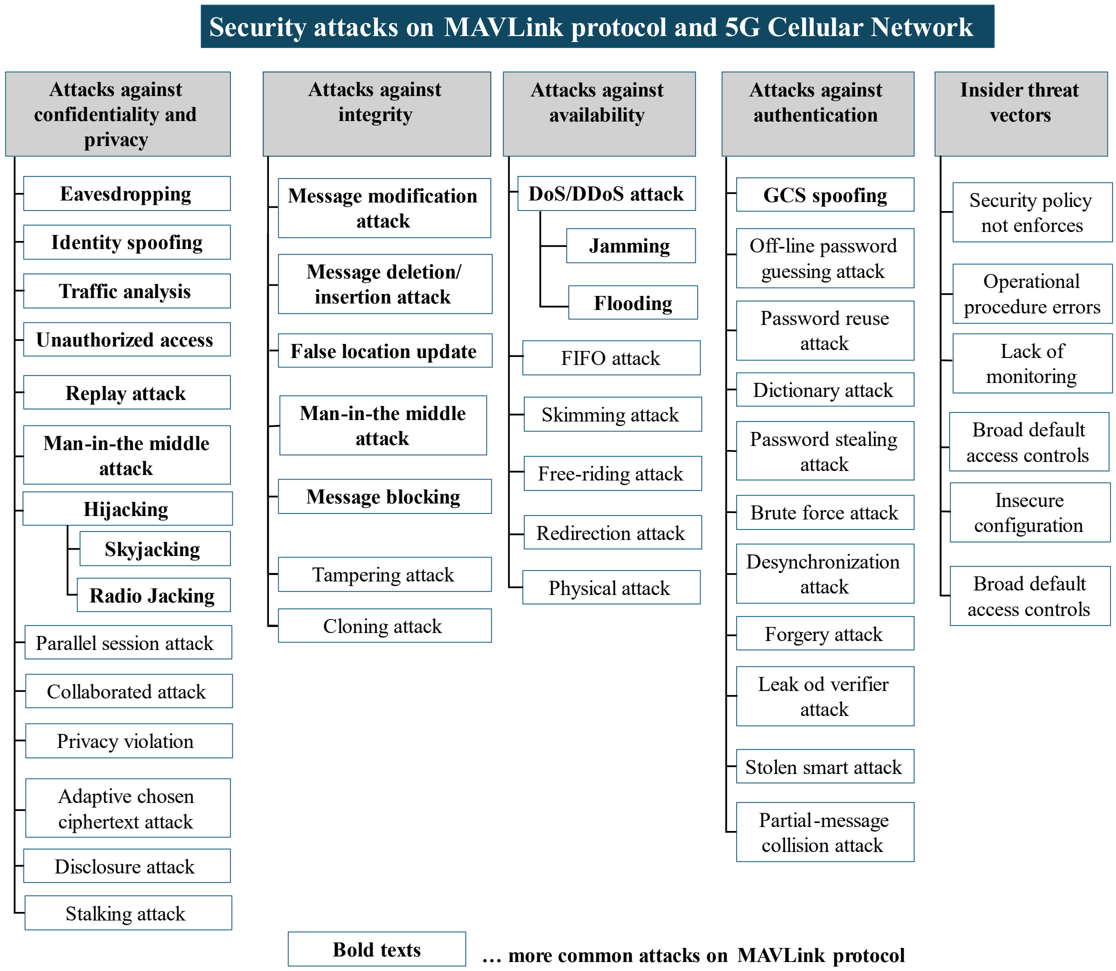

Fig.7.2 Security attacks on MAVLink protocol and 5G cellular network, adapted from [46], [59]

This study highlights the common and popular attacks in both MAVLink protocol and 5G network:

1, Confidentiality and privacy attacks: In this type of attack, an intruder gets unauthorized access to confidential and sensitive information by intercepting data, commands, or messages between UAVs and the GCS. These incidents breach both confidentiality and privacy. Common forms include eavesdropping, identity spoofing, traffic analysis, Man-in-the-middle (MITM) attack, and unauthorized access, often due to security weaknesses in the MAVLink protocol.

Eavesdropping (Communication capture): In this attack, the attacker listens to the communication between UAVs and GCS, eavesdropping on the information exchanged between UAVs and GCS directly from the open environment. After capturing the C&C data sent from GCS to UAVs, the attacker can use these data for more other attacks like replay, traffic analysis or a fabrication attack.

A Man-In-The-Middle (MITM) attack is a significant threat to both the MAVLink protocol and 5G communications. This type of attack exploits MAVLink messages that are sent in plain text in an unencrypted channel without 5G, which become vulnerable when an MITM successfully intermediates the communication channel between UAVs and the GCS. Positioned between the UAVs and GCS, the attacker listens to the data exchanged, can reconstruct MAVLink commands, replay previously recorded packets, alter control commands, and send these corrupted data back to the GCS or the UAV. An MITM attack compromises not only the confidentiality and privacy but also the integrity of the information exchanged between the UAVs and GCS.

Additionally, MITM can easily take UAVs' control, catch, and withhold the UAVs, which is called hijacking. The hijacking contains: *skyjacking* – attack in the WiFi connection to hack UAVs by using airplay-ng software to force disconnecting UAVs-GCS, *radio jacking* – attack in the telemetry via MAVLink protocol if an attacker recognizes the NetID field. However, both these hijackings are not mentioned in any reports about security 5G-connected UAVs.

Identity spoofing: The MAVLink protocol uses the Systems IDs to identify the UAV which sends or is expected to receive the messages, as detailed in Section 4.2.2. Natively, System IDs parameter is not encrypted with the MAVLink messages. Thus, an attacker can compromise the communication link to get the identity of the sending system. This attack can be a first step for attackers to get unauthorized access or to be a MITM.

Traffic analysis represents a type of passive attack where an intruder collects data exchanged over the network to uncover patterns within the 5G network and the communications between UAVs and GCS. This method allows the attacker to gather sensitive information that could be exploited in further attacks.

Unauthorized access: If an attacker gets the information about System IDs (SYSID) or Component IDs (COMPID), he can easily get access to the communications between the UAVs and GCS by duplicating these parameters in a malicious UAV.

2, Integrity attacks aim to modify the data being sent. The attackers try to negatively alter MAVLink messages by modifying them or inserting wrong data into them.

Another kind of this category attacks is false location update. It is a subset of the modification messages attack when the attackers send spoofed MAVLink GPS message containing wrong GPS data sent from UAVs to GCS. This attack makes the operator on the GCS believe that the UAVs are in another location or are following wrong trajectories.

3, Availability attacks: are the type of attacks that compromise the availability of MAVLink and private 5G connections can occur through disruptions in the link used for data exchange between 5G-connected UAVs and the GCS. These disruptions can be executed in several ways, notably through jamming, deletion of critical data, falsification of signals, and Denial of Service (DoS) or Distributed Denial of Service (DDoS) attacks. These methods directly interfere with the communication channels, impeding the operational capabilities of the UAVs and GCS.

A successful DoS attack can lead to a MITM attack. In such an attack, the intruder transmits unauthorized commands in an infinite loop to the UAV or initiates a flooding attack by sending a huge number of various packets in the communication link. This disrupts communication between the GCS and the UAVs, preventing legitimate commands from being executed, as the UAV is continuously occupied with commands issued by the attacker. Consequently, a DoS attack against the UAV makes it unresponsive to the GCS, or vice versa, due to the compromised availability of the system.

Jamming attacks occur when an attacker disrupts the communication link between UAVs and their GCS. This type of attack results in the loss of communication and the state of *lost link*, preventing the controller from functioning properly. Consequently, this leads to the unavailability of services, as the UAVs can no longer receive crucial operational commands or transmit data back to the GCS.

4, Authenticity attacks aim to deceive the GCS or UAV into accepting falsified data as authentic. The authenticity of a MAVLink message can be compromised when malicious data is fabricated to replace legitimate information. Fabrication attacks encompass tactics such as creating counterfeit data and spoofing the GCS, misleading the system into erroneous actions or responses.

7.2 Security in private 5G UNOB network with UAV communication

The private 5G UNOB cellular network, provided by Ericsson Private 5G, is a wireless cellular radio network that incorporates all essential security features of 5G cellular technology as per the 3GPP SA3 standards [60].

Additional fundamental security mechanisms are also adopted from various standards developing organizations (SDOs). For example, the IETF defines essential security protocols like IP layer security (IPsec), Extensible Authentication Protocol (EAP), and Transport Layer Security (TLS), all of which are integrated into the 5G security architecture [61]. The network architecture of 5G, which leverages cloud and virtualization technologies, is further secured by ETSI ISG NFV's guidelines for network functions virtualization. Cryptographic solutions such as the Advanced Encryption Standard (AES) are standardized by the US National Institute of Standards and Technology (NIST). Furthermore, the NESAS framework for security assurance represents a collaborative effort between 3GPP SA3 and GSMA, which also covers interconnect and operational security issues in mobile networks. Additionally, the cloudification of open RAN and their associated security challenges are addressed by the O-RAN Alliance.

In this study, the author focuses specifically on the basic security mechanisms within the private 5G UNOB network, without delving into the comprehensive details of 5G security. This approach ensures compliance with copyright laws by avoiding the disclosure of proprietary information from Ericsson.

7.2.1 Authentication by SIM cards

Similar to public commercial cellular networks, the private network at UNOB is secured using Subscriber Identity Module (SIM) cards, as example in Fig.7.3. These SIM cards are written by local system administrators using a SIM card writer and are physically connected to one of the Ericsson Private 5G network controllers. They are managed through the Network Management Portal (NMP), as presented in Fig. 7.4. Only devices equipped with a valid SIM card are permitted to connect to the Ericsson Private 5G network. Each 5G-connected UAV and terminal device on the GCS is equipped with an authorized and active SIM card. When a device containing a SIM card is active, its status can be readily monitored by the administrator via the NMP.

Fig.7.3 Ericsson Private 5G SIM card

The actual identifier within private 5G UNOB network is the SIM card, not the device into which the SIM card is inserted. If a SIM card is locked to a specified device through the NMP, it can only operate and remain active on that designated device. Conversely, if someone acquires an approved SIM card that is not locked to any device, it can be used in any device, thereby granting that device the same access and privileges as the original device from which the SIM card was removed.

To ensure the integrity of a device is maintained, administrators can use the NMP to enable SIM-to-Device locking, which pairs a specific SIM card (IMSI/SUPI) with a specific device (IMEI). If this configured pair is disrupted, the SIM card will be locked out and disconnected from the system, triggering a security event.

The physical security of any device holding a provisioned SIM card is crucial, especially when there is a need to transfer the SIM card from one device to another. Both the UAV's pilot and the administrator at the GCS must periodically control and verify the authenticity and validity of all devices that contain an active SIM card.

7.2.2 Security architecture with cloud management

The Ericsson Private 5G site equipment consists of radio equipment and other hardware to run the network, for example at UNOB two network controllers as shown in Fig.7.4. It is important to keep these units protected to minimize the risk of someone tampering with the cables or connecting other equipment to the Ericsson Private 5G system.

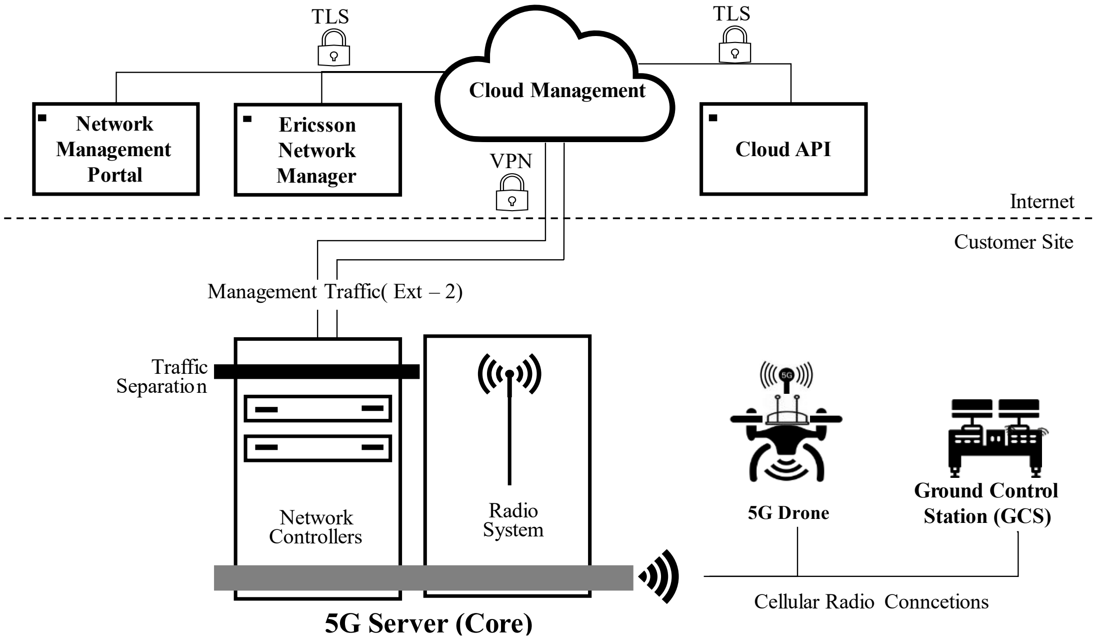

Fig.7.4 Internet and Local Network Access Information, adapted from [62]

The cloud-management connection is used for communication with some Ericsson services and some third-party services. A firewall is also used on this connection to minimize the attack surface of the Ericsson Private 5G equipment and protect the two network controllers. The two network controllers are compact, lifecycle-managed networking appliances that are implemented as a pair of redundant servers, enabling high-availability capabilities.

The Network Management Portal (NMP) is run in the management cloud environment. The role of NMP is helping users of Ericsson Private 5G with installation, configuration, management, and monitoring of their wireless networks. For instance, Fig.7.5 illustrates the active SIM cards (5G devices) on the interface of the NMP.

By monitoring all the private 5G network on NMP, administrators' network and operators on UAVs-GCS system can easily verify the connection of UAVs and GCS to 5G network, monitor and analyze the data traffic between UAVs and GCS. This is crucial to minimize all the security threats mentioned in the previous section. Fig.7.6 depicts the data traffic analyzation of the UAV throughput in the NMP.

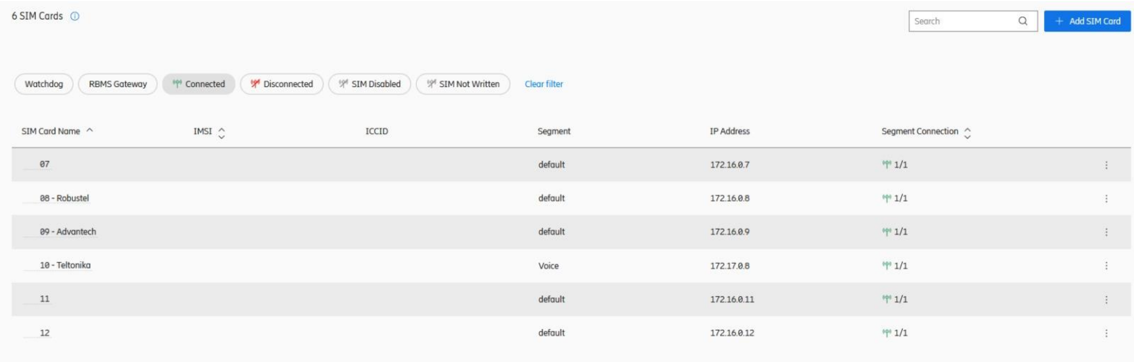

Fig.7.5 NMP monitoring active SIM cards.

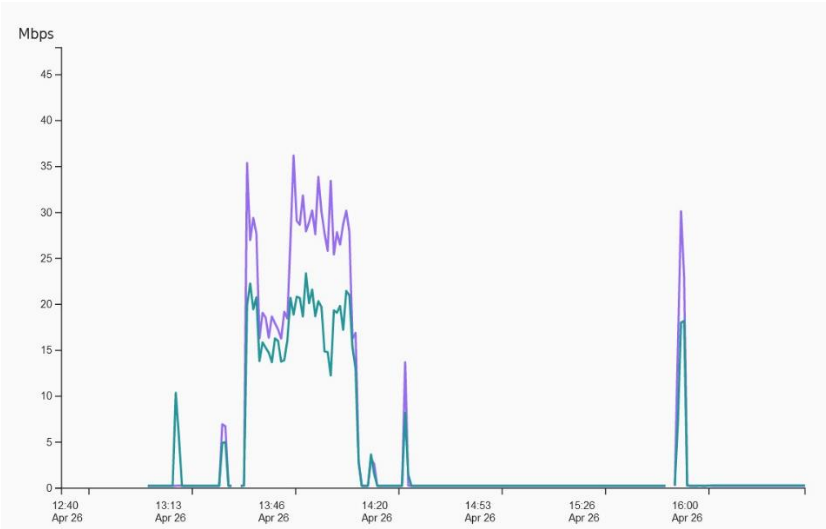

Fig.7.6 NMP analyzes UAV data traffic.

Only the administrator of private 5G UNOB network can access NMP. The strong password requirements, in accordance with the standard National Institute of Standards and Technology (NIST) 800-63b, secure the strength of user account passwords. Secure sign-in method with individual user credentials and Multi-Factor Authentication (MFA) using the Time-based One-time Password (TOTP) algorithm. Valid TOTP providers are Microsoft Authenticator, Google Authenticator and Symantec VIP Access. The security configuration allows protection against brute force attacks on passwords. The mechanism here is logon with wrong passwords leading to locking the account for a time period and increasing lock-out time with the number of failed attempts.

7.2.3 Wireless communication security

Wireless communication security in private 5G UNOB network contains three main parts, which are primary authentication, service-based architecture, and integrity protection of the user plane [62].

When the SBC and the computer on the GCS connect to the private 5G network for the first time, the primary authentication based on different types of credentials besides the credentials stored in the SIM card is initialized. This authentication includes certificates, pre-shared keys, usernames, and passwords.

Depending on the services, the private network supplies different levels of security, which is called Service-based architecture. Higher protocol layers of the ISO/OSI model, e.g. transport and application layer, are given more protection. For the C2 signal using User Datagram Protocol (UDP) protocol (transport layer) and Real-Time Streaming Protocol (RTSP) (application layer) using TCP protocol, which are mostly used in this project, the service-based architecture security is a vital key to protect the air-to-ground connection.

The data exchanged between UAVs and the server on GCS is transferred with suitable rates for each device and ensures its integrity and encryption.

The 5G NR system has the security mechanisms specified by SA3 in TS 3.501 [63], as mentioned at the beginning of this section.

8. EVALUATION

This chapter provides a more detailed evaluation of the potential and limitations of the test results, offers recommendations for UAV applications suited to these findings, and outlines possible directions for future work.

8.1 Test results – Potential and limitations

According to the test results presented in Chapter 6, the private 5G UNOB network fully meets all the UAV communication requirements specified by 3GPP [4], as outlined in Chapter 1. The 3GPP TR 36.777 standard specifies a command and control (C&C) data rate of 60 – 100 kbps and a latency of 50 ms, both of which are comfortably achieved by the private 5G SA UNOB network, with the network even surpassing these rates. Regarding application data, the private 5G UNOB network meets all requirements listed in Table 8.1 below.

Table 8.1 Communication requirements for typical UAV application [6]

UAV Application	Height coverage [m]	Payload traffic latency [ms]	Payload data rate (DL/UL)
Drone delivery	100 m	500 ms	300 Kbps/200 Kbps
Drone filming	100 m	500 ms	300 Kbps/30 Mbps
Access point	500 m	500 ms	50 Mbps/50 Mbps
Surveillance	100 m	3000 ms	300 Kbps/10 Mbps
Infrastructure inspection	100 m	3000 ms	300 Kbps/10 Mbps
Drone fleet show	200 m	100 ms	200 Kbps/200 Kbps
Precision agriculture	300 m	500 ms	300 Kbps/200 Kbps
Search and rescue	100 m	500 ms	300 Kbps/6 Mbps

The private 5G UNOB network, while not intended for civilian use, can effectively meet the requirements for payload traffic latency and data rates in UAV wireless communication, except in scenarios involving access points and drone filming. However, the coverage at higher altitudes remains uncertain, presenting the first limitation noted in this thesis. Test flights were conducted at altitudes no greater than 30 m above ground, due to taking into consideration flight safety, urban flight restrictions, and the VTOL drone's operational constraints under the supervision of the UNOB. Additionally, as mentioned before, these tests complied with the Czech Civil Aviation Authority (CAA) regulations and the EU Regulation 2019/947 set by the European Union Aviation Safety Agency (EASA). Consequently, this study does not explore how 5G KPI indicators vary with flight altitude. Compare to findings in LTE networks as cited in [24], Lassi Sundqvist showed the RSRP parameter initially increases to the maximum and then declines, this study observed minimal changes in RSRP and throughput at altitudes below 30 m in both vertical and horizontal flights.

Secondly, this research is constrained to the specific settings of the private 5G network at UNOB. The results might differ in other environments or with different hardware configurations, and our testing did not account for extreme conditions such as signal interference, potentially limiting the applicability of our findings.

Thirdly, the issue pertains to the mobility of the GCS server. Flight designs that involve the GCS outdoors are observed to have reduced UAV-GCS throughput compared to configurations where the GCS server is positioned at the 5G CORE.

Finally, as the private 5G UNOB network is newly established and still undergoing testing, this research represents one of its initial evaluations. Numerous challenges such as hardware selection and integration of peripheral devices for connection to this private network have been encountered.

When comparing with other studies, although the throughput measurements from both vertical and horizontal UAV-GCS flights align closely with those reported by Festag et al. [34], measuring end-to-end throughput across the T-Mobile commercial mobile network in Germany, involving 6 BSs, these results fail to meet the technical performance specifications for 5G as outlined in Table 5.1, Section 5.1. Specifically, for the 5G eMBB use case, the UL and DL requirements are 10 Gbps and 20 Gbps, respectively, with a user plane latency of no more than 0.5 ms. It is important to note the significant differences in definitions between the ITU [49] standards and this study's end-to-end measurement approach, detailed in Section 5.1.2.

Based on the key findings and evaluation, the author recommends that UAV applications with similar parameters to those in this research can be successfully implemented in Table 8.1. Essentially, the 5G-connected UAV can be remotely controlled within the coverage area of 5G base stations to execute predefined tasks. However, it lacks the capability to adapt to environmental changes, such as avoiding obstacles, tracking objects, etc. While application data can be transmitted to the GCS via the 5G connection, the latency observed does not support real-time control based on this data for missions that require high-frequency MAVLink messages.

8.2 Future work

The findings of this thesis, along with its limitations, suggest several areas for future research:

- Conduct tests on UAV 5G wireless communication across various environments, including both civilian commercial cellular networks and private 5G UNOB networks, and compare these in urban versus rural settings under different interference conditions.

- Explore the long-term stability and security of civilian commercial mobile networks and private 5G UNOB networks, particularly in relation to their connections with 5G-connected UAVs.
- Examine the potential of integrating 5G technology with other established communication technologies in UAV applications.
- For the private 5G UNOB network, consider positioning the server for the GCS at the CORE. While this may not address the mobility issue of the GCS, it could alleviate problems related to data throughput.

9. CONCLUSION

As explored in Chapter 1, a comprehensive study on UAV wireless communications was undertaken to delineate various types of wireless communications for UAVs, highlighting their respective advantages and disadvantages. This analysis is crucial in understanding why cellular networks, especially 5G, are increasingly considered a better choice for UAV applications. The ongoing development of cellular technologies and the expansion of research into integrating cellular networks into UAV communication, as discussed in Chapters 2 and 3, highlight the importance and practicality of this type of connection in UAV communications.

This thesis primarily focuses on the deployment and evaluation of a private 5G UNOB network for UAV communication and control. The key accomplishments of this thesis are summarized as follows:

- Testbed development: A testbed setup for a 5G-connected UAV and GCS was successfully established. This setup encompassed both hardware on the UAV and GCS, along with detailed software configurations. Significant challenges in hardware integration and driver installation for 5G modules were encountered and overcome, as detailed in Chapter 4. The careful selection and optimization of 5G modules within the private 5G network were crucial. The software selected met the measurement and compatibility requirements with the chosen hardware, aligning with the research objectives and available resources.
- Private 5G UNOB network exploration: The thesis introduces the concept of the private 5G UNOB network, detailing its data flow and the functional network devices employed in UAV control and measurement tests. Insights from Chapters 2, 5, and 6 illustrate the network's efficacy in urban settings for all conducted tests and measurements, answering the question of the feasibility of real-time UAVs control via 5G at extended distances.
- Parameter measurement and evaluation: The research established key parameters to assess the quality of the 5G signal and end-to-end Quality of Service (QoS), specifically for 5G UAV-GCS communications. These included key performance indicators such as RSRP, SINR, and RSRQ, as well as throughput and latency metrics. A tailored measurement program was developed to systematically assess the quality of the private 5G UNOB network.
- Test scenarios and results: The measurement program was executed across various test scenarios. Results indicated that at an altitude of 30 m, there was no significant decline in downlink and uplink throughput, nor in the 5G signal parameters, as the altitude of the 5G-connected UAV varied. Both vertical and horizontal flights demonstrated this stability. However, at greater distances from the 5G base station, uplink performance varied significantly, though downlink quality remained high. The study also highlighted how signal quality deteriorates with increased distance

from the antenna due to energy attenuation, exacerbated by urban infrastructural elements like physical obstructions.

- Antenna coverage evaluation: The coverage of each 5G antenna at Černá Pole and Šumavská barracks was analyzed. It was determined that optimal signal quality for controlling 5G-connected UAVs within the private 5G UNOB network occurs within 150 m of the antenna, where RSRP exceeds -80 dBm and SINR surpasses 25 dBm. The smaller, obstacle-free UAV testing area at Šumavská barracks facilitated superior signal integrity compared to Černá Pole.
- Remote control verification: The study confirmed the feasibility of remote UAVs control via the private 5G network under conditions of adequate signal quality. Additionally, in civilian commercial cellular networks, remote control was also achieved through the establishment of an OpenVPN Server to facilitate UAV-GCS connectivity.
- Autonomous control of 5G-connected UAV: The study developed a program to evaluate the potential for autonomous UAV control via 5G, utilizing application data from onboard sensors. The requirement for a high frequency of control messages, such as those using the MAVLink protocol, highlighted the challenges of achieving real-time control with the existing hardware and software configuration. This limitation presents significant challenges that warrant further investigation in future research to enhance the responsiveness and effectiveness of autonomous UAV operations.
- Security in UAV-GCS communication within private 5G UNOB network: The thesis addressed the specific security requirements for 5G UAV-GCS connectivity, identifying potential security risks and proposing corresponding mitigation strategies. Additionally, it elucidated how the private 5G UNOB network addresses general security concerns and specifically fortifies UAV communications against vulnerabilities. This comprehensive analysis of security measures ensures a robust framework for safe and secure UAV operations within the private 5G network context.

This master's thesis presents a comprehensive investigation into the control of UAVs via the 5G network, specifically using the private 5G UNOB network. The study addresses a range of issues essential for achieving effective UAV control through 5G, including the selection of appropriate hardware and software, assessing network quality, and the control of UAVs in real-world flight tests within this network environment, as well as evaluating security measures.

The author confirms that the objectives set out at the beginning of this research have been met, marking this work as one of the first studies in the application of UNOB's private 5G network for UAV control when this network has been recently deployed. Despite facing numerous challenges and encountering some imperfections inherent in a novel area of study, significant progress has been made.

Looking forward, there are several areas identified for future research which include optimizing software programs, addressing latency issues, testing UAV 5G wireless communication across different environments, evaluating in urban and rural settings under varied interference conditions, etc. These enhancements will continue to build on the foundation laid by this thesis, advancing the capabilities and reliability of 5G-connected UAVs in complex operational environments.

LITERATURE

[1] GSMA, ‘A look into the future of mobile-enabled drones’, 2019, Accessed: Oct. 26, 2023. [Online]. Available: https://www.gsma.com/iot/wp-content/uploads/2019/02/22166-Connected-Drones-Infographic-v3-002.pdf

[2] Inc.com, ‘With 1 announcement, the FAA just created an $82 billion market and 100,000 new jobs’. Accessed: Oct. 26, 2023. [Online]. Available: https://www.inc.com/yoram-solomon/with-one-rule-the-faa-just-created-an-82-billion-market-and-100000-new-jobs.html

[3] ITU, ‘Characteristics of unmanned aircraft systems and spectrum requirements to support their safe operation in non-segregated airspace M Series Mobile, radiodetermination, amateur and related satellites services’, 2009. [Online]. Available: http://www.itu.int/ITU-R/go/patents/en

[4] 3GPP TR 36.777, ‘Technical specification group radio access network: study on enhanced LTE support for aerial vehicles, v.15.0.0.’ Accessed: Oct. 31, 2023. [Online]. Available: https://portal.3gpp.org/desktopmodules/Specifications/SpecificationDetails.aspx?specificationId=3231

[5] A. Chriki, H. Touati, H. Snoussi, and F. Kamoun, ‘FANET: Communication, mobility models and security issues’, *Computer Networks*, vol. 163, 2019, doi: 10.1016/j.comnet.2019.106877.

[6] Y. Zeng, Q. Wu, and R. Zhang, ‘Accessing from the Sky: A Tutorial on UAV Communications for 5G and beyond’, *Proceedings of the IEEE*, vol. 107, no. 12, 2019, doi: 10.1109/JPROC.2019.2952892.

[7] C. Cox, *An Introduction to 5G*. 2021. doi: 10.1002/9781119602682.ch13.

[8] 3GPP TR 22.891, ‘Feasibility Study on New Services and Markets Technology Enablers; Stage 1, (Release 14)’, *3rd Generation Partnership Project (3GPP), TR 22.891 V14.2.0*, 2016.

[9] ITU-R, ‘IMT Vision – Framework and overall objectives of the future development of IMT for 2020 and beyond’, *Recommendation Itu-R M.2083-0*, vol. 0, 2015.

[10] ITU, *Setting the Scene for 5G: Opportunities & Challenges*. 2018.

[11] Ericsson, ‘Ericsson Mobility Report June 2023’, Stokhom, Sweden, 2023. Accessed: Oct. 10, 2023. [Online]. Available: https://www.ericsson.com/49dd9d/assets/local/reports-papers/mobility-report/documents/2023/ericsson-mobility-report-june-2023.pdf

[12] GSA, ‘5G-Market Snapshot May 2023’, 2023. Accessed: Oct. 10, 2023. [Online]. Available: https://gsacom.com/paper/5g-market-snapshot-may-2023/

[13] Precedence Research, ‘5G Infrastructure Market’. Accessed: Oct. 11, 2023. [Online]. Available: https://www.precedenceresearch.com/5g-infrastructure-market
[14] A. Introduction *et al.*, ‘Network Functions Virtualisation,An Introduction, Benefits, Enablers, Challenges & Call for Action’, *Citeseer,* no. 1, 2012.
[15] A. Osseiran, J. F. Monserrat, and P. Marsch, *5G mobile and wireless communications technology*. 2016. doi: 10.1017/CBO9781316417744.
[16] V. G. Nguyen, A. Brunstrom, K. J. Grinnemo, and J. Taheri, ‘SDN/NFV-Based Mobile Packet Core Network Architectures: A Survey’, *IEEE Communications Surveys and Tutorials,* vol. 19, no. 3, 2017, doi: 10.1109/COMST.2017.2690823.
[17] D. B. Rawat and S. R. Reddy, ‘Software Defined Networking Architecture, Security and Energy Efficiency: A Survey’, *IEEE Communications Surveys and Tutorials,* vol. 19, no. 1. 2017. doi: 10.1109/COMST.2016.2618874.
[18] A. Kaloxylos, ‘A Survey and an Analysis of Network Slicing in 5G Networks’, *IEEE Communications Standards Magazine,* vol. 2, no. 1, 2018, doi: 10.1109/MCOMSTD.2018.1700072.
[19] I. Afolabi, T. Taleb, K. Samdanis, A. Ksentini, and H. Flinck, ‘Network slicing and softwarization: A survey on principles, enabling technologies, and solutions’, *IEEE Communications Surveys and Tutorials,* vol. 20, no. 3, 2018, doi: 10.1109/COMST.2018.2815638.
[20] Univerzita Obrany, ‘Univerzita bude mít vlastní 5G mobilní síť’. Accessed: Dec. 09, 2023. [Online]. Available: https://unob.cz/univerzita-bude-mit-vlastni-5g-mobilni-sit/
[21] M. Wzorek, D. Landen, and P. Doherty, ‘GSM Technology as a Communication Media for an Autonomous Unmanned Aerial Vehicle’, *21th Bristol UAV Systems Conference,* no. April, 2006.
[22] N. Goddemeier, K. Daniel, and C. Wietfeld, ‘Coverage evaluation of wireless networks for unmanned aerial systems’, in *2010 IEEE Globecom Workshops, GC’10,* 2010. doi: 10.1109/GLOCOMW.2010.5700244.
[23] F. Gonzalez, R. Walker, N. Rutherford, and C. Turner, ‘Assessment of the suitability of public mobile data networks for aircraft telemetry and control purposes’, *Progress in Aerospace Sciences,* vol. 47, no. 3. 2011. doi: 10.1016/j.paerosci.2010.08.001.
[24] Lassi Sundqvist, ‘Cellular controlled drone experiment: evaluation of network requirements’, Espoo, Finland, 2015.
[25] S. J. Maeng, O. Ozdemir, I. Guvenc, M. L. Sichitiu, R. Dutta, and M. Mushi, ‘AERIQ: SDR-Based LTE I/Q Measurement and Analysis Framework for Air-to-Ground Propagation Modeling’, in *IEEE Aerospace Conference Proceedings,* 2023. doi: 10.1109/AERO55745.2023.10115787.

[26] M. Gharib, S. Nandadapu, and F. Afghah, ‘An Exhaustive Study of Using Commercial LTE Network for UAV Communication in Rural Areas’, in *2021 IEEE International Conference on Communications Workshops, ICC Workshops 2021 - Proceedings*, 2021. doi: 10.1109/ICCWorkshops50388.2021.9473547.

[27] L. Afonso, N. Souto, P. Sebastião, M. Ribeiro, T. Tavares, and R. Marinheiro, ‘Feature article: Cellular for the skies: Exploiting mobile network infrastructure for low altitude air-to-ground communications’, *IEEE Aerospace and Electronic Systems Magazine*, vol. 31, no. 8, 2016, doi: 10.1109/MAES.2016.150170.

[28] R. Amorim, H. Nguyen, P. Mogensen, I. Z. Kovács, J. Wigard, and T. B. Sørensen, ‘Radio Channel Modeling for UAV Communication over Cellular Networks’, *IEEE Wireless Communications Letters*, vol. 6, no. 4, 2017, doi: 10.1109/LWC.2017.2710045.

[29] R. Amorim, I. Z. Kovacs, J. Wigard, G. Pocovi, T. B. Sorensen, and P. Mogensen, ‘Improving drone’s command and control link reliability through dual-network connectivity’, in *IEEE Vehicular Technology Conference*, 2019. doi: 10.1109/VTCSpring.2019.8746579.

[30] X. Lin *et al.*, ‘Mobile Network-Connected Drones: Field Trials, Simulations, and Design Insights’, *IEEE Vehicular Technology Magazine*, vol. 14, no. 3, 2019, doi: 10.1109/MVT.2019.2917363.

[31] Qualcomm, ‘LTE unmanned aircraft systems’, May 2017. Accessed: Dec. 08, 2023. [Online]. Available: https://www.qualcomm.com/documents/lte-unmannedaircraft-systems-trial-report,

[32] B. Van Der Bergh, A. Chiumento, and S. Pollin, ‘LTE in the sky: Trading off propagation benefits with interference costs for aerial nodes’, *IEEE Communications Magazine*, vol. 54, no. 5, 2016, doi: 10.1109/MCOM.2016.7470934.

[33] I. Bor-Yaliniz, M. Salem, G. Senerath, and H. Yanikomeroglu, ‘Is 5G ready for drones: A look into contemporary and prospective wireless networks from a standardization perspective’, *IEEE Wirel Commun*, vol. 26, no. 1, 2019, doi: 10.1109/MWC.2018.1800229.

[34] A. Festag, S. Udupa, L. Garcia, R. Wellens, M. Hecht, and P. Ulfig, ‘End-to-End Performance Measurements of Drone Communications in 5G Cellular Networks’, in *IEEE Vehicular Technology Conference*, 2021. doi: 10.1109/VTC2021-Fall52928.2021.9625429.

[35] J. Sae, P. Kurvi, S. Andreev, and M. Valkama, ‘Agile 5G Network Measurements: Operator Benefits of Employing Aerial Mobility’, *IEEE Internet of Things Magazine*, vol. 5, no. 2, 2022, doi: 10.1109/iotm.002.2200023.

[36] R. Muzaffar, C. Raffelsberger, A. Fakhreddine, J. L. Luque, D. Emini, and C. Bettstetter, ‘First experiments with a 5G-Connected drone’, in *Proceedings of the 6th ACM Workshop on Micro Aerial Vehicle Networks, Systems, and Applications, DroNet 2020*, 2020. doi: 10.1145/3396864.3400304.
[37] M. Agiwal, H. Kwon, S. Park, and H. Jin, ‘A Survey on 4G-5G Dual Connectivity: Road to 5G Implementation’, *IEEE Access*, vol. 9, 2021, doi: 10.1109/ACCESS.2021.3052462.
[38] A. H. Fahim Raouf, S. Joon Maeng, I. Guvenc, Ö. Özdemir, and M. Sichitiu, ‘Spectrum Monitoring and Analysis in Urban and Rural Environments at Different Altitudes’, in *IEEE Vehicular Technology Conference*, 2023. doi: 10.1109/VTC2023-Spring57618.2023.10200994.
[39] V. Platzgummer, V. Raida, G. Krainz, P. Svoboda, M. Lerch, and M. Rupp, ‘UAV-Based coverage measurement method for 5G’, in *IEEE Vehicular Technology Conference*, 2019. doi: 10.1109/VTCFall.2019.8891252.
[40] M. Gharib, B. Hopkins, J. Murrin, A. Koka, and F. Afghah, ‘5G Wings: Investigating 5G-Connected Drones Performance in Non-Urban Areas’, Jul. 2023.
[41] Van Phi Nguyen, ‘Autonomous unmanned aerial vehicle landing using artificial intelligence’, University of Defence, Brno, 2022.
[42] Leela S. Karumbunathan, ‘NVIDIA Jetson AGX Orin Series: A Giant Leap Forward for Robotics and Edge AI Applications’, 2022. Accessed: Nov. 19, 2023. [Online]. Available: https://www.nvidia.com/content/dam/en-zz/Solutions/gtcf21/jetson-orin/nvidia-jetson-agx-orin-technical-brief.pdf
[43] Jon Dugan, Seth Elliott, Bruce A. Mah, Jeff Poskanzer, and Kaustubh Prabhu, ‘iPerf - The ultimate speed test tool for TCP, UDP and SCTP’. Accessed: Nov. 17, 2023. [Online]. Available: https://iperf.fr/
[44] Cisco Meraki, ‘Troubleshooting Client Speed using iPerf’. Accessed: Nov. 18, 2023. [Online]. Available: https://documentation.meraki.com/General_Administration/Tools_and_Troubleshooting/Troubleshooting_Client_Speed_using_iPerf
[45] 5G PPP, ‘White Paper KPIs Measurement Tools From KPI definition to KPI validation enablement’, Mar. 2023. Accessed: Nov. 19, 2023. [Online]. Available: https://5g-ppp.eu/wp-content/uploads/2023/05/TMV-KPI-Measurement-Tools_1.0-published.pdf
[46] A. Koubaa, A. Allouch, M. Alajlan, Y. Javed, A. Belghith, and M. Khalgui, ‘Micro Air Vehicle Link (MAVlink) in a Nutshell: A Survey’, *IEEE Access*, vol. 7, 2019, doi: 10.1109/ACCESS.2019.2924410.
[47] MAVLink and Dronecode Project, ‘MAVLink Packet Serialization’.

[48] MAVLink and DroneCode Project, ‘MAVLINK Common Message Set’. Accessed: May 15, 2024. [Online]. Available: https://mavlink.io/en/messages/common.html
[49] ITU-R, ‘Minimum requirements related to technical performance for IMT-2020 radio interface(s)’, Nov. 2017. Accessed: Nov. 20, 2023. [Online]. Available: https://www.itu.int/dms_pub/itu-r/opb/rep/R-REP-M.2410-2017-PDF-E.pdf
[50] Quectel, ‘RG50xQ&RM5xxQ Series AT Commands Manual’, Aug. 2021.
[51] SIMCom, ‘SIM8300 Series_ AT Command Manual’, 2022.
[52] ModalAI Inc., ‘Qualcomm Flight RB5 Connect to GCS’. Accessed: May 20, 2024. [Online]. Available: https://docs.modalai.com/Qualcomm-Flight-RB5-user-guide-connect-gcs/#connecting-to-qgc-over-5g
[53] G. Bradski, ‘The OpenCV Library’, *Dr. Dobb’s Journal of Software Tools*, 2000.
[54] J. Wubben *et al.*, ‘Accurate landing of unmanned aerial vehicles using ground pattern recognition’, *Electronics (Switzerland)*, vol. 8, no. 12, 2019, doi: 10.3390/electronics8121532.
[55] J. B. V. K. Van Phi Nguyen, ‘Precision landing of multirotor drones using computer vision’, in *Proceedings I of the 29th Conference STUDENT EEICT 2023*, Assoc. Prof. Vítězslav Novák, Ed., Brno: Brno University of Technology, Faculty of Electrical Engineering and Communication, 2023, pp. 156–159.
[56] Nathan Jennings, ‘Socket Programming in Python (Guide)’. Accessed: May 21, 2024. [Online]. Available: https://realpython.com/python-sockets/
[57] DroneCode Project, ‘MAVLink Landing Target Protocol’.
[58] D. He, S. Chan, and M. Guizani, ‘Communication Security of Unmanned Aerial Vehicles’, *IEEE Wirel Commun*, vol. 24, no. 4, 2016, doi: 10.1109/MWC.2016.1600073WC.
[59] M. Khaled, ‘Ericsson Security Presentation US TTI event’, 2023. Accessed: May 06, 2024. [Online]. Available: https://ustti.org/wp-content/uploads/2023/06/20230607-Ericsson-USTTI-Security.pdf
[60] TSGS, ‘TS 133 501 - V15.4.0 - 5G; Security architecture and procedures for 5G System (3GPP TS 33.501 version 15.4.0 Release 15)’, 2019. [Online]. Available: https://portal.etsi.org/TB/ETSIDeliverableStatus.aspx
[61] E. R. D. S. Eva Fogelström, ‘Security standards and their role in 5G and 6G’. Accessed: May 20, 2024. [Online]. Available: https://www.ericsson.com/en/blog/2023/10/security-standards-role-in-5g
[62] Ericsson, ‘Hardening Guideline - Ericsson Private 5G’, 2023.
[63] Ericsson, ‘Security User Guide - Ericsson Private 5G’, 2023.

SYMBOLS AND ABBREVIATIONS

Abbreviations:

3GPP	Third Generation Partnership Project
5G NR	5G New Radio
AAS	Advanced Antenna System
AR/VR	Augmented Reality/Virtual Reality
ATC	Air Traffic Control
BS	Base Station
CAA	Czech Civil Aviation Authority
CAN	Controller Area Network (Bus)
CNPC	Control and Non-Payload Communication
COM	Communication Port
CPU	Central Processing Unit
C-RAN	Cloud - Radio Access Network
CSI	Camera Serial Interface
CUDA	Compute Unified Device Architecture
DC	Direct Current
DiffServ	Differentiated Services
DL	Downlink
DMIC	Digital Microphone
DP	Double-Precision
EASA	European Union Aviation Safety Agency
EDGE	Enhanced Data Rates for GSM Evolution
eMBB	Enhanced Mobile Broadband
eMMC	Embedded Multimedia Card
eNodeB	Evolved Node B
FANET	Flying Ad-Hoc Networks
FCU	Fused Connection Unit
FWA	Fixed Wireless Access
GCS	Ground Control Station
GNSS	Global Navigation Satellite System
GPIO	General-Purpose Input/Output (Interface)
GPRS	General Packet Radio Service
GPS	Global positioning system
GPU	Graphics processing unit
GSM	Global System for Mobile Communications
HSPA	High-Speed Packet Access
I/Q	In-Phase/ Quadrature-Phase
I2C	Inter-Integrated Circuit

I2S	Inter-IC Sound
ICMP	Internet Control Message Protocol
IEEE	Institute of Electrical and Electronics Engineers
IP	Internet Protocol
ITU	International Telecommunication Union
JTAG	Joint Test Action Group (header)
KPI	Key Performance Indicator
LiDAR	Light Detection and Ranging
LoS	Line of Sight
LTE	Long Term Evolution
LTE-A	Long Term Evolution Advanced
MANET	Mobile Ad-Hoc Network
MAVLink	Micro Air Vehicle Link
MBIM	Mobile Broadband Interface Model
MIMO	Multiple-Input Multiple-Output
MIPI	Mobile Industry Processor Interface
mmWave	Millimeter Wave
MTC	Massive Machine-Type Communication
NEO	Network Operation
NF	Network Function
NFV	Network Function Virtualization
NSA	Non-standalone
PCI	Peripheral Component Interconnect
PVA	Programmable Vision Accelerator
QoE	Quality of Experience
QoS	Quality of Service
RAM	Random Access Memory
RF	Radio frequency
RSRP	Reference Signal Received Power
RSRQ	Reference Signal Received Quality
RSSI	Reference Signal Strength Indicator
RTC	Real Time Clock (battery)
RTT	Round-Trip Time
RX	Receiver
SA	Standalone
SBC	Single-Board Computer
SCTP	Stream Control Transmission Protocol
SDN	Software Defined Networking
SDR	Software Defined Radio
SIM	Subscriber Identity Module

SINR	Signal to Interference & Noise Ratio
SPI	Serial Peripheral Interface
SS	Synchronization Signals
TCP	Transmission Control Protocol
TDD	Time Division Duplex
TX	Transmitter
UART	Universal Asynchronous Receiver-Transmitter
UASs	Unmanned Aircraft Systems
UAVs	Unmanned Aerial Vehicles
UDP	User Datagram Protocol
UE	User Equipment
UL	Uplink
UMTS	Universal Mobile Telecommunication System
URLLC	Ultra-reliable Low-latency Communication
USB	Universal Serial Bus
VANET	Vehicle Ad-Hoc Networks
VTOL	Vertical Take-Off and Landing
VNF	Virtualized Network Function

Appendix A - Throughput UAV-GSC

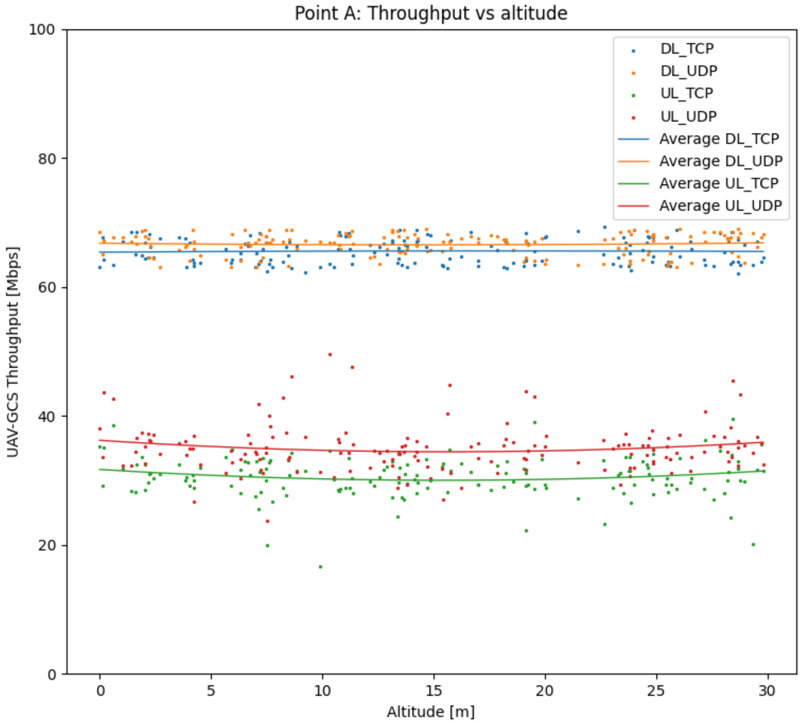

Fig.9.1 Measurement results in the vertical flights at point A: Throughput vs altitude

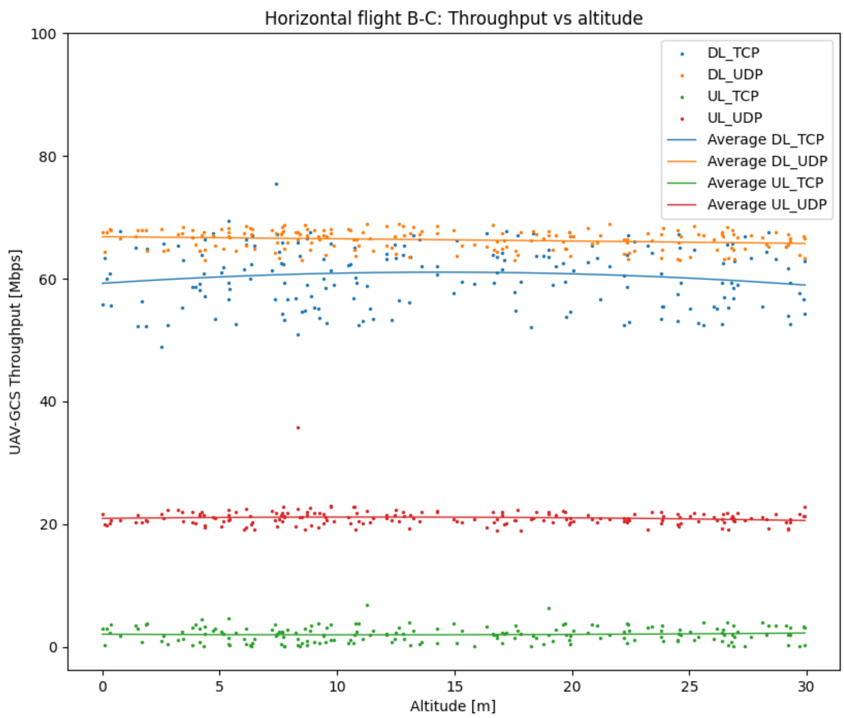

Fig.9.2 Measurement results in the horizontal flight at B-C: Throughput vs altitude

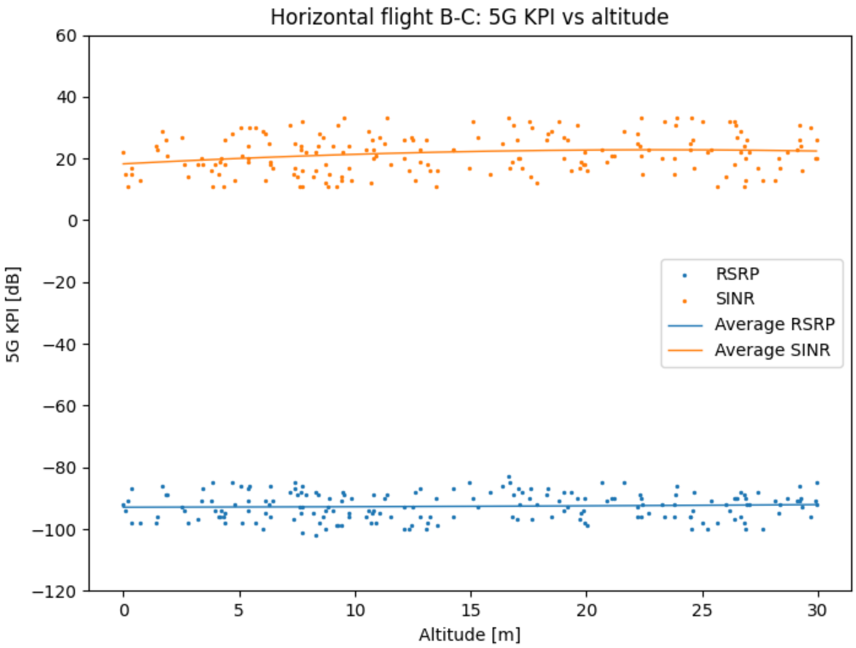

Fig.9.3 Measurement results in the horizontal flights at B-C: 5G KPI vs altitude

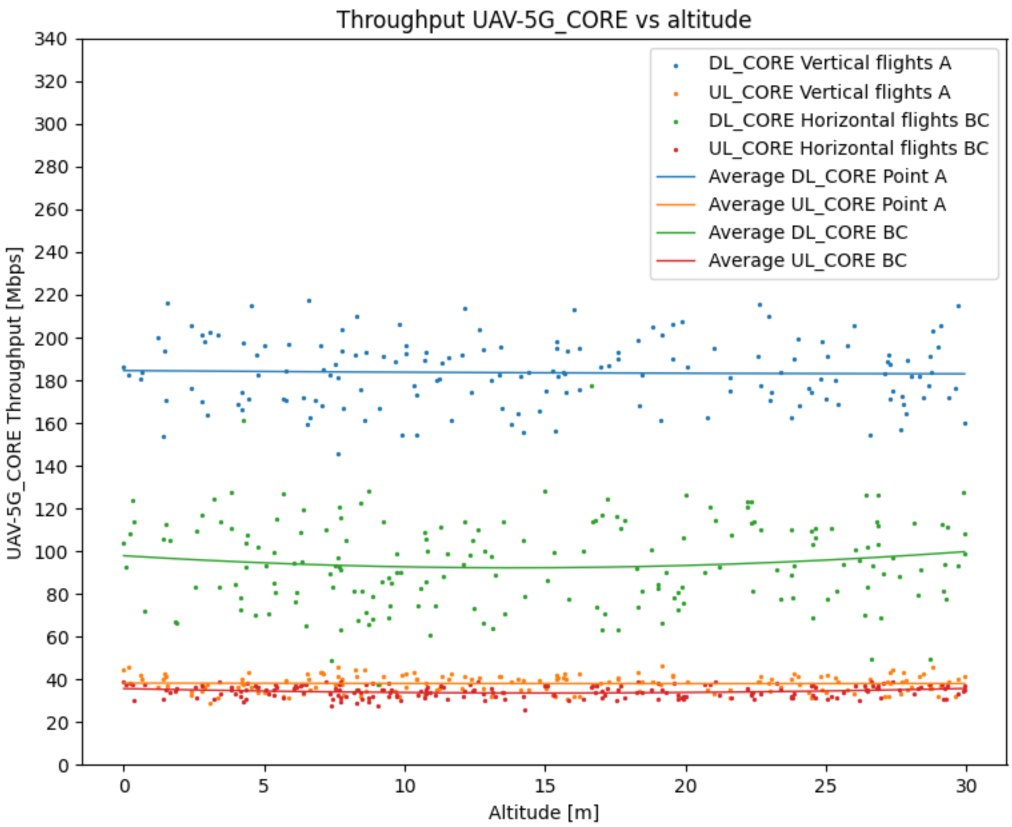

Fig.9.4 Measurement results in both flights: Throughput UAV-CORE vs altitude

Appendix B - Content of Electronic Appendix

The electronic appendix includes programs for measuring the maximum throughput between the UAV and the GCS in the private 5G UNOB network. Each program is named according to the test scenario it represents. Additionally, the appendix includes simulation scripts for Gazebo/ROS tailored to the precision landing mode of the MAVLink protocol. It also provides the AT command guide for the two 5G modules included in this study.

```
/…………………………………………..root directory of electronic appendix
|__ 5G_UAV
    |__ Gazebo-ROS………….………………...simulation for Scenario 4
    |    |__GCS.py
    |    |__UAV_in_ROS.py
    |
    |__ measure_KPI_5G_and_Throughput_Scenario_1.py
    |
    |__ measure_only_KPI_5G_Scenario_2.py
    |
    |__ Quectel_AT_Commands.pdf
    |
    |__ SIMCom_Series_AT_Command.pdf
```